

Bayesian inference and uncertainty quantification in *ab initio* nuclear physics

Andreas Ekström

Chalmers University of Technology

Why UQ?

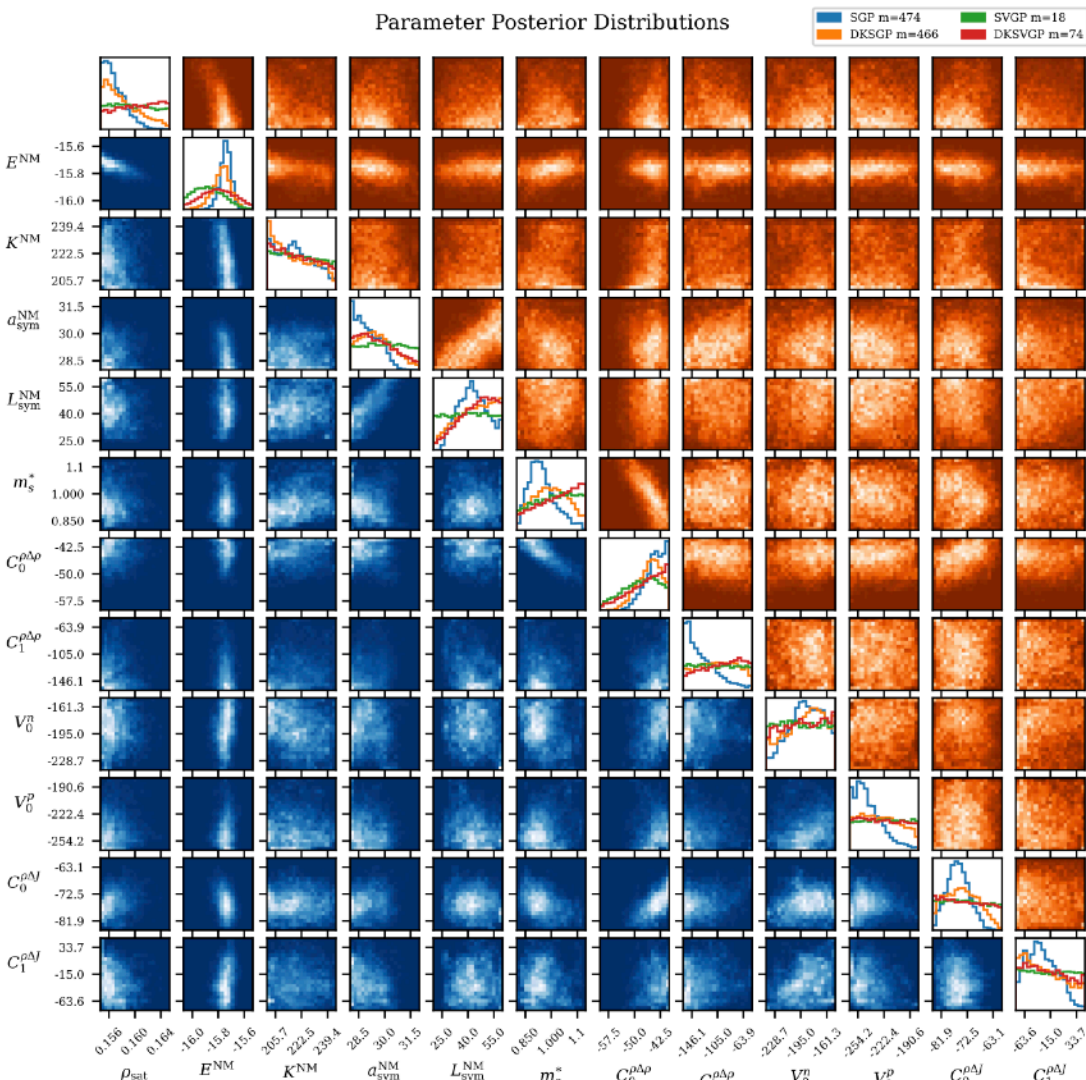
What is *ab initio*?

Methods & Applications

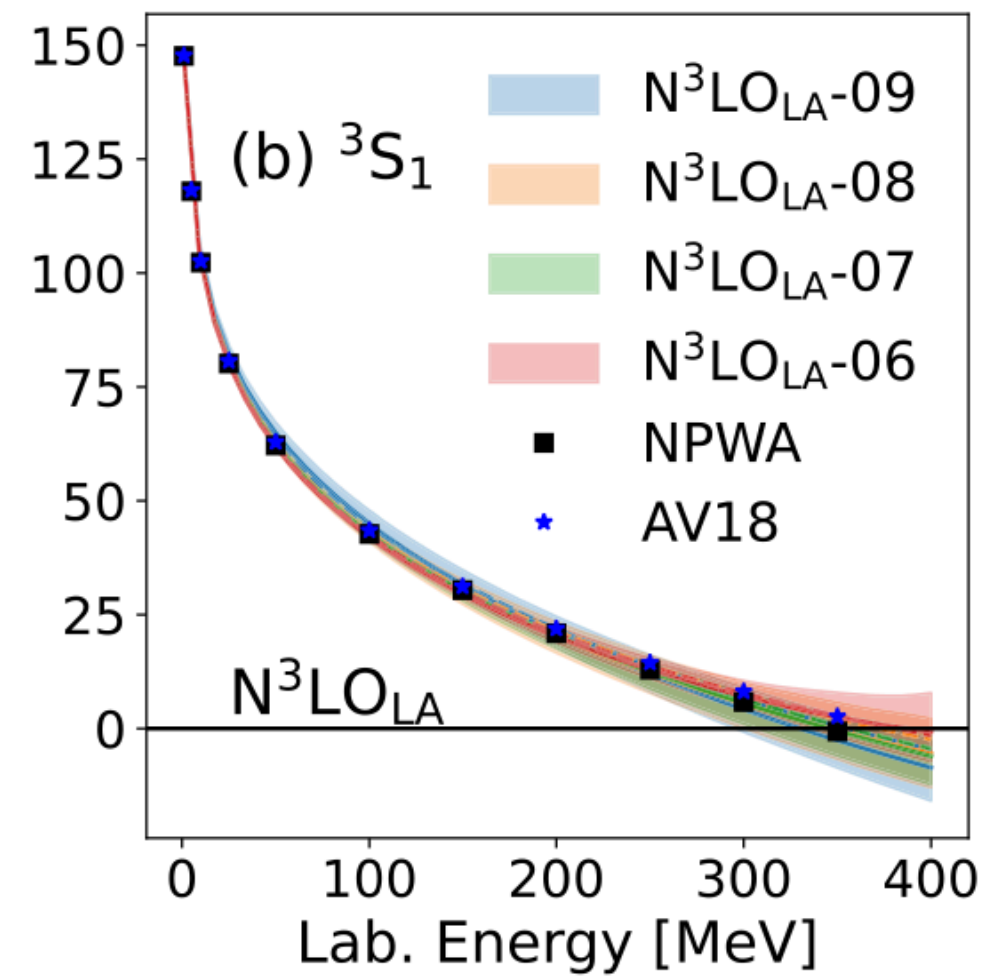
Modified Weinberg's PC



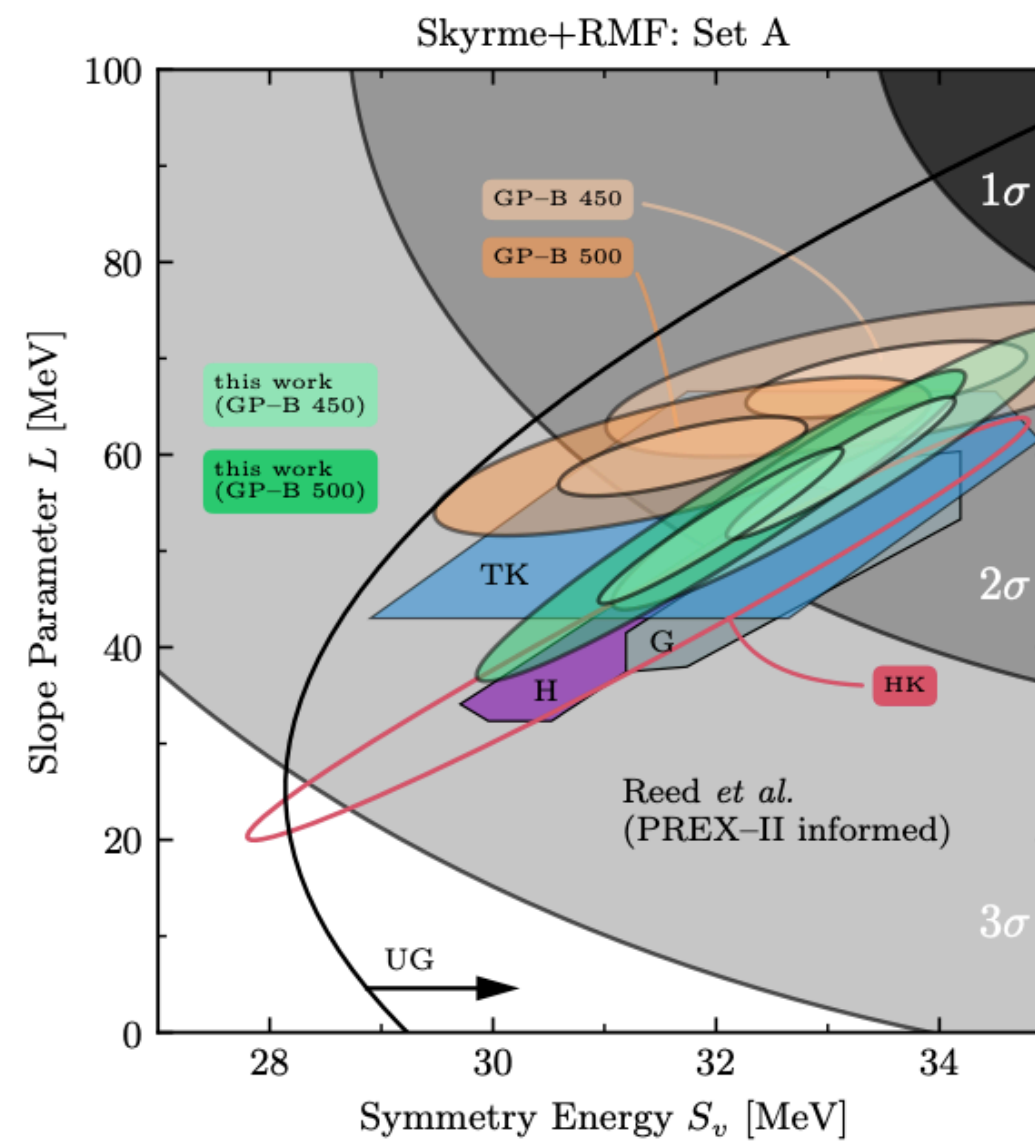
There's a lot of UQ in NP (2024 snapshots)



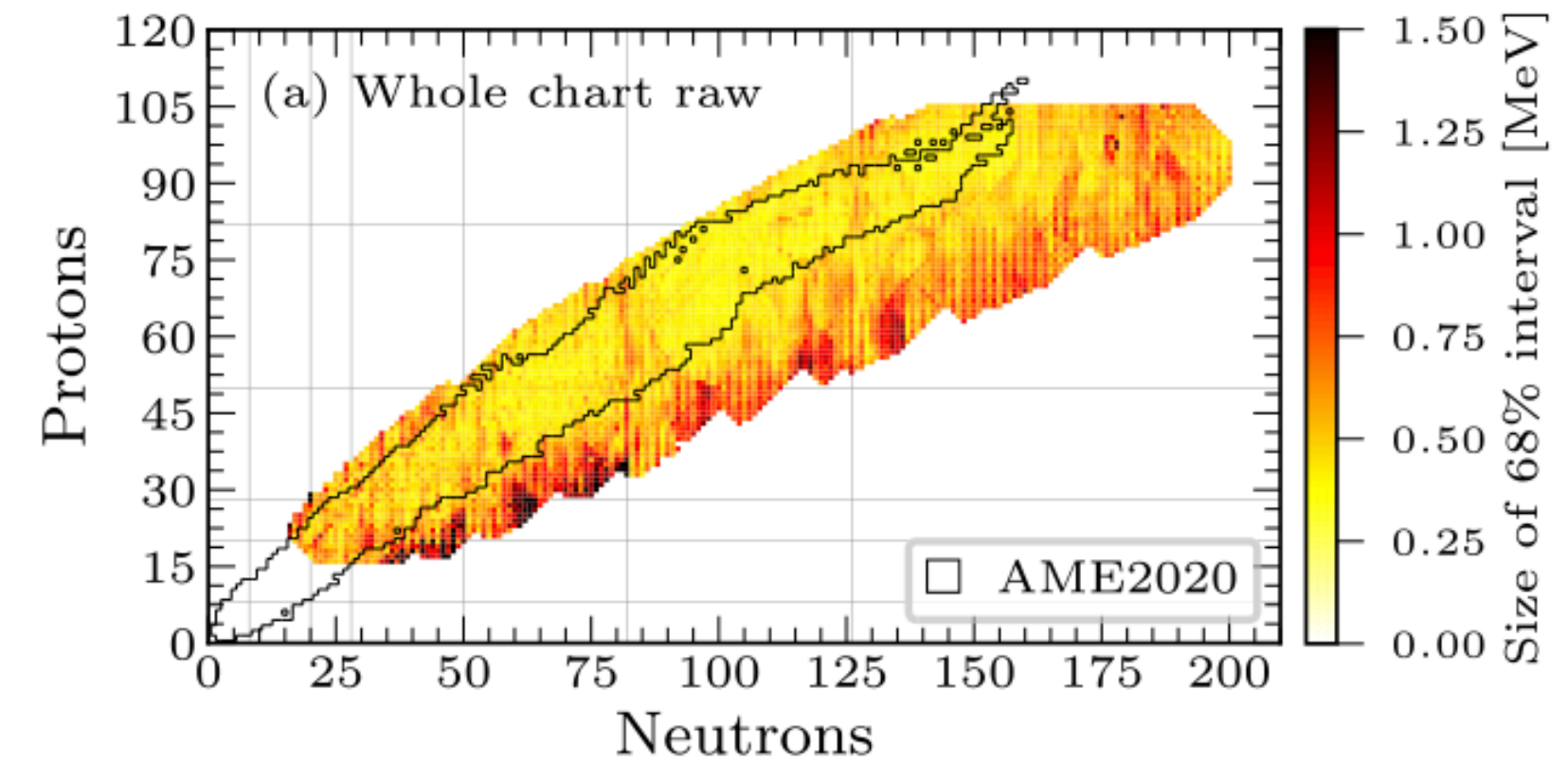
nuclear DFT: Stetzler arXiv (2024)
Posterior using GP emulators



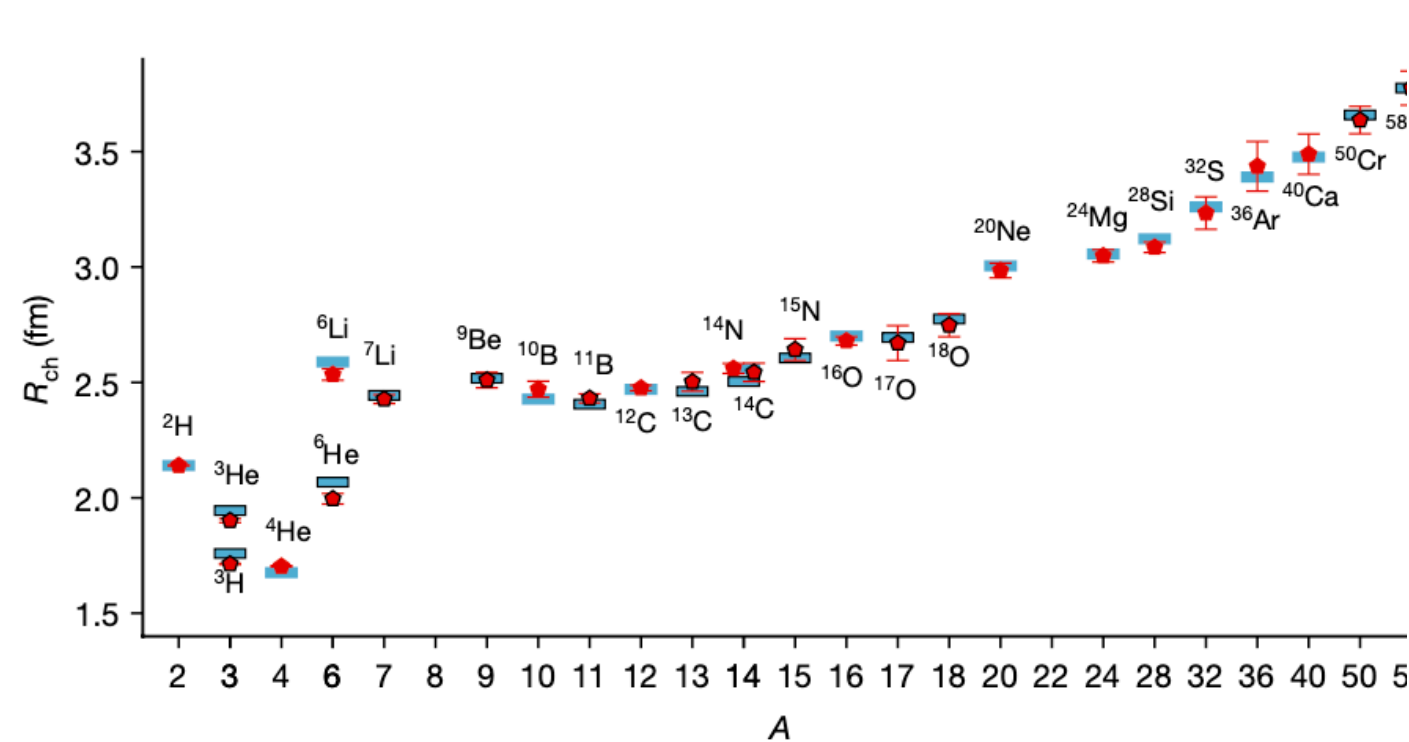
χ EFT: Somasundaram PRC (2024)
Bayesian inference and MC



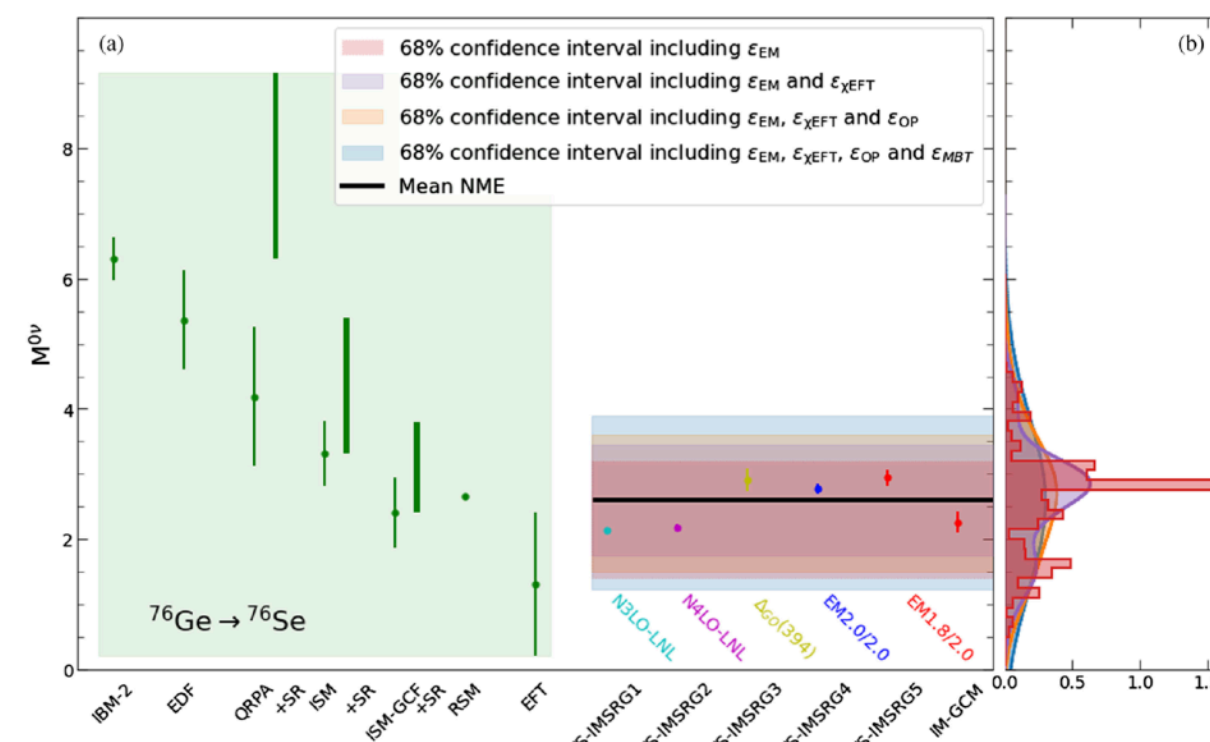
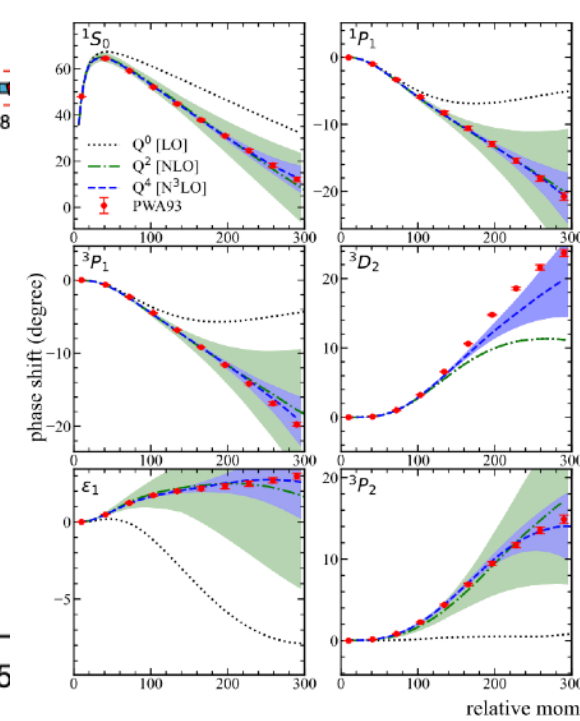
Nuclear Matter: Drischler arXiv (2024)
Bayesian mixture model



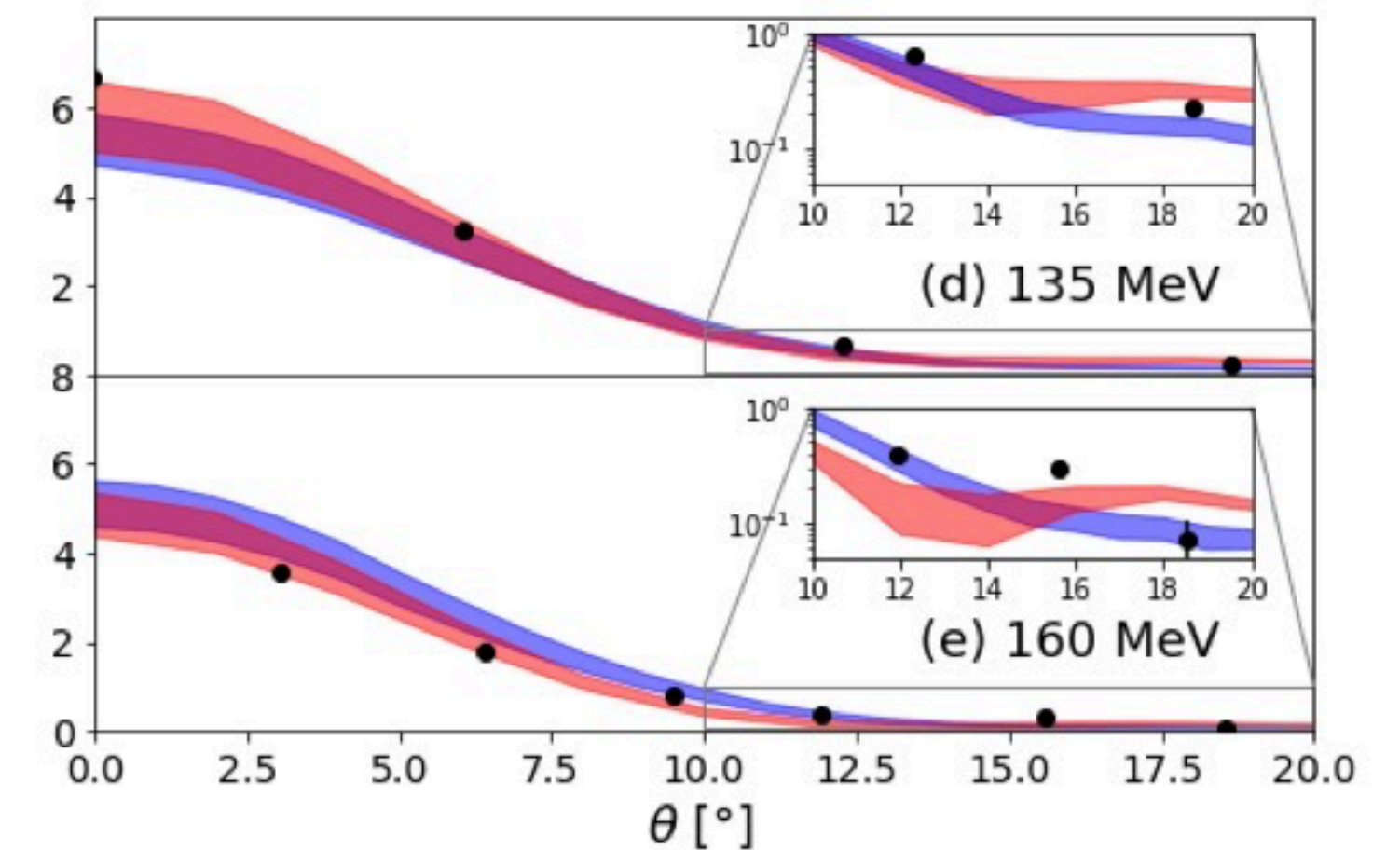
Nuclear mass models: Saito PRC (2024)
Bayesian model averaging



Lattice EFT predictions: Elhatisari Nature (2024)
History matching, MCMC, emulators



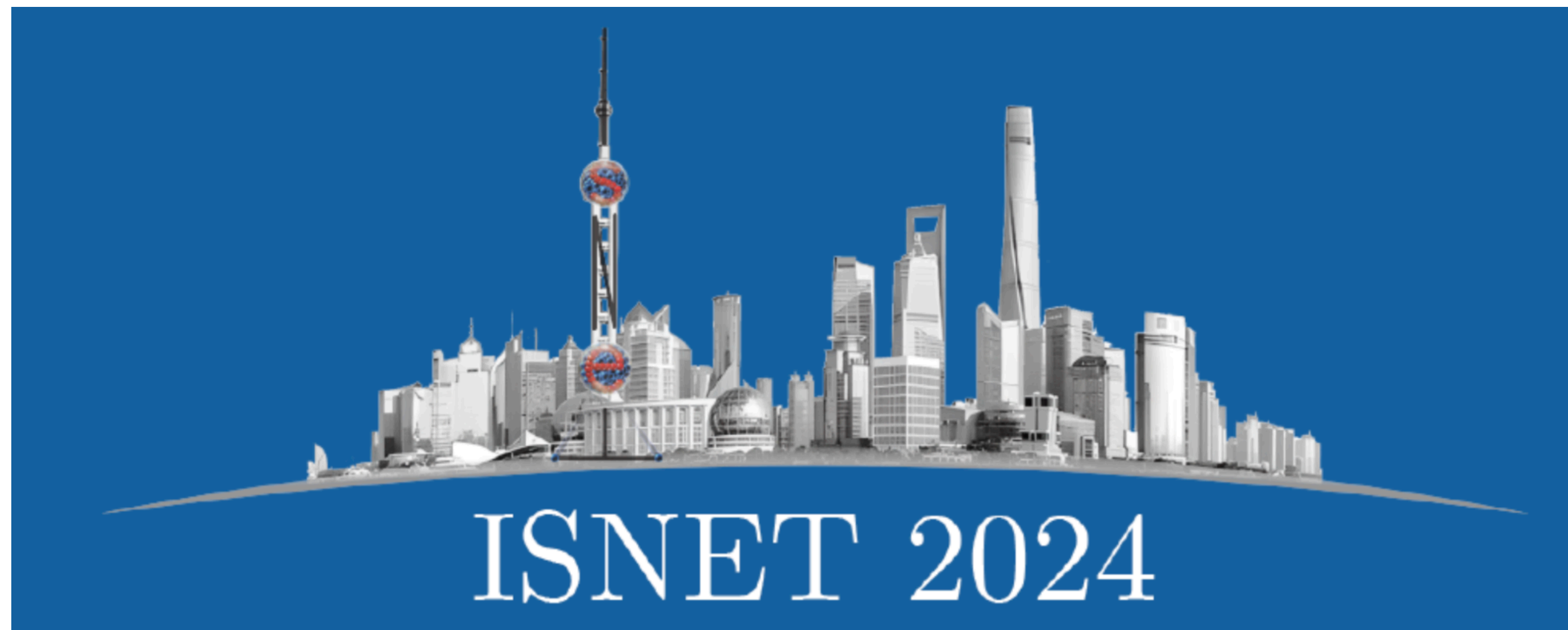
UQ fo $0\nu\beta\beta$ decay: Belley PRL (2024)
Posteriors, history matching, resampling, GP emulators



Nuclear reactions: Smith PRC (2024)
posteriors predictive distributions

ISNET-11 in Shanghai, November 10-15, 2024

@The Jiangwan Campus of Fudan University



Topics covered:

- Uncertainty quantification and statistical analysis
- Emulators and optimization
- Model mixing and data mining
- Machine learning
- Bayesian inference
- Statistics techniques in nuclear experiments
- New frontiers of nuclear physics

Apply at <https://napp.fudan.edu.cn/indico/event/757/> before July 15

More about ISNET: <https://isnet-series.github.io/>

Why uncertainty quantification?

Why uncertainty quantification?

- Predicting future data \tilde{y} from past data y is an uncertain process.
- Quantifying this uncertainty with probability:
 - enhances transparency and communication of results
 - helps improve decision-making, model reliability, and scientific understanding

Why uncertainty quantification?

- Predicting future data \tilde{y} from past data y is an uncertain process.
- Quantifying this uncertainty with probability:
 - enhances transparency and communication of results
 - helps improve decision-making, model reliability, and scientific understanding

Challenge: how to measure probabilities?
cognitive biases, philosophical interpretations,
domain standards, real-world complexity

Why uncertainty quantification?

- Predicting future data \tilde{y} from past data y is an uncertain process.
- Quantifying this uncertainty with probability:
 - enhances transparency and communication of results
 - helps improve decision-making, model reliability, and scientific understanding

Challenge: how to measure probabilities?
cognitive biases, philosophical interpretations,
domain standards, real-world complexity

Why Bayesian inference?

The probability for \tilde{y} given y is called the *posterior predictive distribution*, and this quantity is fundamental to Bayesian inference.

$$p(\tilde{y} | y, I)$$

Here, I denotes *your* background knowledge. To enable quantitative statements, we construct a *model* M . Any model comes with uncertain parameters $\vec{\alpha}$.

$$p(\tilde{y} | y, M, I) = \int p(\tilde{y} | \vec{\alpha}, M, I) p(\vec{\alpha} | y, M, I) d\vec{\alpha}$$

Bayes' rule: from likelihood & prior to posterior

- Collect N data points that we gather in a data vector y
- To explain the data, propose some model M , depending on parameters $\vec{\alpha}$
- Apply Bayes' rule

$$p(\vec{\alpha} | y, M, I) = \frac{\text{Likelihood} \cdot \text{Prior}}{\text{Marginal likelihood}} = \frac{p(y | \vec{\alpha}, M, I) \cdot p(\vec{\alpha} | M, I)}{p(y | M, I)}$$



most likely not Rev. T. Bayes

- The **prior** encodes our knowledge about the parameter values before analyzing the data
- The **likelihood** is the probability of the data given a set of parameters
- The **marginal likelihood** (or model evidence) provides normalization of the posterior
- The **posterior** is the complete inference and resulting probability density for the parameters $\vec{\alpha}$

Bayes' rule: from likelihood & prior to posterior

- Collect N data points that we gather in a data vector y
- To explain the data, propose some model M , depending on parameters $\vec{\alpha}$
- Apply Bayes' rule

Challenge: formulating the prior and likelihood. Computational costs

$$p(\vec{\alpha} | y, M, I) = \frac{\text{Likelihood} \cdot \text{Prior}}{\text{Marginal likelihood}}$$
$$p(\vec{\alpha} | y, M, I) = \frac{p(y | \vec{\alpha}, M, I) \cdot p(\vec{\alpha} | M, I)}{p(y | M, I)}$$



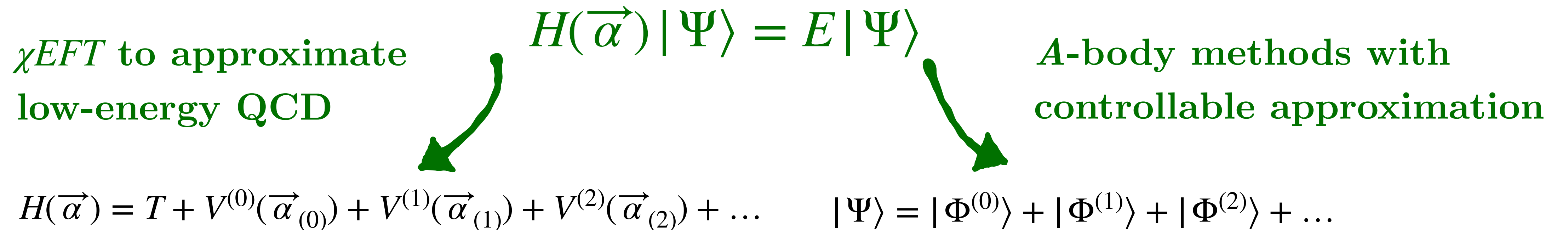
most likely not Rev. T. Bayes

- The **prior** encodes our knowledge about the parameter values before analyzing the data
- The **likelihood** is the probability of the data given a set of parameters
- The **marginal likelihood** (or model evidence) provides normalization of the posterior
- The **posterior** is the complete inference and resulting probability density for the parameters $\vec{\alpha}$

Ab initio offers an inferential advantage

$$y_{\text{exp}}(\vec{x}) = \underbrace{y_{\text{th}}(\vec{\alpha}; \vec{x}) + \delta y_{\text{th}}(\vec{\alpha}; \vec{x})}_{\text{'Model'}} + \delta y_{\text{exp}}(\vec{x})$$

Nuclear *ab initio*: a *systematically improvable* approach for quantitatively describing nuclei using the finest resolution scale possible while maximizing its predictive capabilities.



This systematicity creates an *inferential advantage*. We can test our assumptions about the model and the model discrepancy as we increase the fidelity of M .

Ab initio offers an inferential advantage

$$y_{\text{exp}}(\vec{x}) = \underbrace{y_{\text{th}}(\vec{\alpha}; \vec{x}) + \delta y_{\text{th}}(\vec{\alpha}; \vec{x})}_{\text{'Model'}} + \delta y_{\text{exp}}(\vec{x})$$

Nuclear *ab initio*: a *systematically improvable* approach for quantitatively describing nuclei using the finest resolution scale possible while maximizing its predictive capabilities.

χ EFT to approximate
low-energy QCD

$$H(\vec{\alpha}) |\Psi\rangle = E |\Psi\rangle$$

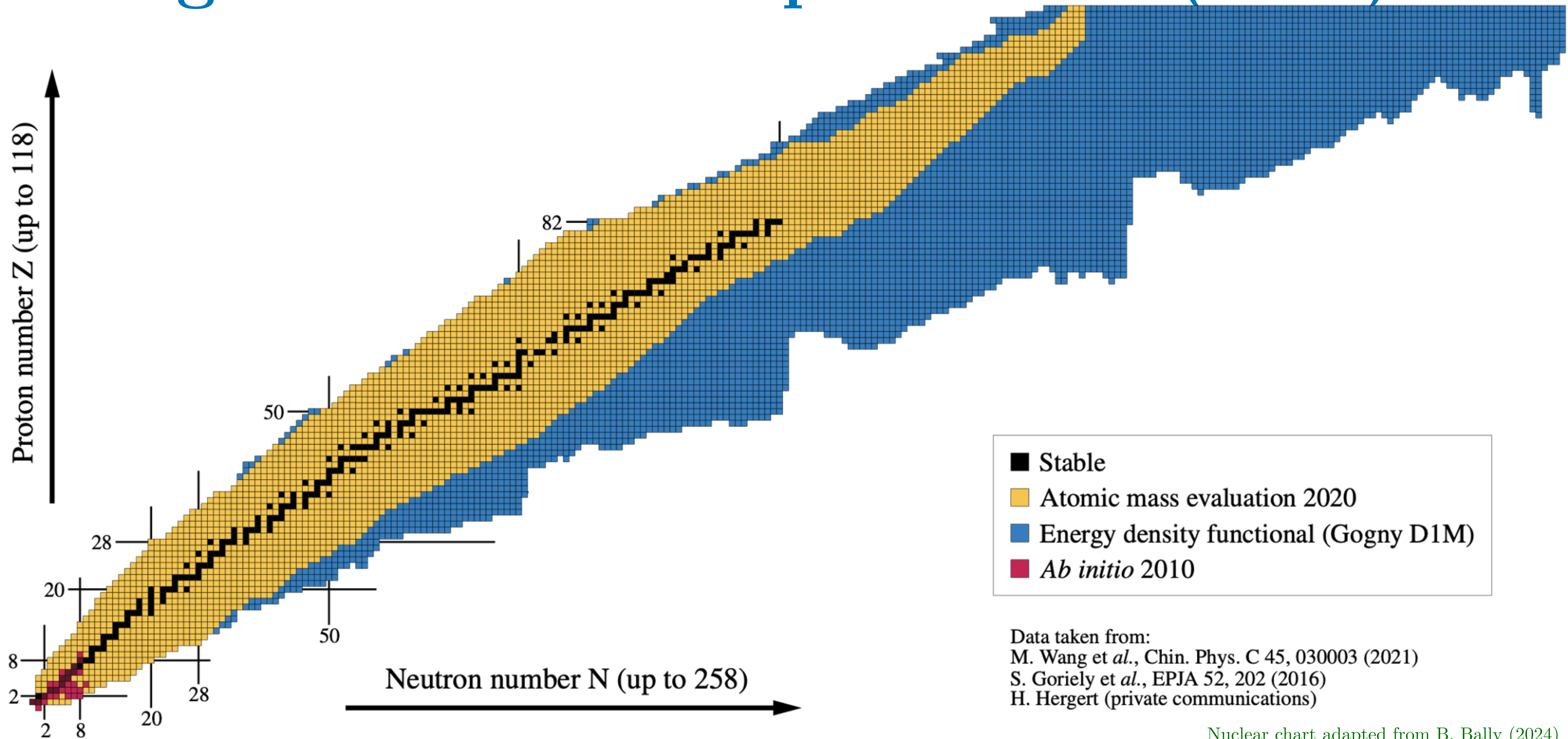
A-body methods with
controllable approximation

$$H(\vec{\alpha}) = T + V^{(0)}(\vec{\alpha}_{(0)}) + V^{(1)}(\vec{\alpha}_{(1)}) + V^{(2)}(\vec{\alpha}_{(2)}) + \dots \quad |\Psi\rangle = |\Phi^{(0)}\rangle + |\Phi^{(1)}\rangle + |\Phi^{(2)}\rangle + \dots$$

This systematicity creates an *inferential advantage*. We can test our assumptions about the model and the model discrepancy as we increase the fidelity of M .

Challenge: estimating errors in *ab initio* many-body predictions

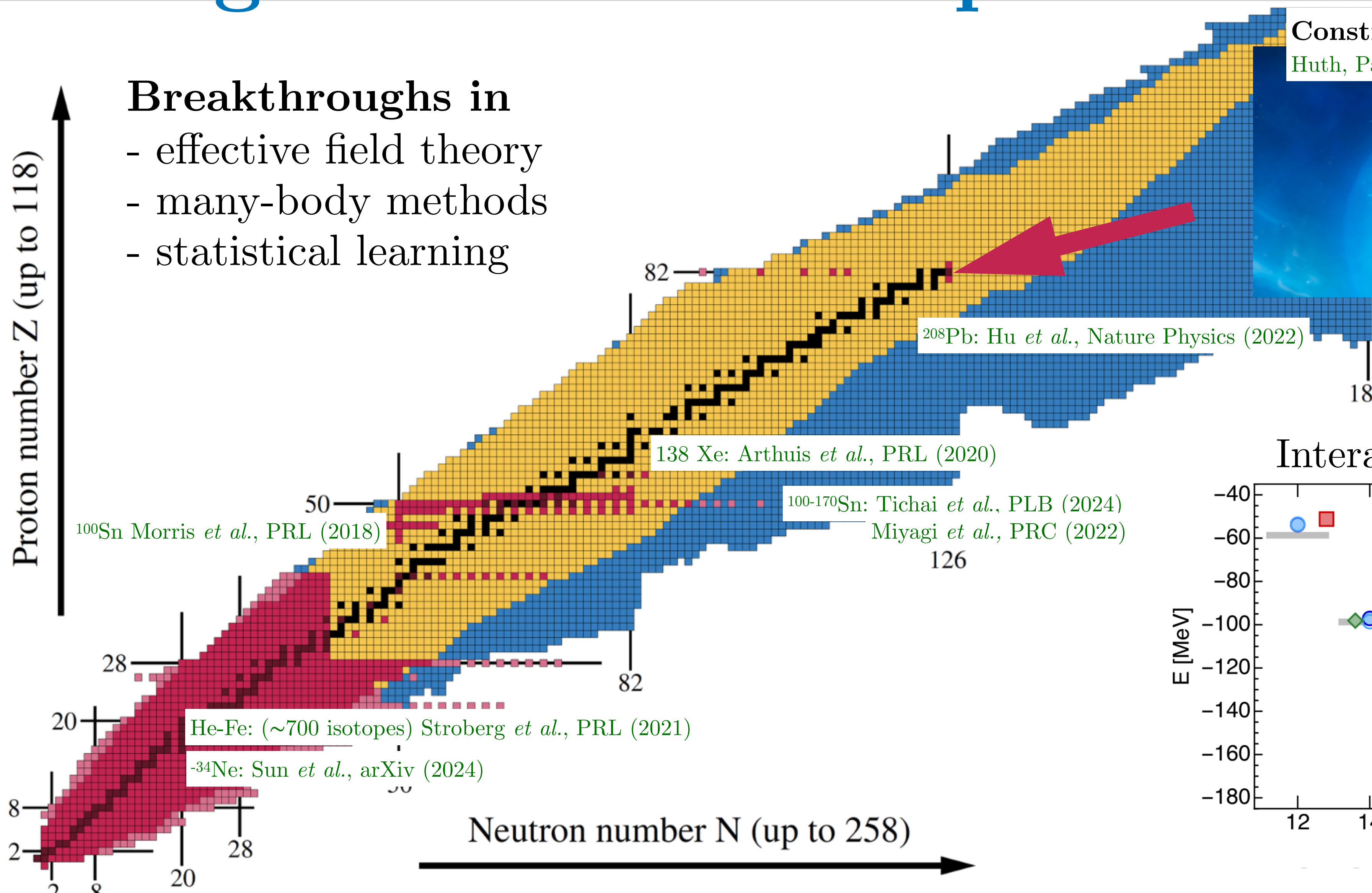
Progress in *Ab initio* predictions (2010)



Progress in *Ab initio* predictions (2024)

Breakthroughs in

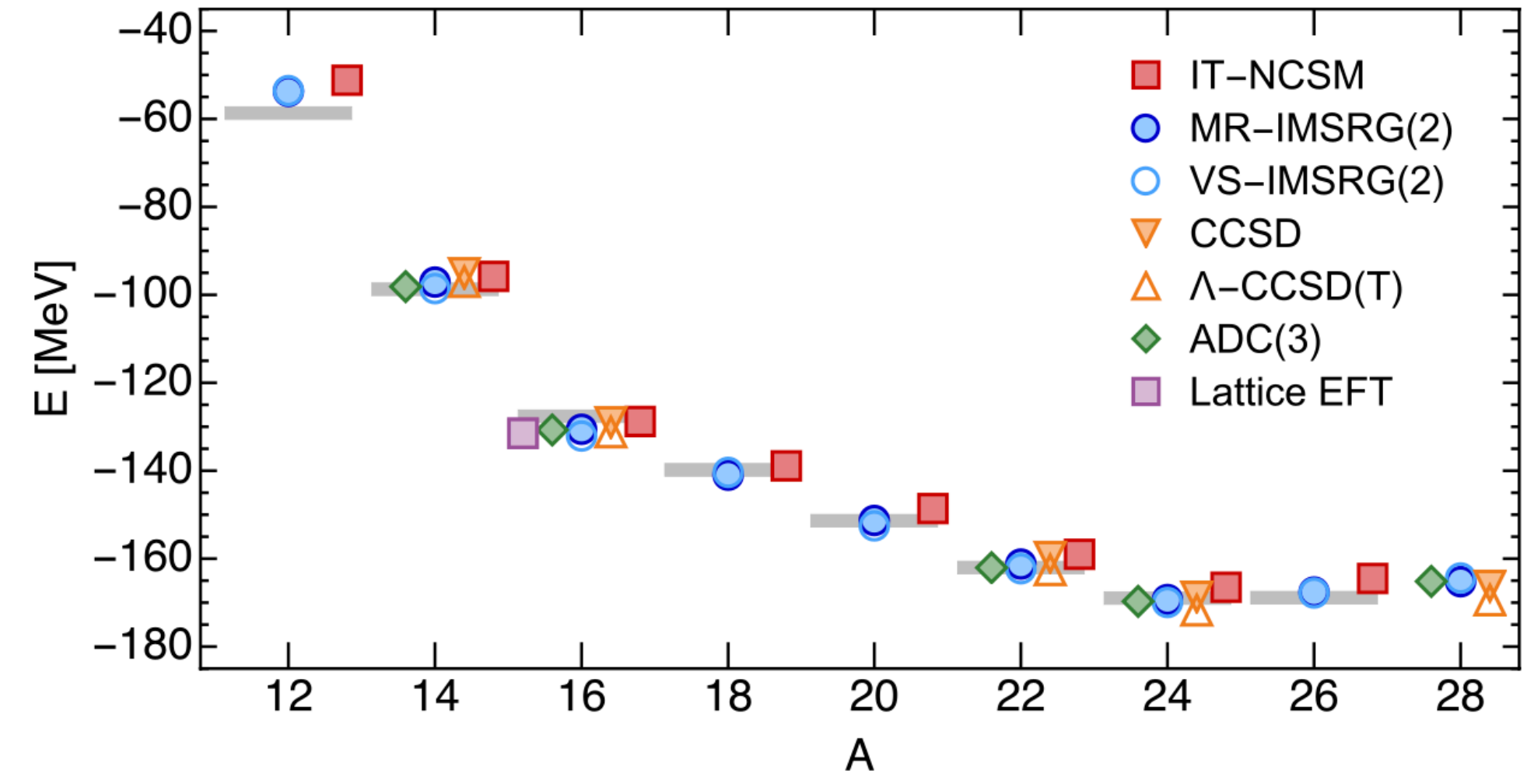
- effective field theory
- many-body methods
- statistical learning



Constraining neutron star matter
Huth, Pang, Tews, Le Fèvre, Schwenk, et al Nature (2022)

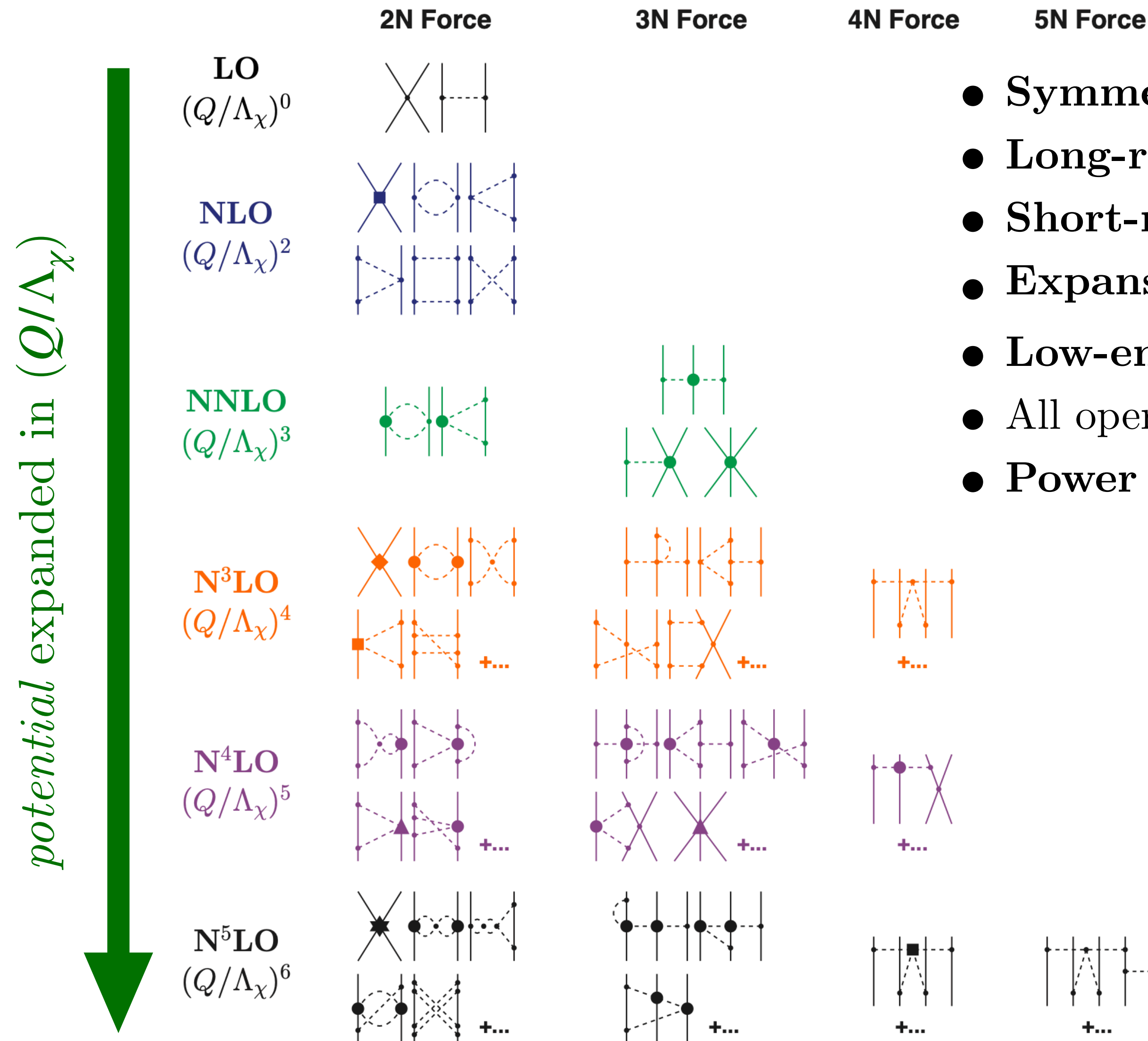


Interaction uncertainty dominates



Nuclear chart adapted from B. Bally (2024)

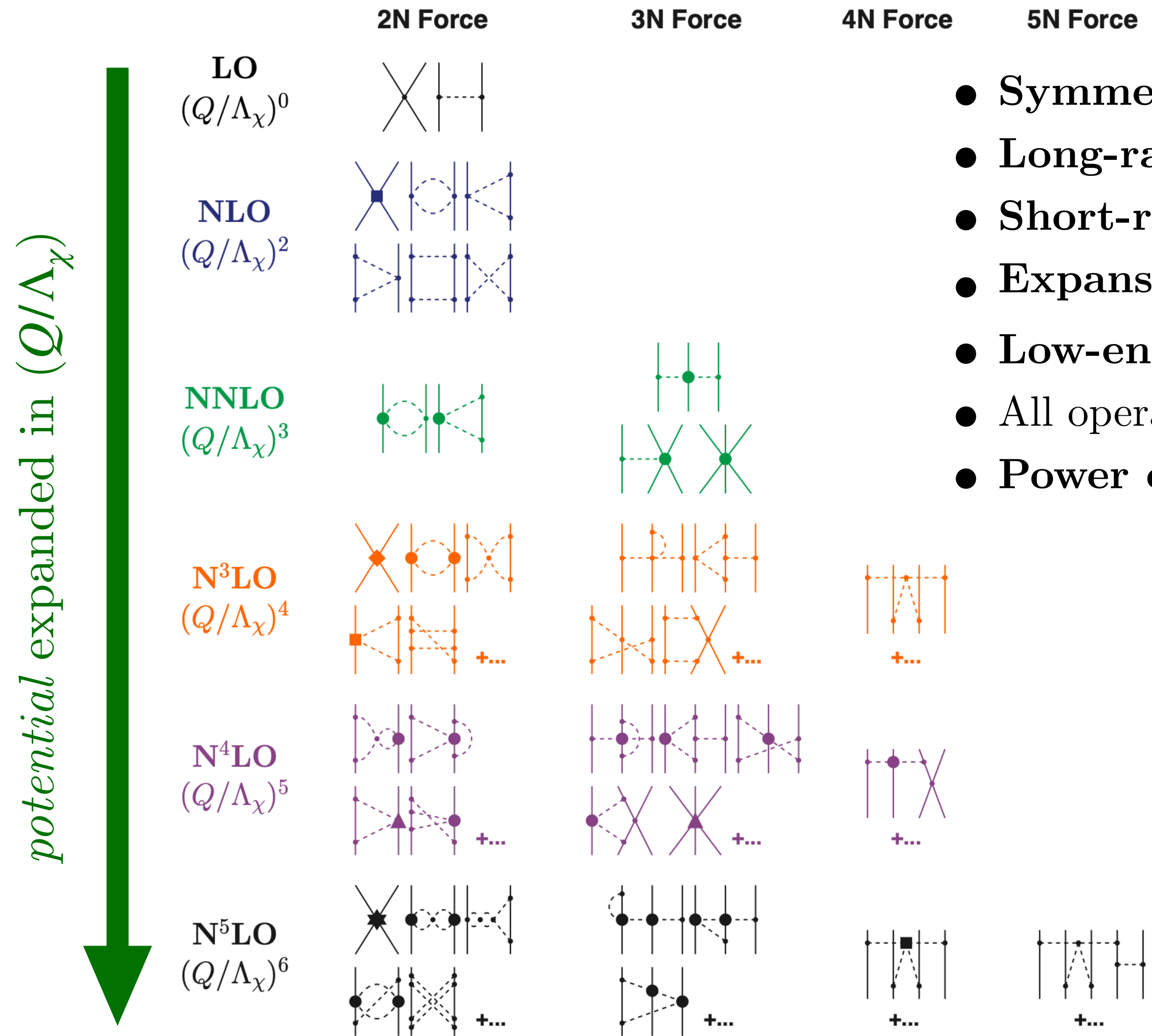
Ab initio based on χ EFT



- **Symmetries** of QCD dictate contents of effective Lagrangian
- **Long-ranged** physics governed by pion exchanges
- **Short-ranged** physics determined by a set of contact interactions
- **Expansion** in (Q/Λ_χ) [soft scale ($\sim m_\pi$) over hard scale ($\sim m_N$)]
- **Low-energy** constants (LECs) must be fit from data once
- All operators must be regulated \Rightarrow **cutoff dependence**
- **Power counting** organizes contributions (diagrams) at each order

Ab initio based on χ EFT

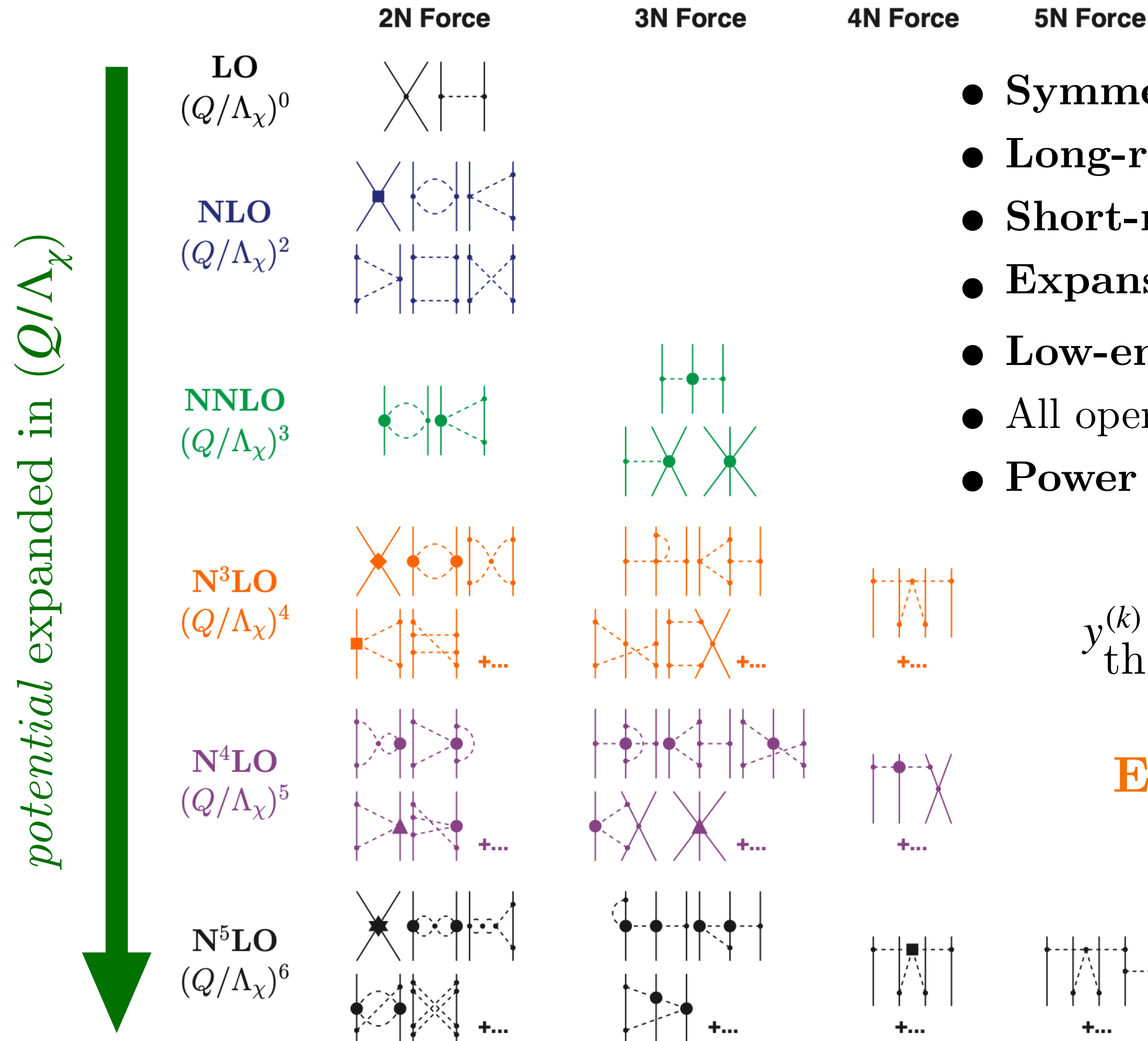
Challenge: which power counting (if any) will generate a pionfull theory for the nuclear interaction that actually is an EFT of low-energy QCD?



- **Symmetries** of QCD dictate contents of effective Lagrangian
- **Long-ranged** physics governed by pion exchanges
- **Short-ranged** physics determined by a set of contact interactions
- **Expansion** in (Q/Λ_χ) [soft scale ($\sim m_\pi$) over hard scale ($\sim m_N$)]
- **Low-energy** constants (LECs) must be fit from data once
- All operators must be regulated \Rightarrow **cutoff dependence**
- **Power counting** organizes contributions (diagrams) at each order

Ab initio based on χ EFT

Challenge: which power counting (if any) will generate a pionfull theory for the nuclear interaction that actually is an EFT of low-energy QCD?



- **Symmetries** of QCD dictate contents of effective Lagrangian
- **Long-ranged** physics governed by pion exchanges
- **Short-ranged** physics determined by a set of contact interactions
- **Expansion** in (Q/Λ_χ) [soft scale ($\sim m_\pi$) over hard scale ($\sim m_N$)]
- **Low-energy** constants (LECs) must be fit from data once
- All operators must be regulated \Rightarrow **cutoff dependence**
- **Power counting** organizes contributions (diagrams) at each order

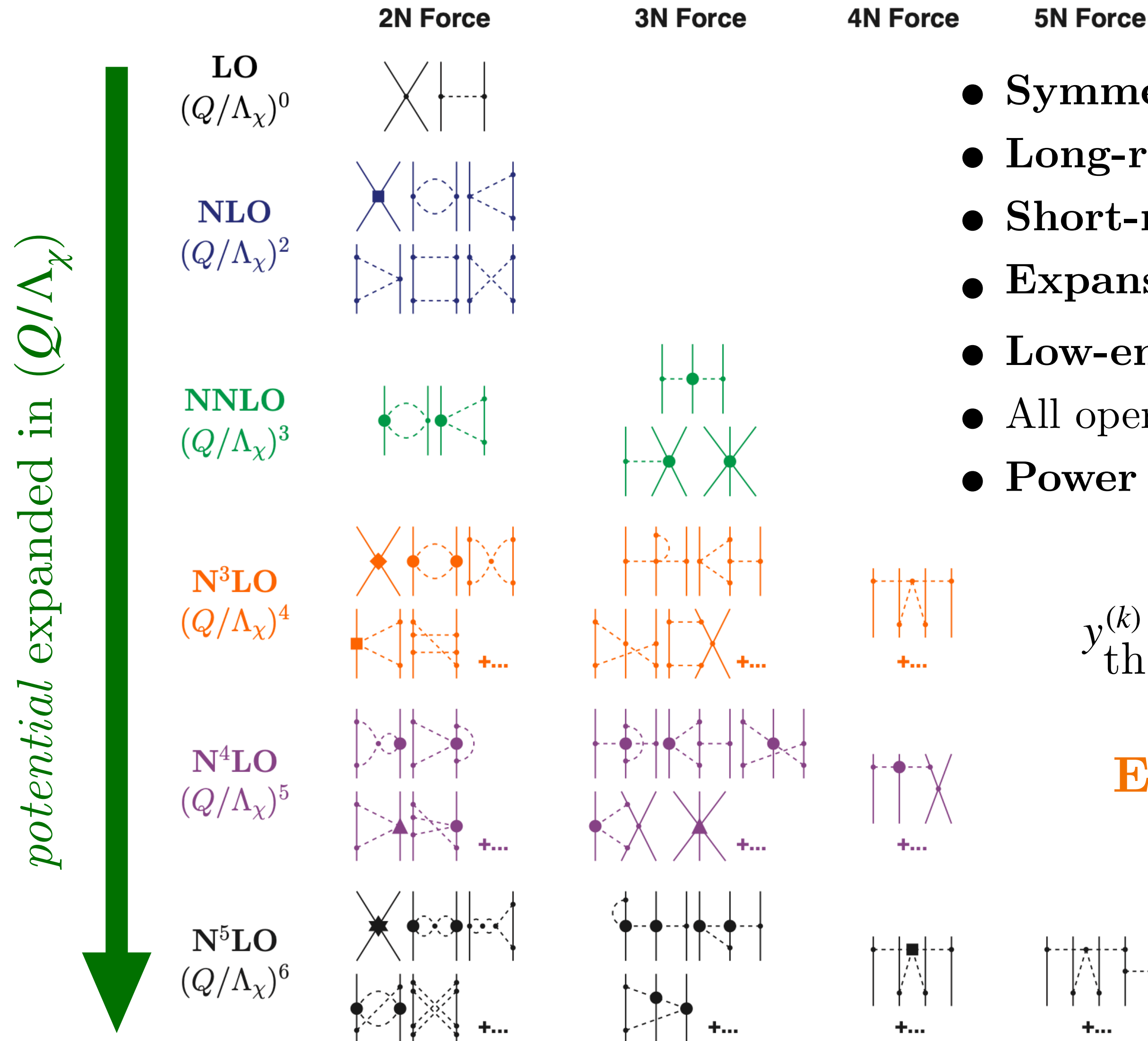
$$y_{\text{th}}^{(k)} = y_{\text{ref}} \sum_{\nu=0}^k c_\nu \left(\frac{Q}{\Lambda_\chi} \right)^\nu \quad \text{and} \quad \delta y_{\text{th}}^{(k)} = y_{\text{ref}} \sum_{\nu=k+1}^{\infty} c_\nu \left(\frac{Q}{\Lambda_\chi} \right)^\nu$$

EFT prediction

EFT truncation error

Ab initio based on χ EFT

Challenge: which power counting (if any) will generate a pionfull theory for the nuclear interaction that actually is an EFT of low-energy QCD?



- **Symmetries** of QCD dictate contents of effective Lagrangian
- **Long-ranged** physics governed by pion exchanges
- **Short-ranged** physics determined by a set of contact interactions
- **Expansion** in (Q/Λ_χ) [soft scale ($\sim m_\pi$) over hard scale ($\sim m_N$)]
- **Low-energy** constants (LECs) must be fit from data once
- All operators must be regulated \Rightarrow **cutoff dependence**
- **Power counting** organizes contributions (diagrams) at each order

$$y_{\text{th}}^{(k)} = y_{\text{ref}} \sum_{\nu=0}^k c_\nu \left(\frac{Q}{\Lambda_\chi} \right)^\nu \quad \text{and} \quad \delta y_{\text{th}}^{(k)} = y_{\text{ref}} \sum_{\nu=k+1}^{\infty} c_\nu \left(\frac{Q}{\Lambda_\chi} \right)^\nu$$

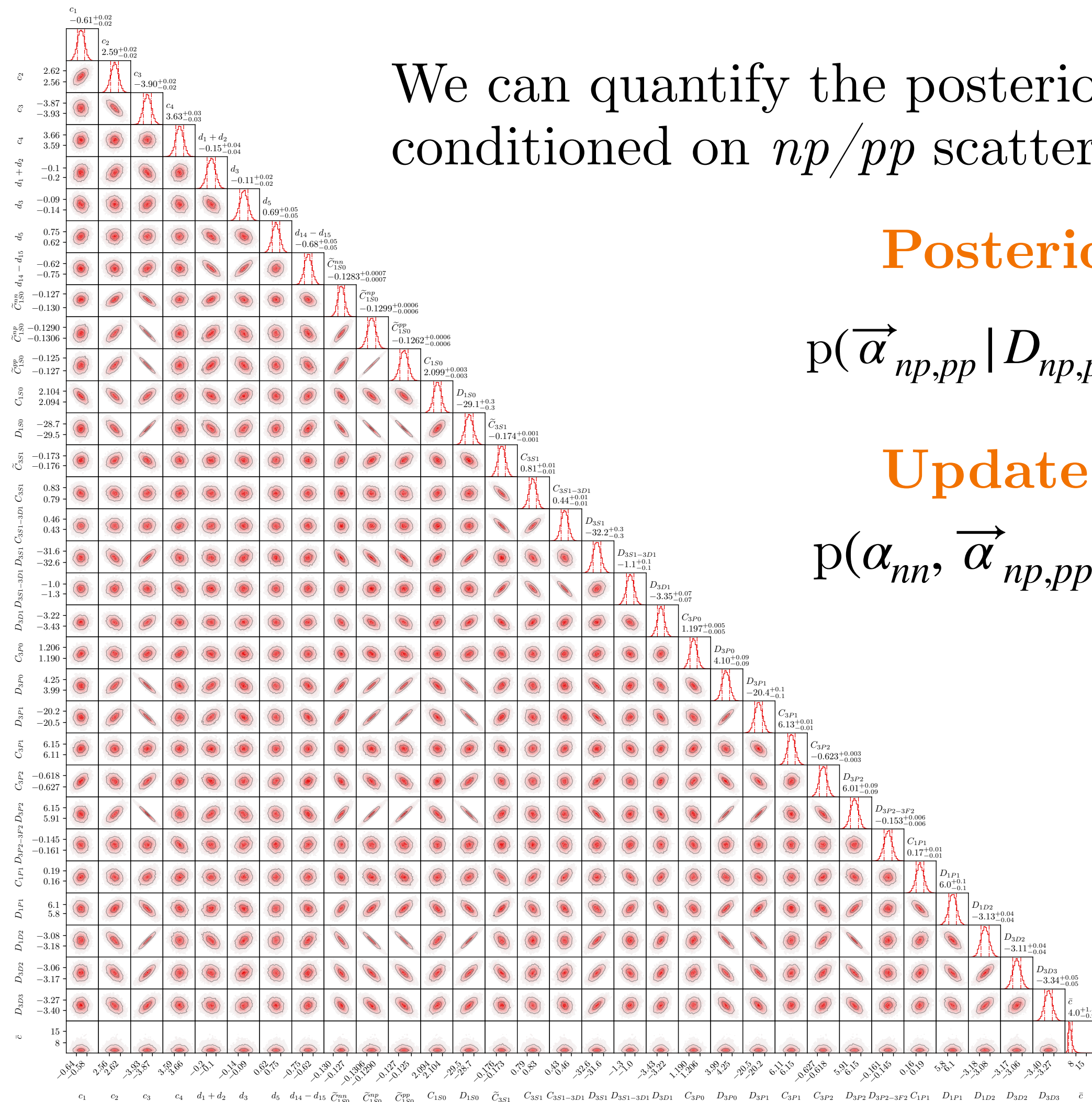
EFT prediction

EFT truncation error

Challenge: irregular convergence patterns, correlated predictions, multiple scales

Quantifying uncertainties

Low energy NN scattering



We can quantify the posterior pdf $p(\alpha_{nn}, \vec{\alpha}_{np,pp} | a_{nn}^{\text{exp}}, D_{np,pp}, I)$ up to N3LO, conditioned on np/pp scattering cross sections and the nn scattering length.

Posterior

Likelihood

Prior

$$p(\vec{\alpha}_{np,pp} | D_{np,pp}, I) \propto \exp \left[-\frac{1}{2} \vec{r}^T (\Sigma_{\text{exp}} + \Sigma_{\text{th}})^{-1} \vec{r} \right] \cdot \mathcal{N}(\mu_{NN}, \Sigma_{NN}) \cdot \mathcal{N}(\mu_{\pi N}, \Sigma_{\pi N})$$

Update

$$p(\alpha_{nn}, \vec{\alpha}_{np,pp} | a_{nn}^{\text{exp}}, D_{nn,np}, I) = p(\alpha_{nn}, | a_{nn}^{\text{exp}}, \vec{\alpha}_{np,pp}, I) \cdot p(\vec{\alpha}_{np,pp} | D_{np,pp}, I)$$

We place a multivariate normal **prior** on the πN LECs following the Roy-Steiner analysis by *Hoferichter et al.* and an uncorrelated $\mathcal{N}(0, 5^2)$ prior (in appropriate units) on the NN contact LECs up to N3LO.

Sample (31+1) dimensional posterior using HMC

Quantifying uncertainties

Low-energy NN scattering: correlated UQ

$$y_{\text{exp}}(\vec{x}) = y_{\text{th}}^{(k)}(\vec{\alpha}; \vec{x}) + \delta y_{\text{exp}}(\vec{x}) + \delta y_{\text{th}}^{(k)}(\vec{x}).$$

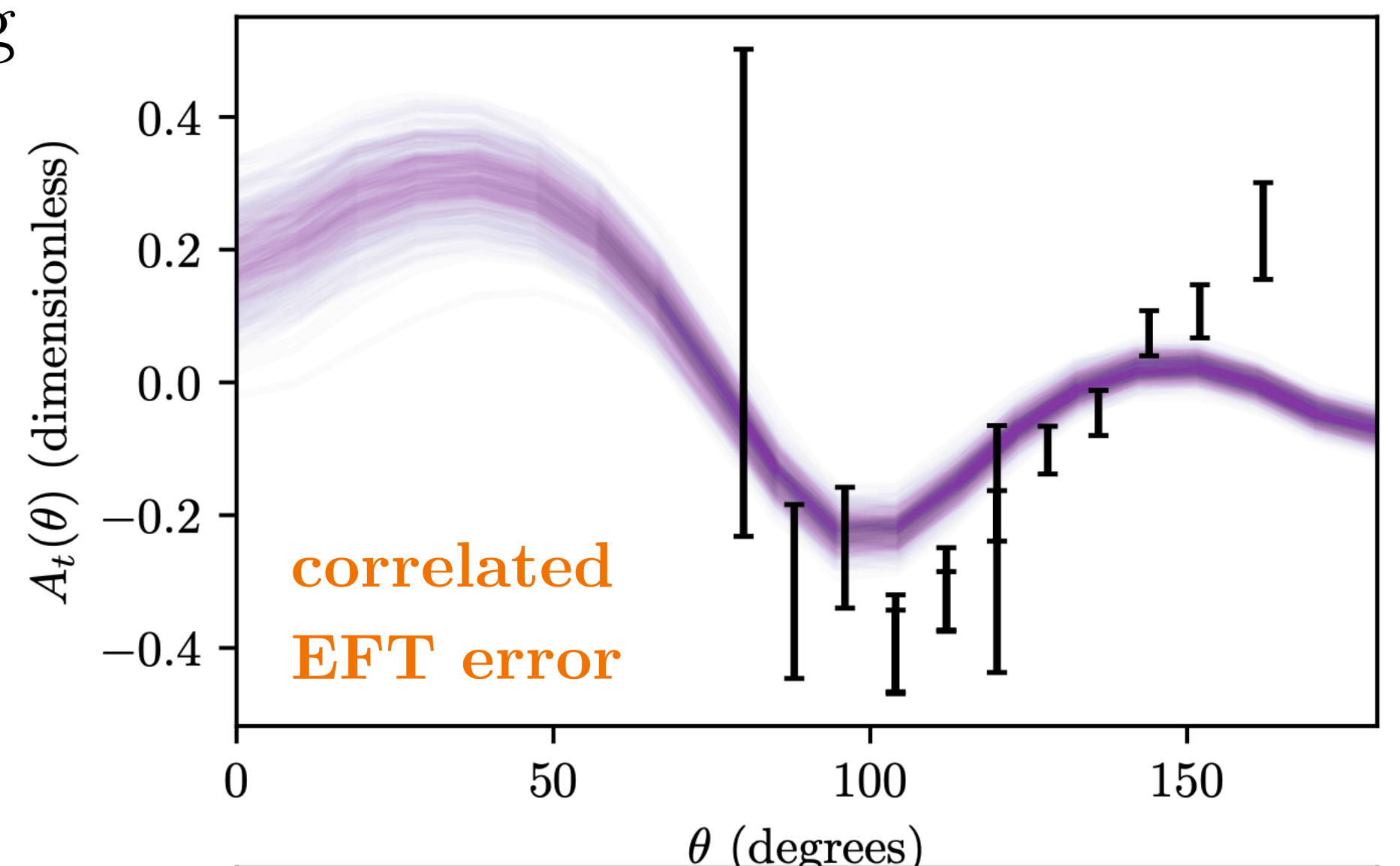
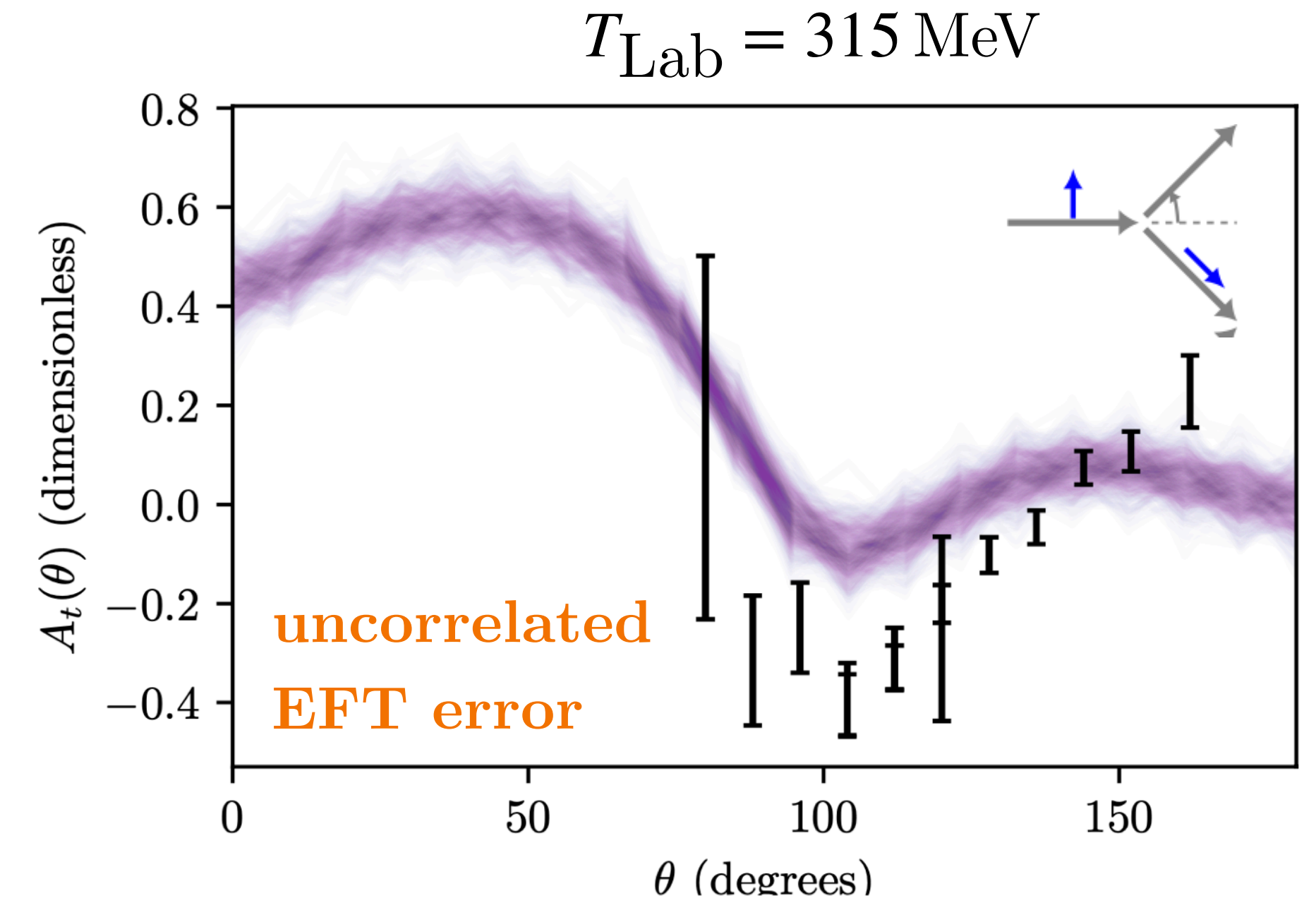
Model correlations across kinematics $\vec{x} = (T_{\text{lab}}, \theta)$,

$$(\Sigma_{\text{th},y})_{mn} = \text{cov}[\delta y_{\text{th}}^{(k)}(\vec{x}_m), \delta y_{\text{th}}^{(k)}(\vec{x}_n)] \quad \text{GP-model}$$

Correlation lengths for np scattering: 45–83 MeV & 24–39 deg

Accounting for correlations:

- reduces the effective number of independent NN data with factors 8 and 4 at NLO and NNLO.
- leaves LEC posterior mode location, but doubles the posterior width.
- yields a smoother and more realistic uncertainty estimate.



Quantifying uncertainties

Low-energy NN scattering: correlated UQ

$$y_{\text{exp}}(\vec{x}) = y_{\text{th}}^{(k)}(\vec{\alpha}; \vec{x}) + \delta y_{\text{exp}}(\vec{x}) + \delta y_{\text{th}}^{(k)}(\vec{x}).$$

Model correlations across kinematics $\vec{x} = (T_{\text{lab}}, \theta)$,

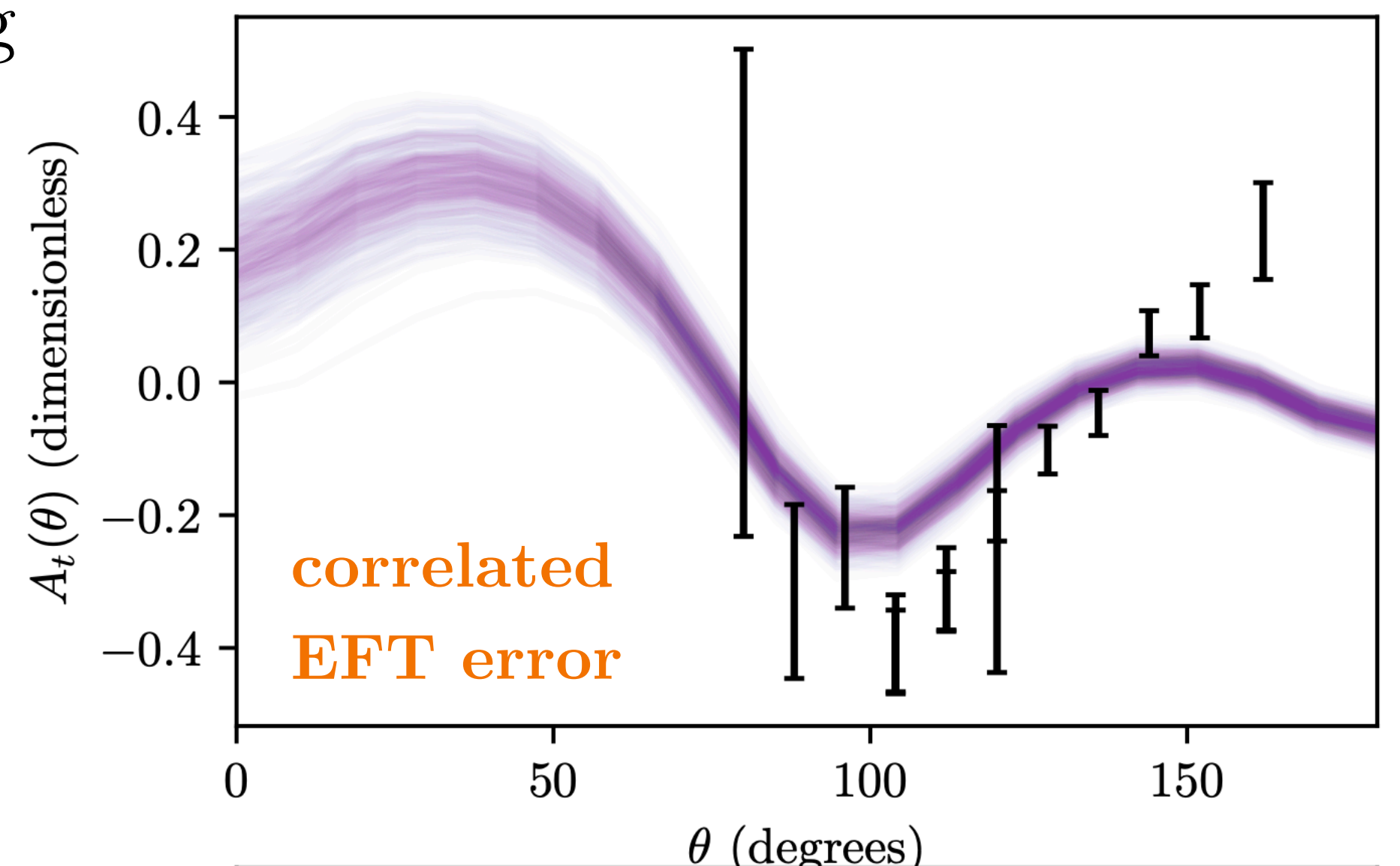
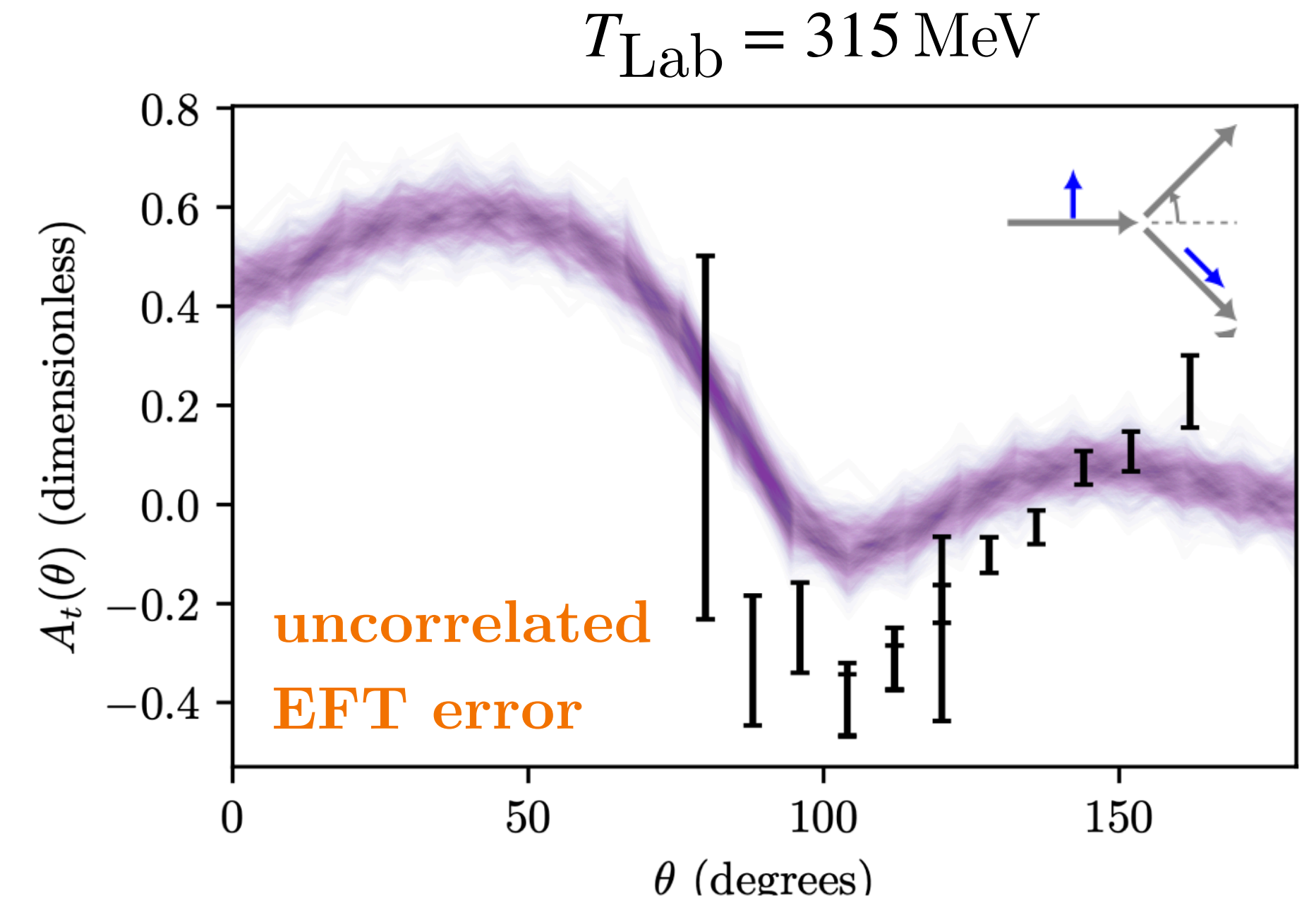
$$(\Sigma_{\text{th},y})_{mn} = \text{cov}[\delta y_{\text{th}}^{(k)}(\vec{x}_m), \delta y_{\text{th}}^{(k)}(\vec{x}_n)] \quad \text{GP-model}$$

Correlation lengths for np scattering: 45–83 MeV & 24–39 deg

Accounting for correlations:

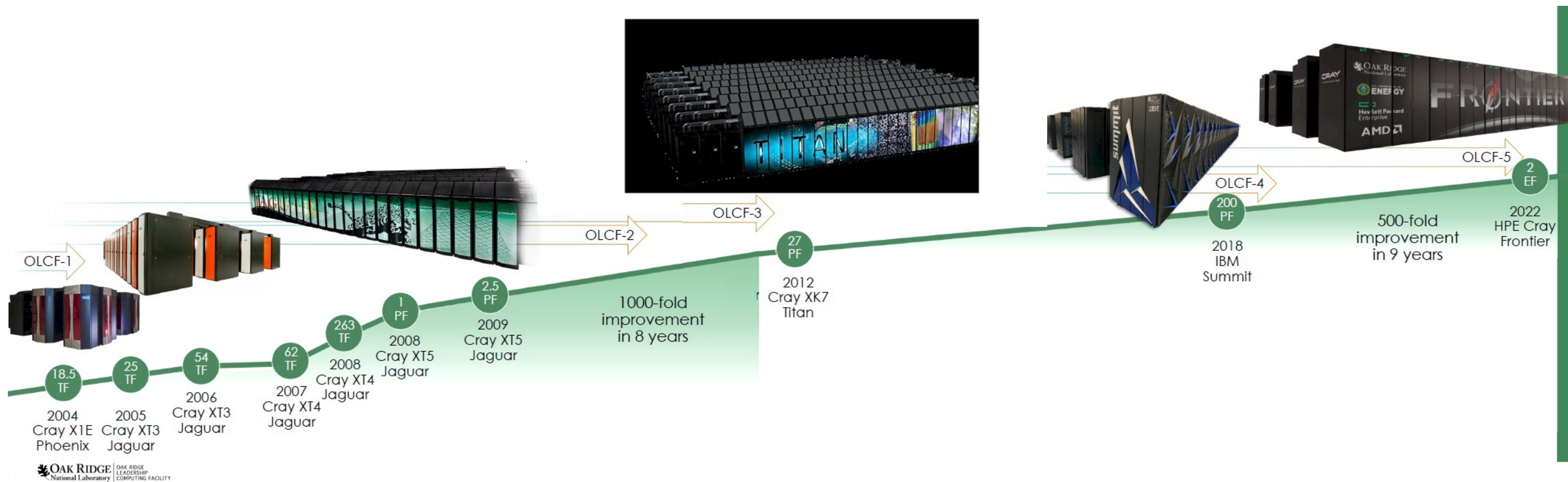
- reduces the effective number of independent NN data with factors 8 and 4 at NLO and NNLO.
- leaves LEC posterior mode location, but doubles the posterior width.
- yields a smoother and more realistic uncertainty estimate.

Challenge: sample ppd:s for $A > 2$ nuclear systems



Computing nuclei: an HPC problem

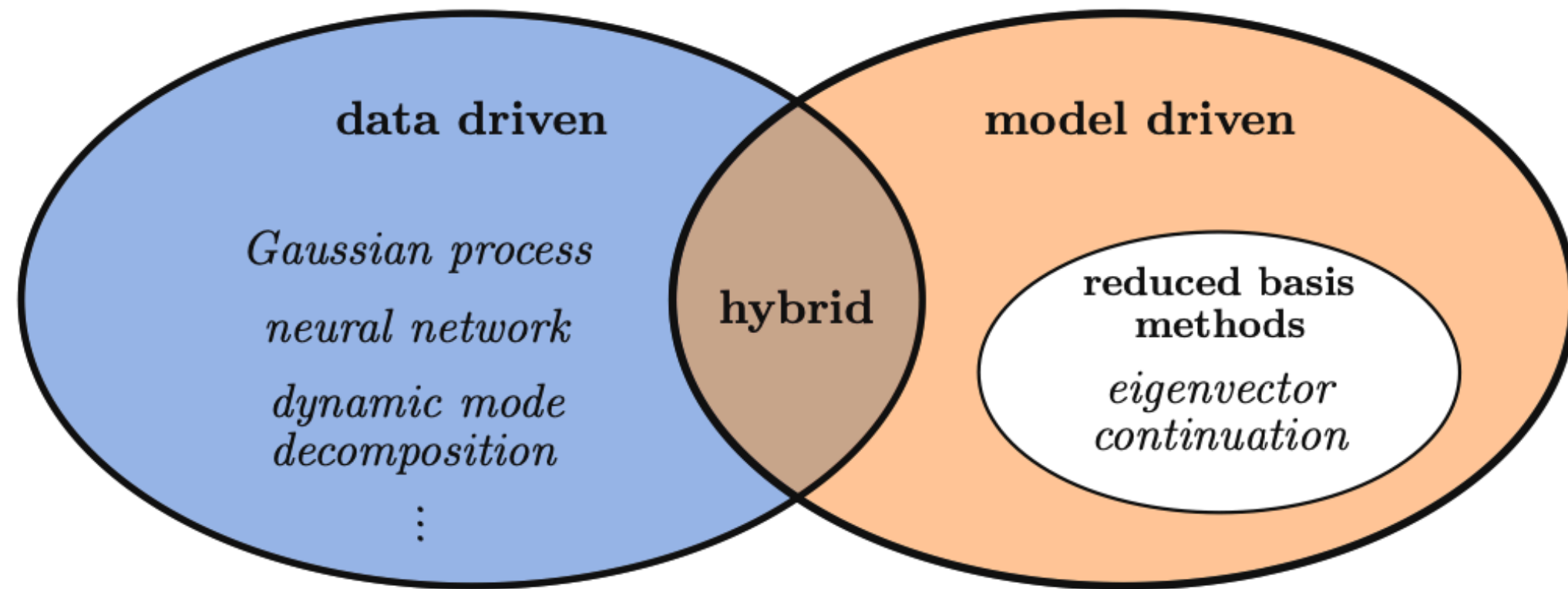
Solving the Schrödinger equation for a large collection of strongly interacting nucleons typically requires substantial high-performance computing resources. Naively, the computational cost to solve the Schrödinger equation grows exponentially with nucleon number and basis size. Polynomially scaling methods exist but are still computationally expensive.



Emulators to the rescue

Eigenvector continuation (EC): a reduced-basis method (RBM)

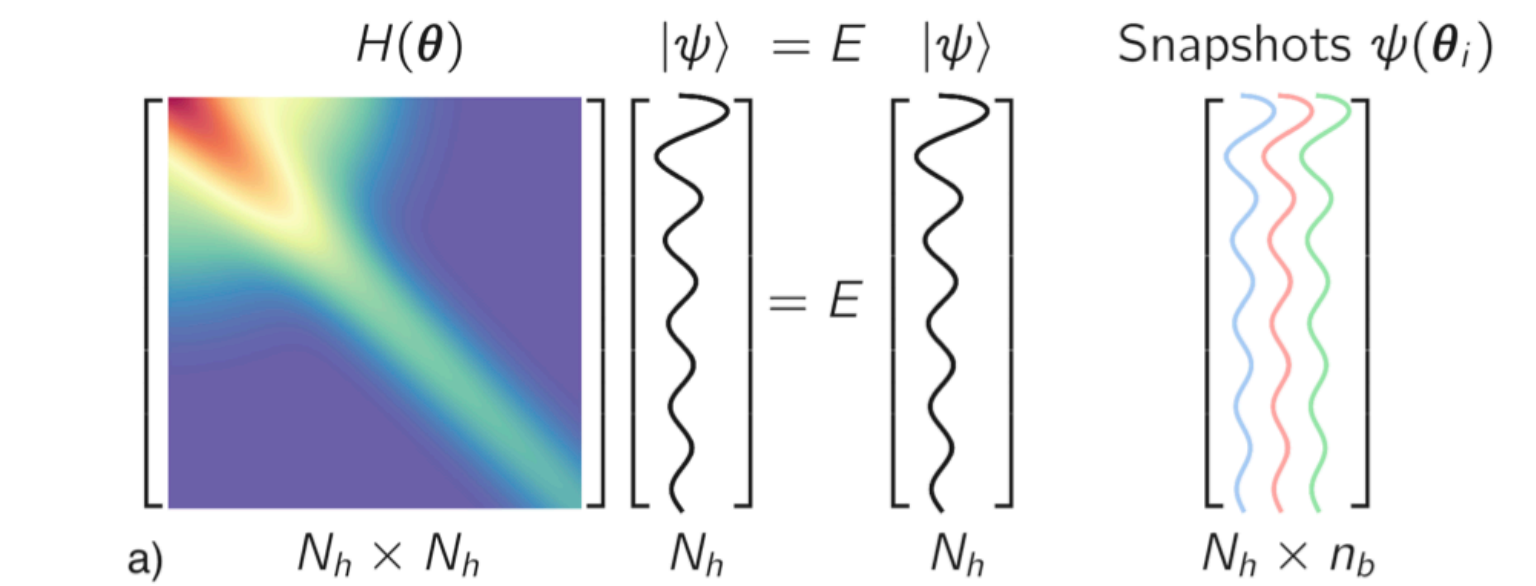
reduced order models



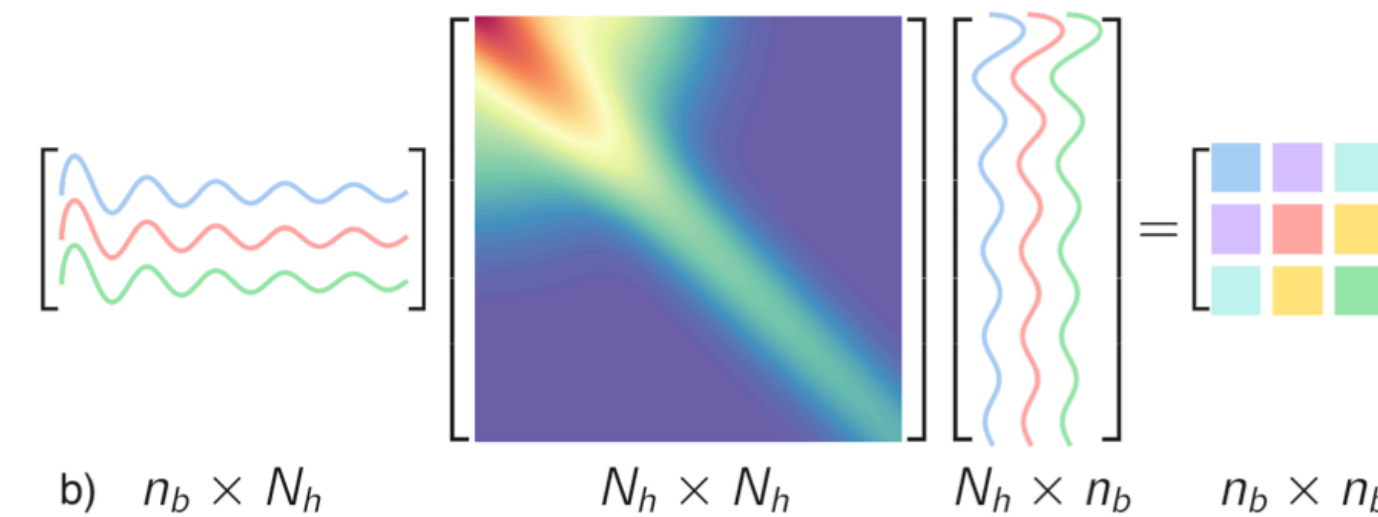
$$H(\alpha) = H_0 + \alpha H_1$$

continuous parameter

Eigenvector trajectories from Hamiltonian changes lie in a low-dimensional manifold.



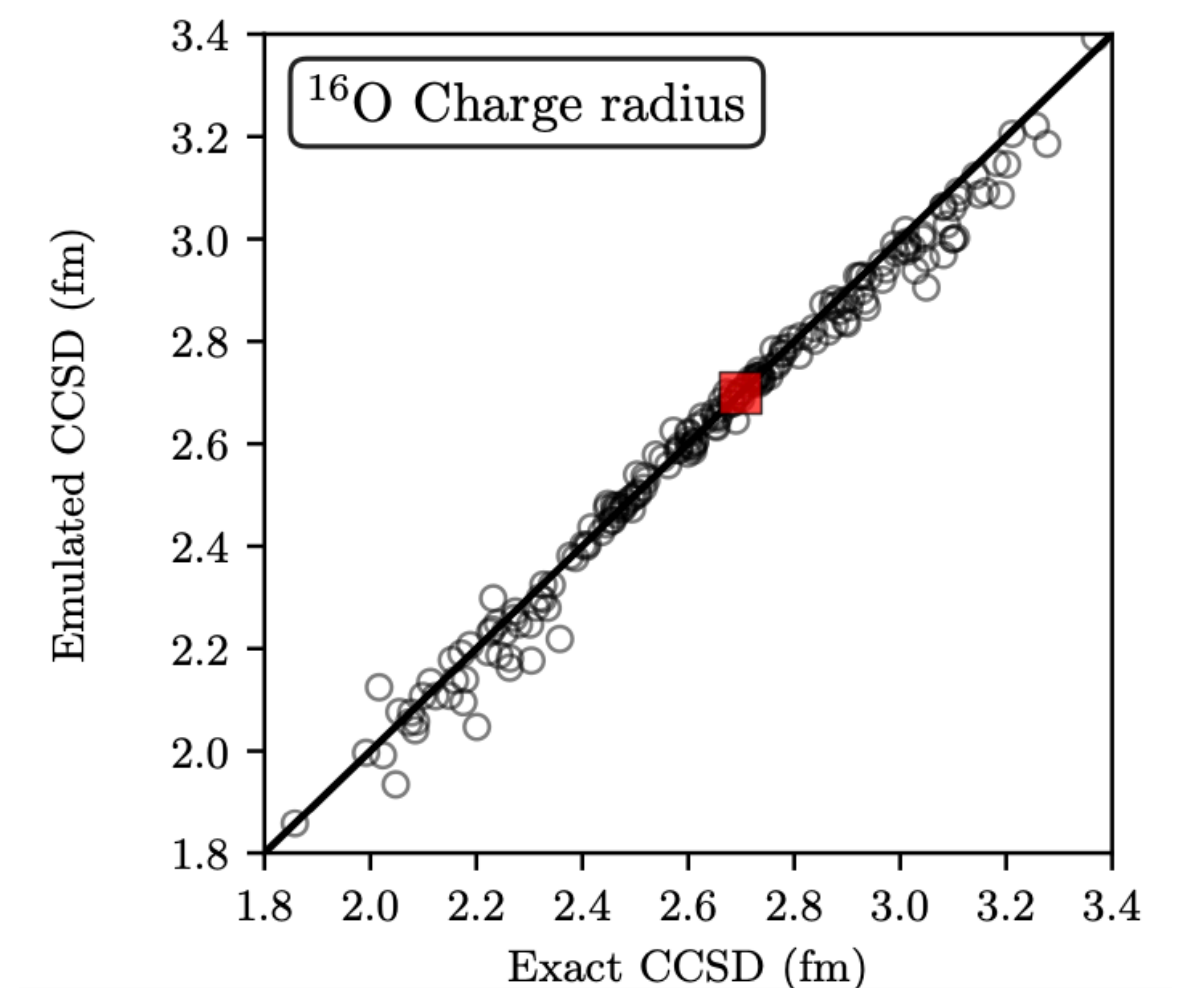
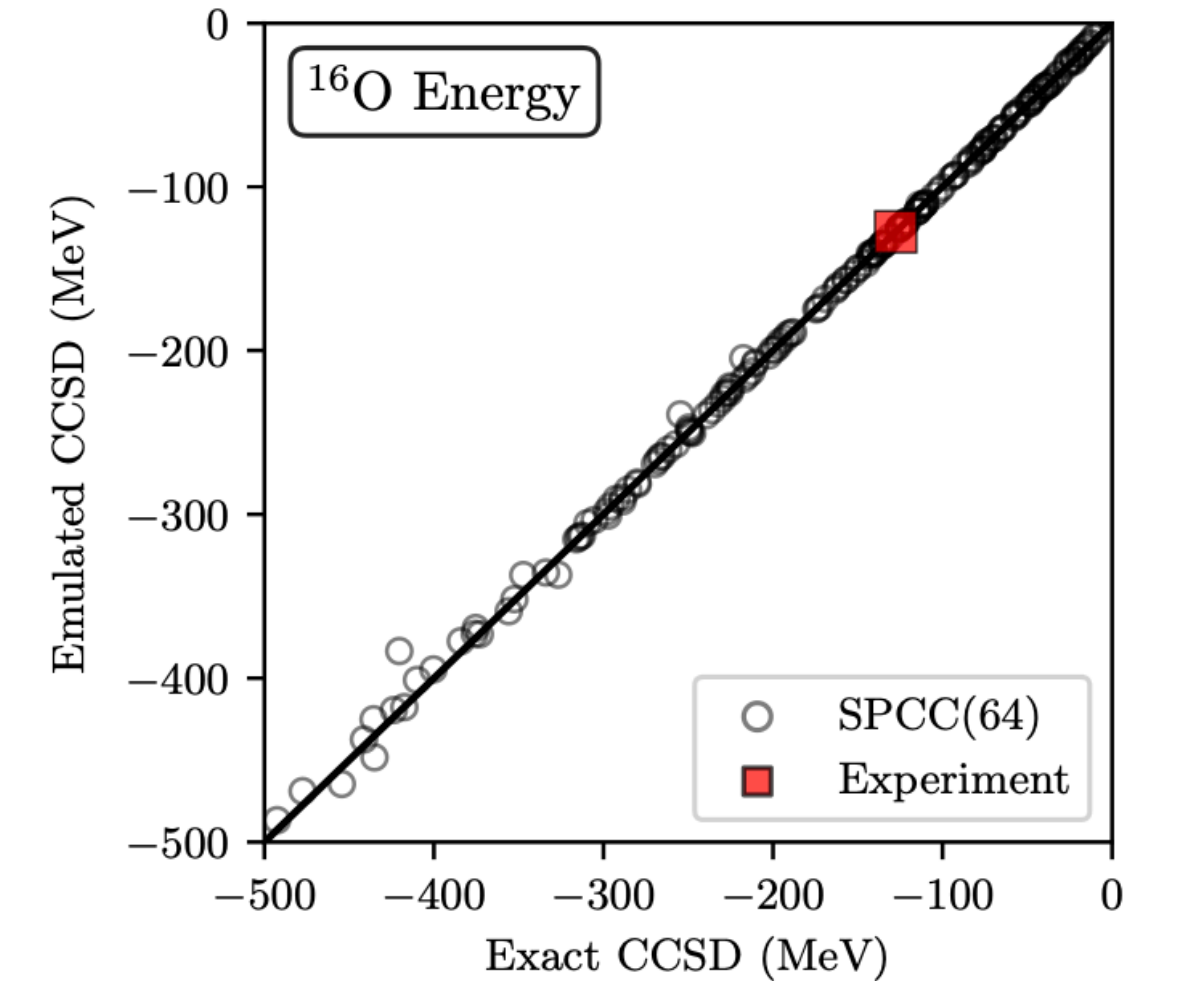
Projection (after orthonormalizing snapshots)



Emulation ($E \approx \tilde{E}$)

$$\tilde{H}(\theta) \quad \tilde{\beta} = \tilde{E} \tilde{N} \tilde{\beta}$$

c) All size- n_b operations



History matching: exploring the parameter space

Analyzing the first observation of ^{28}O

Explore the vast parameter space of χEFT using emulators and *history matching*.

$$M_i(\vec{\alpha}) = \widetilde{M}_i(\vec{\alpha}) + \varepsilon_{\text{emulator},i}$$

$$z_i = \widetilde{M}_i(\vec{\alpha}) + \varepsilon_{\text{exp},i} + \varepsilon_{\text{model},i} + \varepsilon_{\text{method},i} + \varepsilon_{\text{emulator},i}$$

Identify a region in 17-dimensional LEC-space of $\Delta\text{NNLO}(394)$ where the model reproduces seen (historical) data within specified uncertainties

$$I^2(\vec{\alpha}) = \max_{i \in \mathcal{Z}} \frac{|\widetilde{M}_i(\vec{\alpha}) - z_i|^2}{\text{Var}(\widetilde{M}_i(\vec{\alpha}) - z_i)}$$

LEC $\vec{\alpha}$ values with $I(\vec{\alpha}) > c = 3$ *implausible*, and reject them!

Target	z	ε_{exp}	$\varepsilon_{\text{model}}$	$\varepsilon_{\text{method}}$	$\varepsilon_{\text{emulator}}$
$E(^2\text{H})$	-2.2298	0.0	0.05	0.0005	0.001%
$r_p^2(^2\text{H})$	3.9030	0.0	0.02	0.0005	0.001%
$Q(^2\text{H})$	0.27	0.01	0.003	0.0005	0.001%
$E(^3\text{H})$	-8.4818	0.0	0.17	0.0005	0.005%
$E(^4\text{He})$	-28.2956	0.0	0.55	0.0005	0.005%
$r_p^2(^4\text{He})$	2.1176	0.0	0.045	0.0005	0.05%
$E(^{16}\text{O})$	127.62	0.0	0.75	1.5	0.5%
$r_p^2(^{16}\text{O})$	6.660	0.0	0.16	0.05	1%
$\Delta E(^{22,16}\text{O})$	-34.41	0.0	0.4	0.5	1%
$\Delta E(^{24,22}\text{O})$	-6.35	0.0	0.4	0.5	4%
$E_{2+}(^{24}\text{O})$	4.79	0.0	0.5	0.25	2%
$\Delta E(^{25,24}\text{O})$	0.77	0.02	0.4	0.25	—

History matching: exploring the parameter space

Analyzing the first observation of ^{28}O

Explore the vast parameter space of χEFT using emulators and *history matching*.

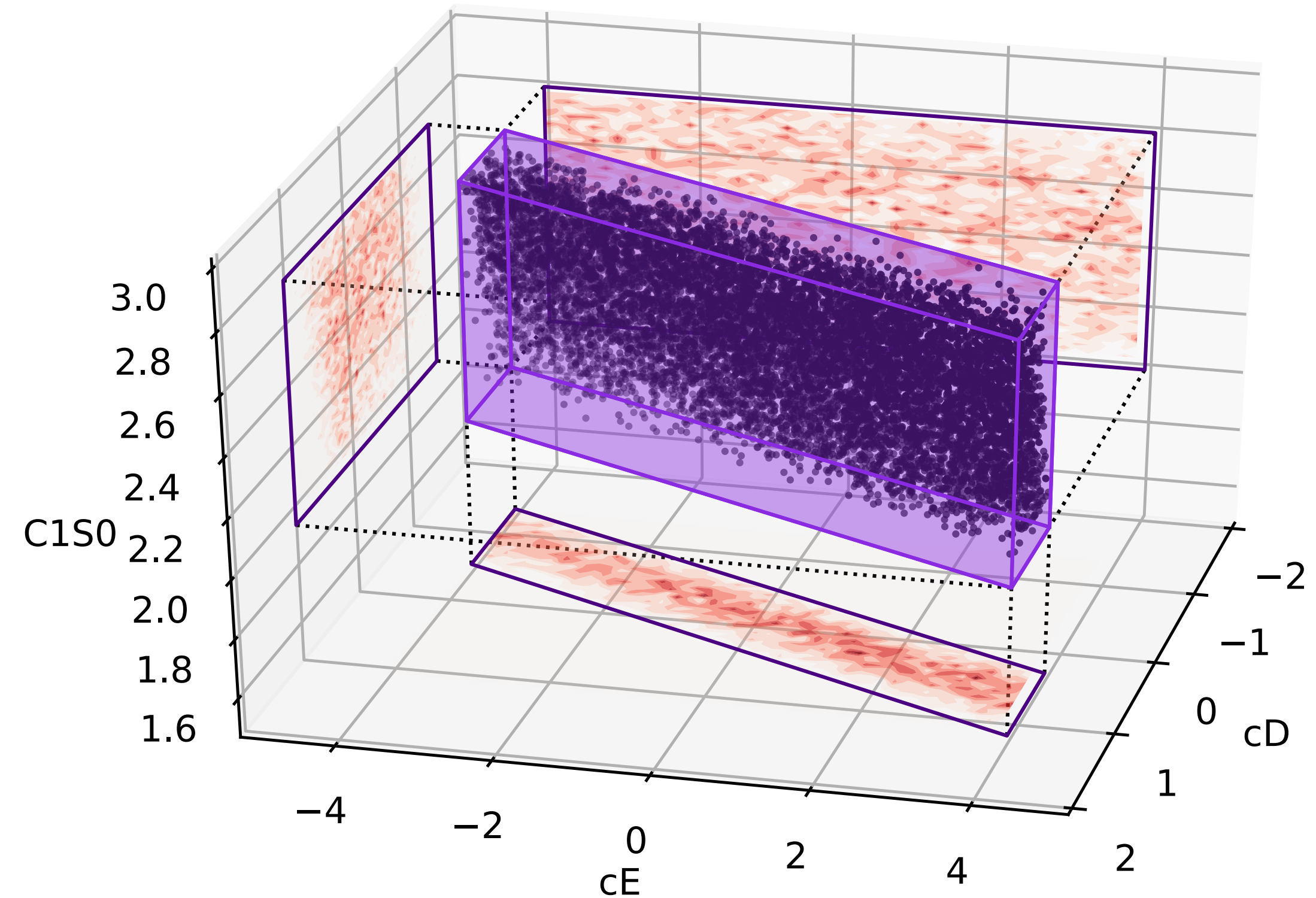
$$M_i(\vec{\alpha}) = \widetilde{M}_i(\vec{\alpha}) + \varepsilon_{\text{emulator},i}$$

$$z_i = \widetilde{M}_i(\vec{\alpha}) + \varepsilon_{\text{exp},i} + \varepsilon_{\text{model},i} + \varepsilon_{\text{method},i} + \varepsilon_{\text{emulator},i}$$

Identify a region in 17-dimensional LEC-space of $\Delta\text{NNLO}(394)$ where the model reproduces seen (historical) data within specified uncertainties

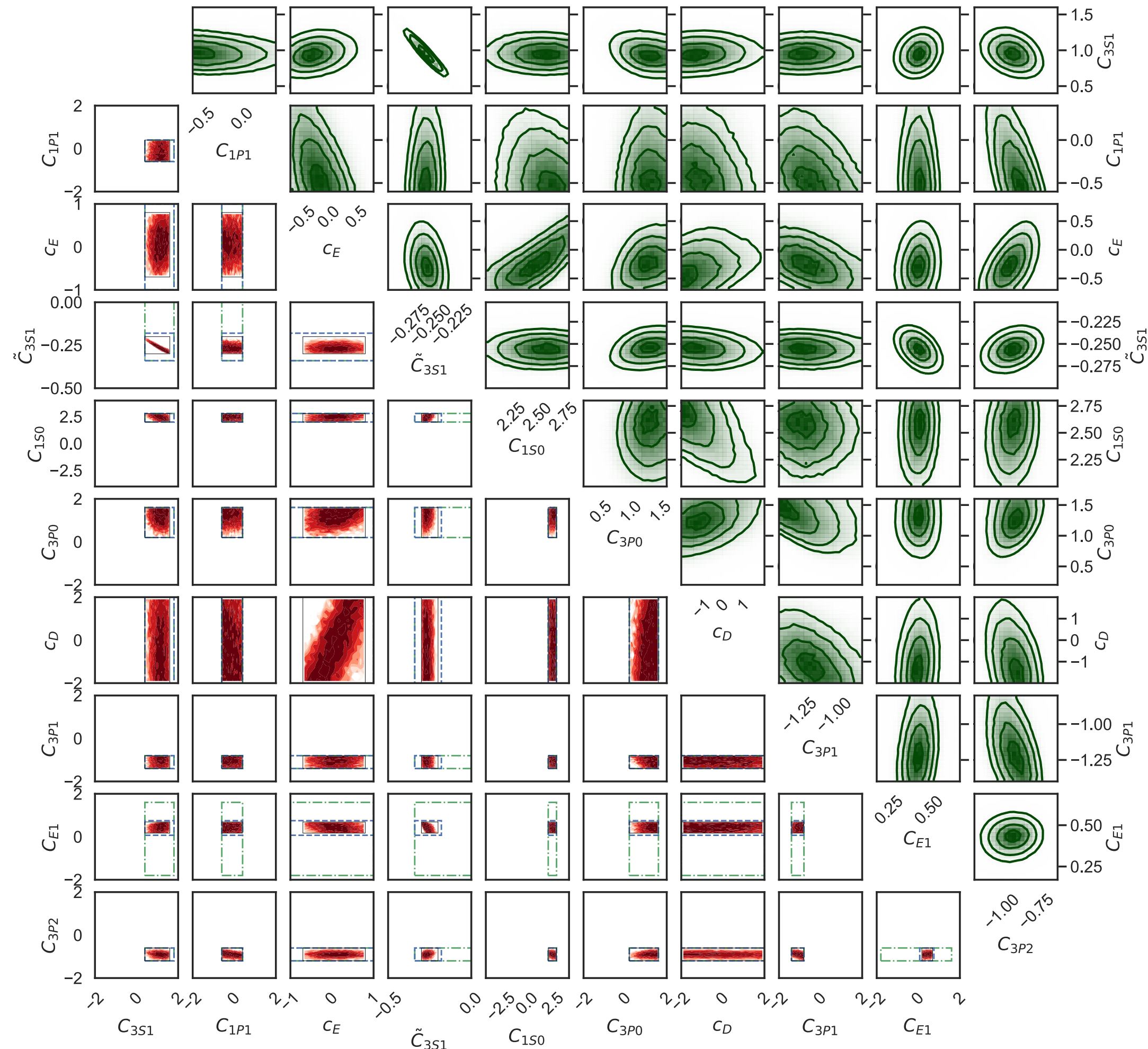
$$I^2(\vec{\alpha}) = \max_{i \in \mathcal{Z}} \frac{|\widetilde{M}_i(\vec{\alpha}) - z_i|^2}{\text{Var}(\widetilde{M}_i(\vec{\alpha}) - z_i)}$$

LEC $\vec{\alpha}$ values with $I(\vec{\alpha}) > c = 3$ *implausible*, and reject them!



Sampling the posterior predictive distribution

Bayesian posterior pdf



history matching

- **History matching** identifies the parameter region where we expect the LEC posterior distribution to reside.
- **MCMC + emulators** to draw 10^8 samples of the LEC posterior at ΔNNLO with $\text{NN}+3\text{N}$ interaction.

$$p(\vec{\alpha}|A = 2 - 24)$$

- We assume uniform prior + uncorrelated normal likelihood
- Informative to update the parameter posterior with $\Delta E(25\text{O}, 24\text{O})$. Subsequently draw 121 parameter samples that we employ in our prediction of oxygen-27/28.

$$\vec{\alpha} \sim p(\vec{\alpha}|A = 2 - 25)$$

PPD for complex nuclei

^{28}O separation energies

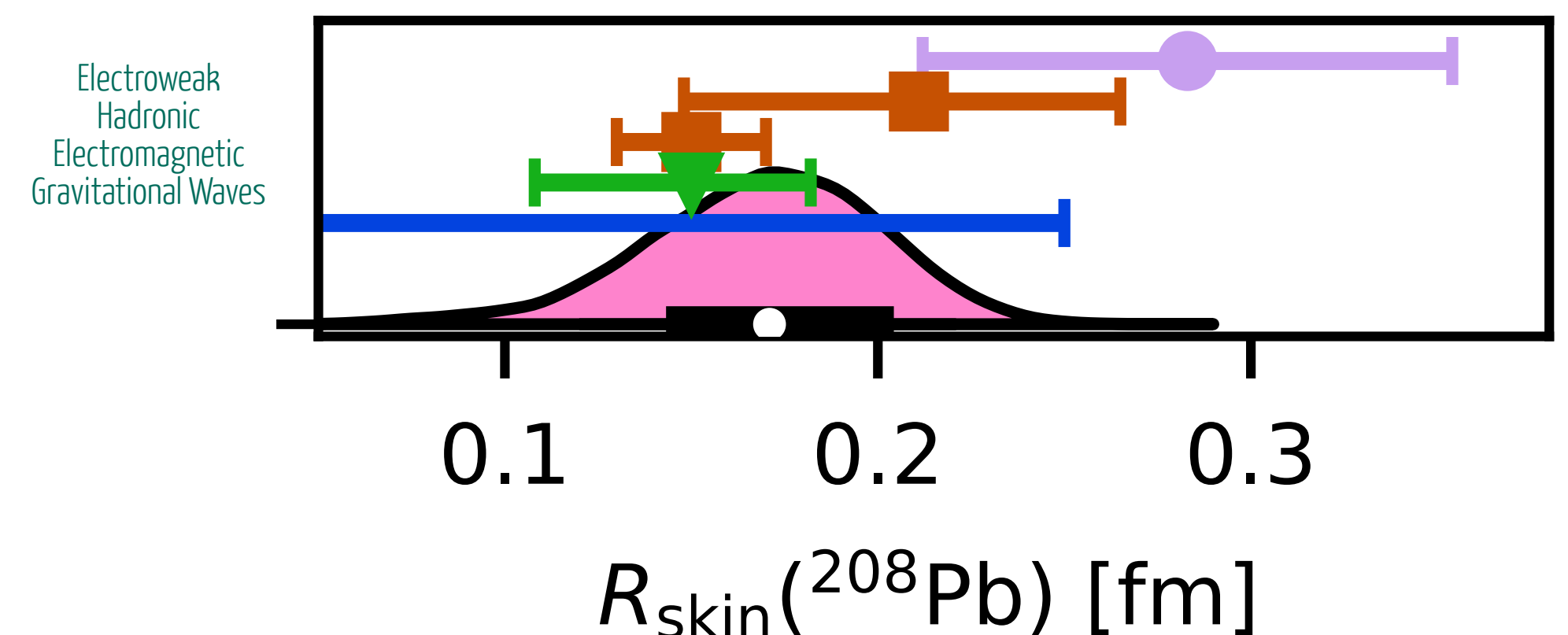
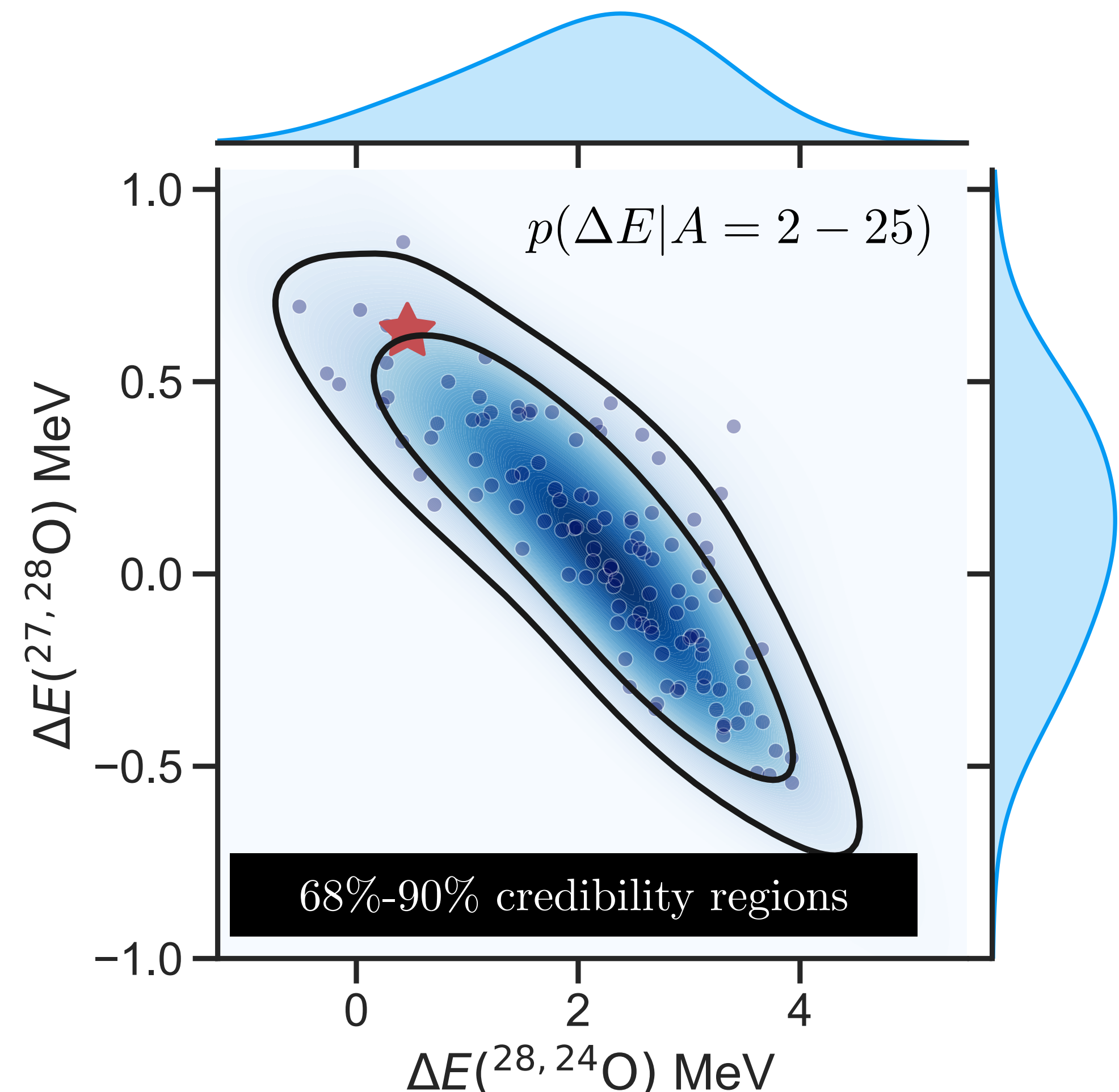
- We claim with 98% certainty that ^{28}O is unbound with respect to ^{24}O :
- The experimental data point (red star) is away from the posterior maximum. This suggests that only a few finely-tuned chiral interactions are able to reproduce low-energy and exotic oxygen structure Y. Kondo et al. Nature (2023)

^{208}Pb neutron skin-thickness

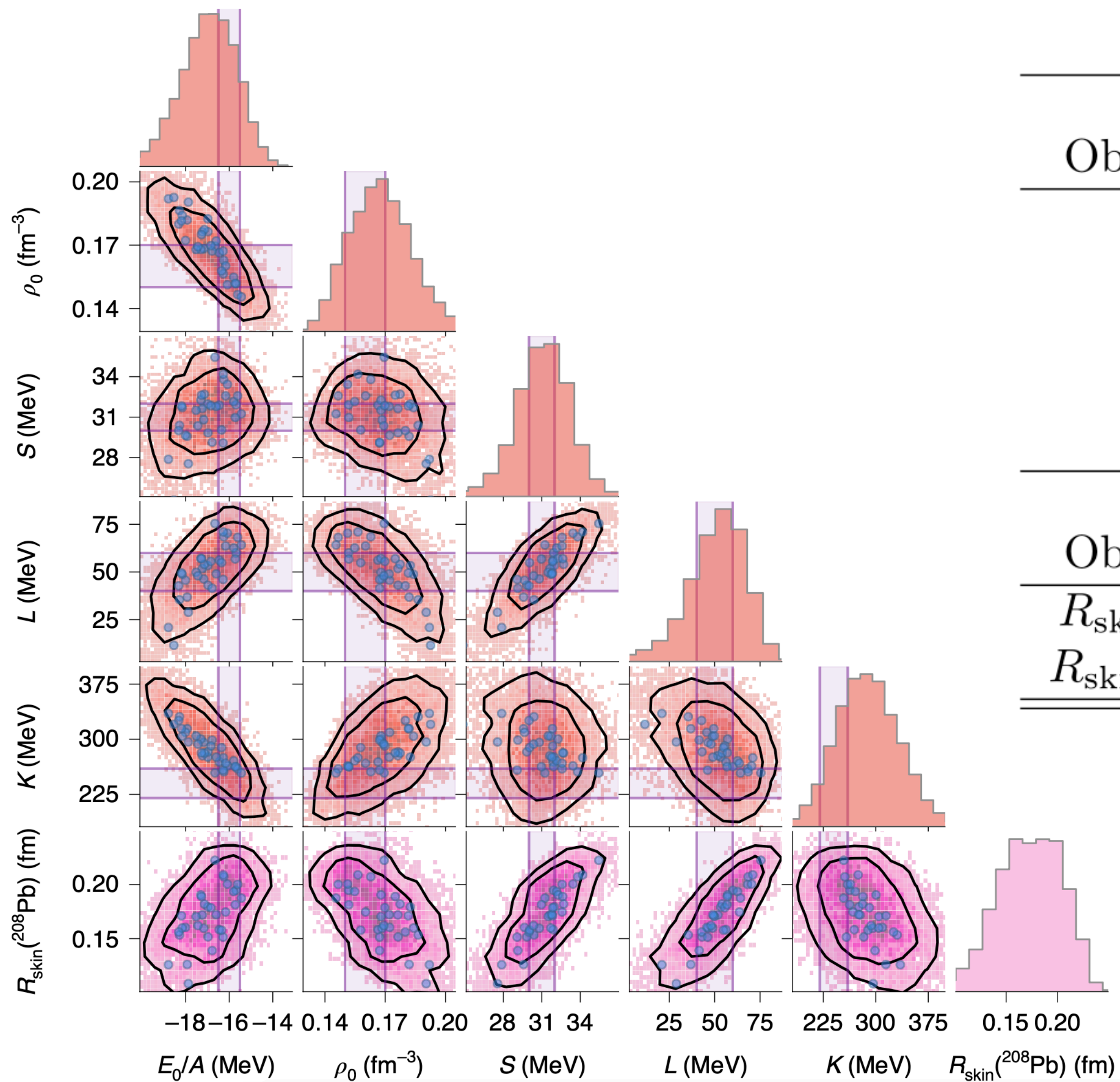
n.b. similarly curated history matching data

- We predict a small skin thickness 0.14-0.20 fm in mild (1.5σ) tension with electroweak (PREX) measurement.

B. Hu et al Nature Physics (2022)



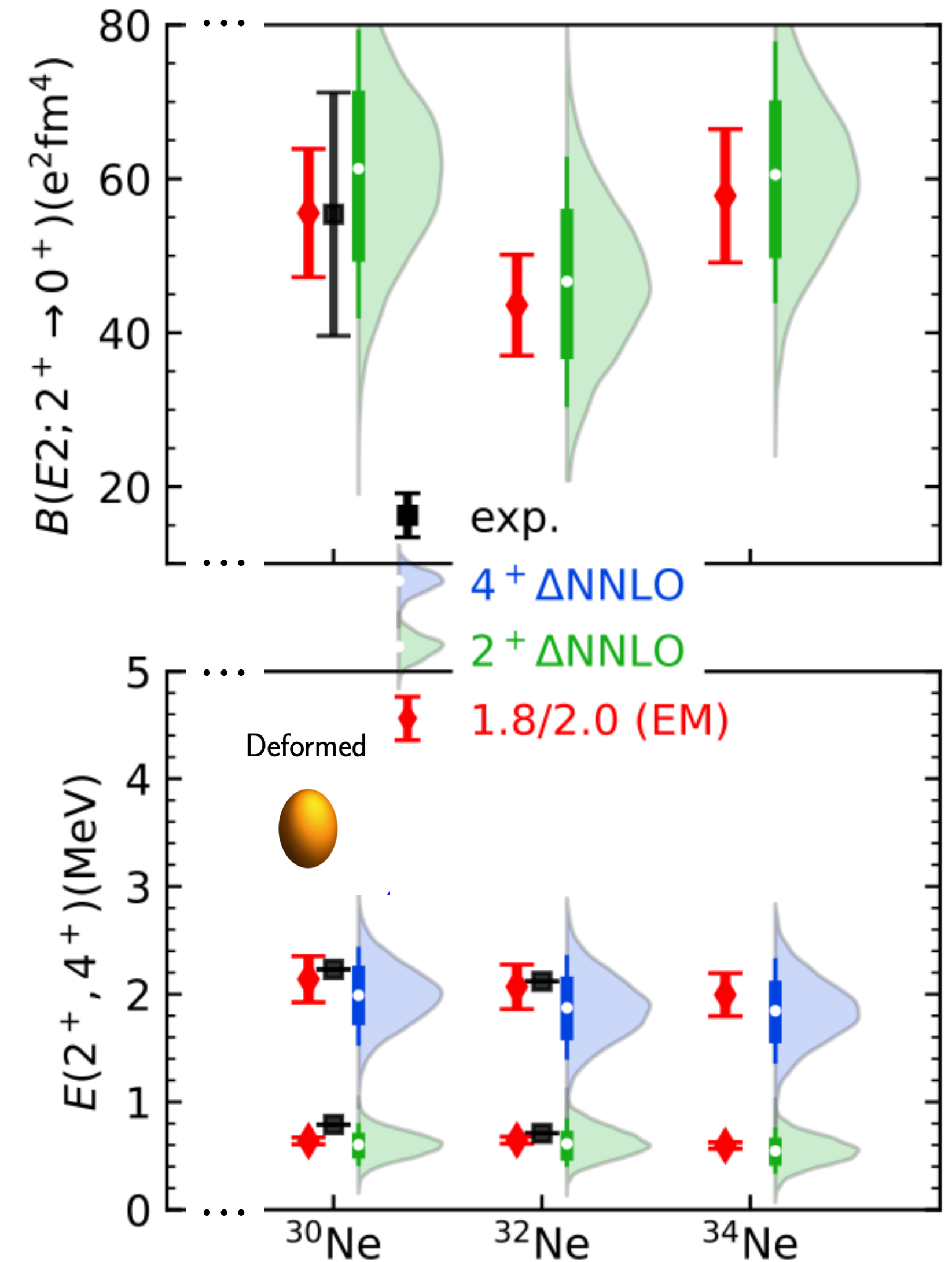
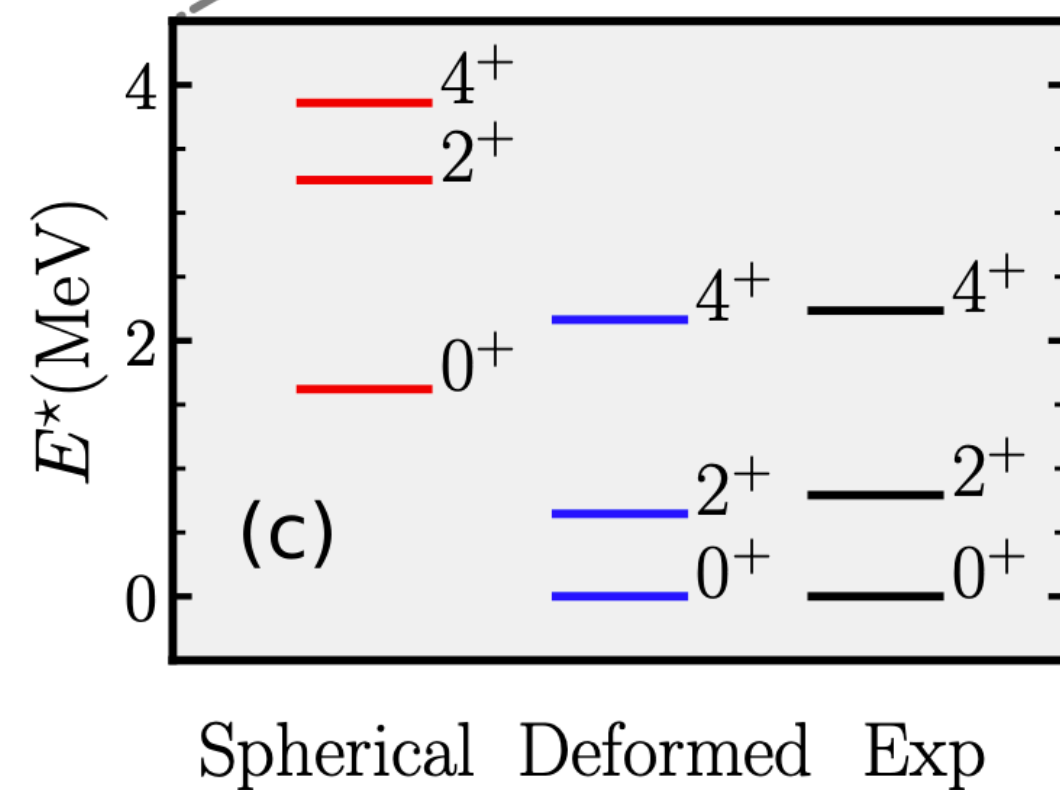
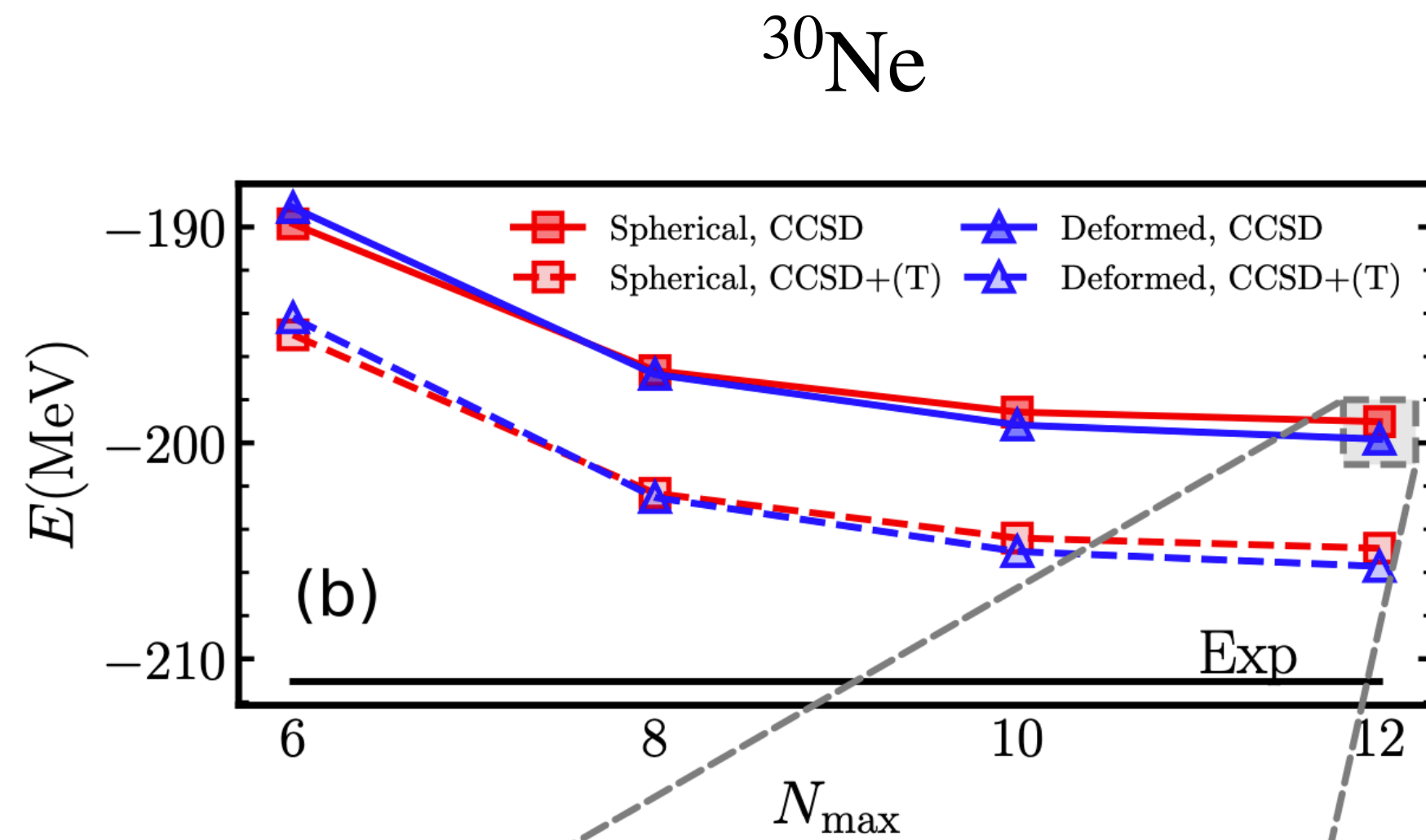
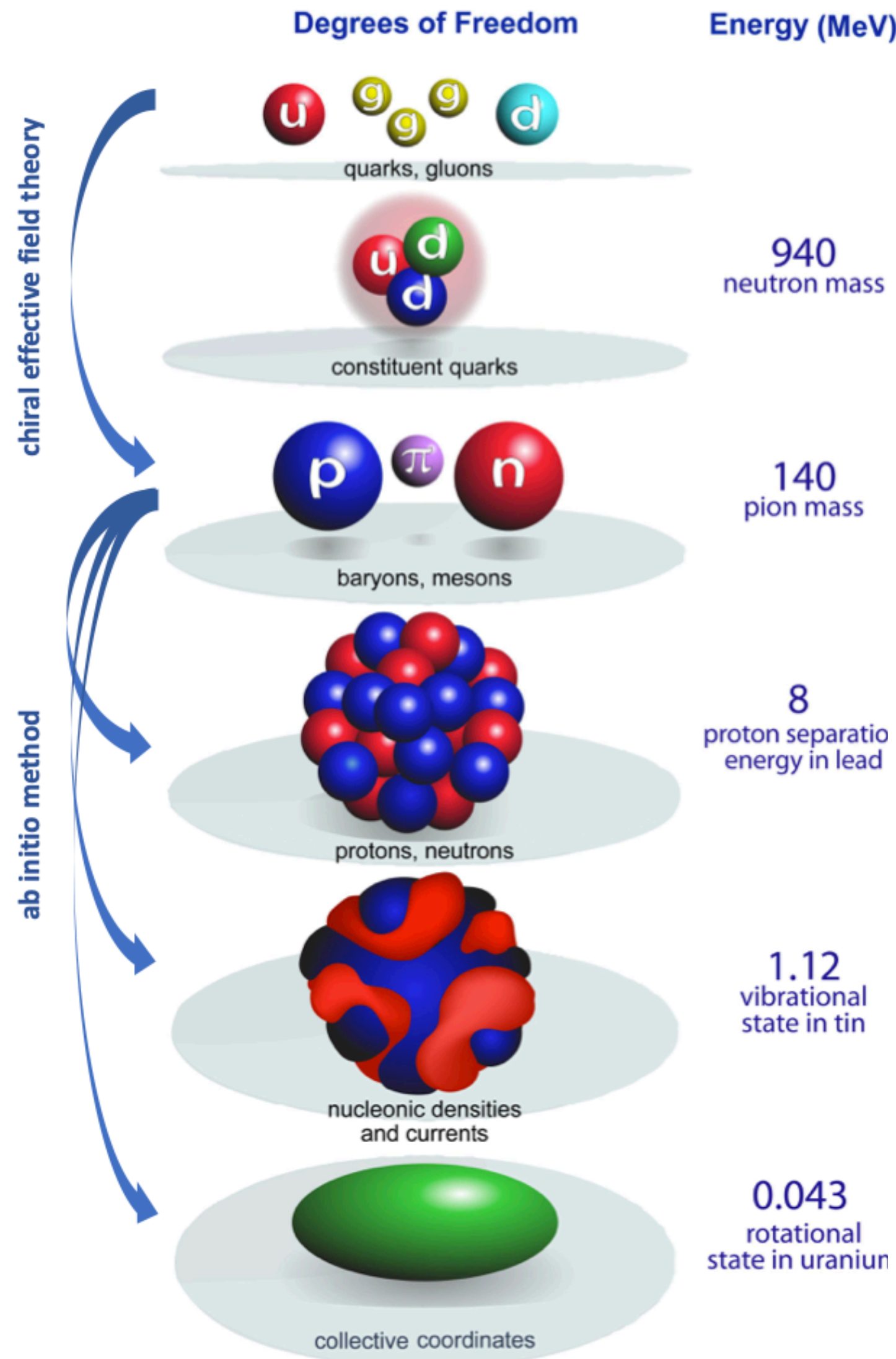
PPD skin thickness and nuclear matter at saturation



Nuclear matter properties			
Observable	median	68% CR	90% CR
E_0/A	-16.9	[-17.9, -15.4]	[-19.1, -14.9]
ρ_0	0.167	[0.150, 0.181]	[0.142, 0.194]
S	31.1	[29.1, 33.2]	[27.6, 34.6]
L	52.7	[38.3, 68.5]	[23.9, 76.2]
K	287	[242, 331]	[216, 362]
Neutron skins			
Observable	median	68% CR	90% CR
$R_{\text{skin}}(^{48}\text{Ca})$	0.164	[0.141, 0.187]	[0.123, 0.199]
$R_{\text{skin}}(^{208}\text{Pb})$	0.171	[0.139, 0.200]	[0.120, 0.221]

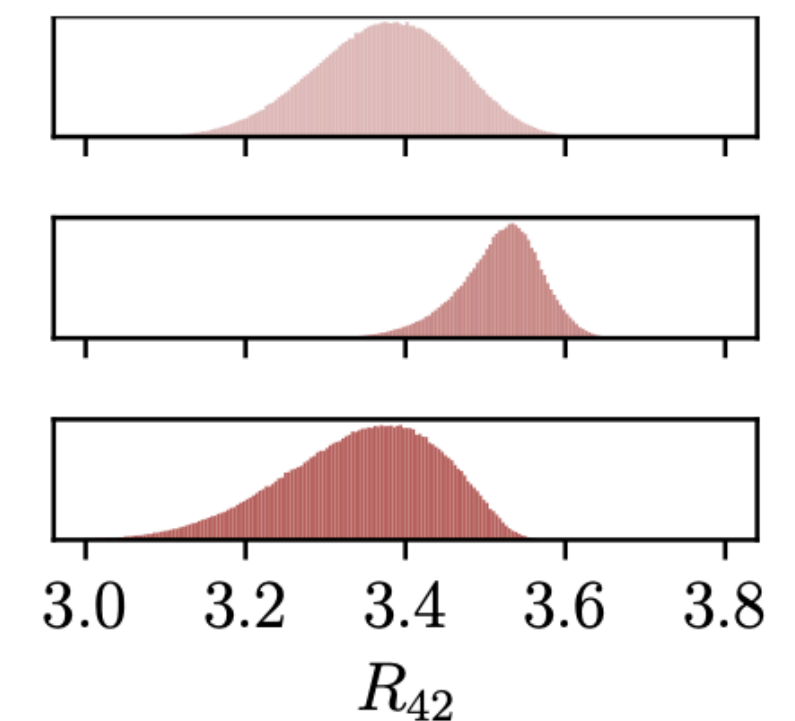
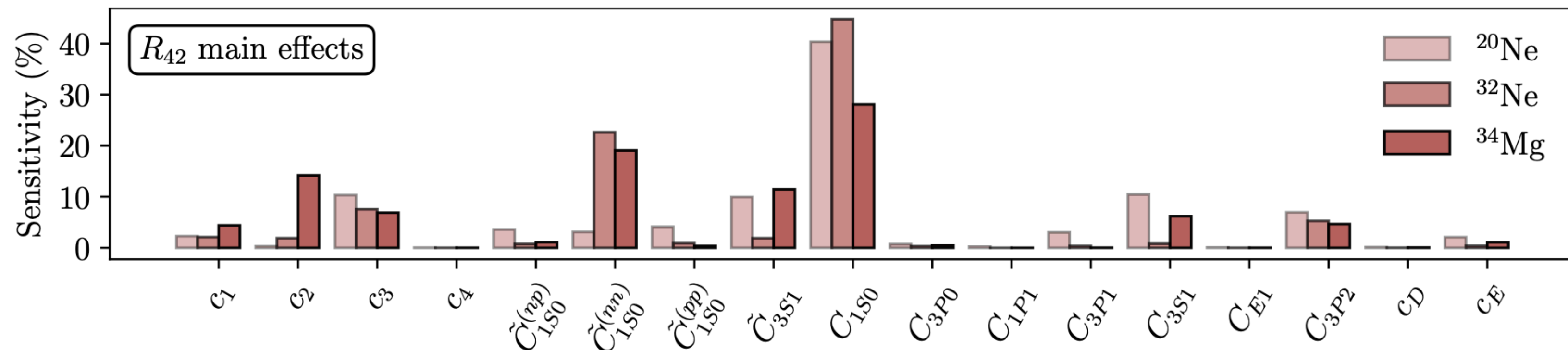
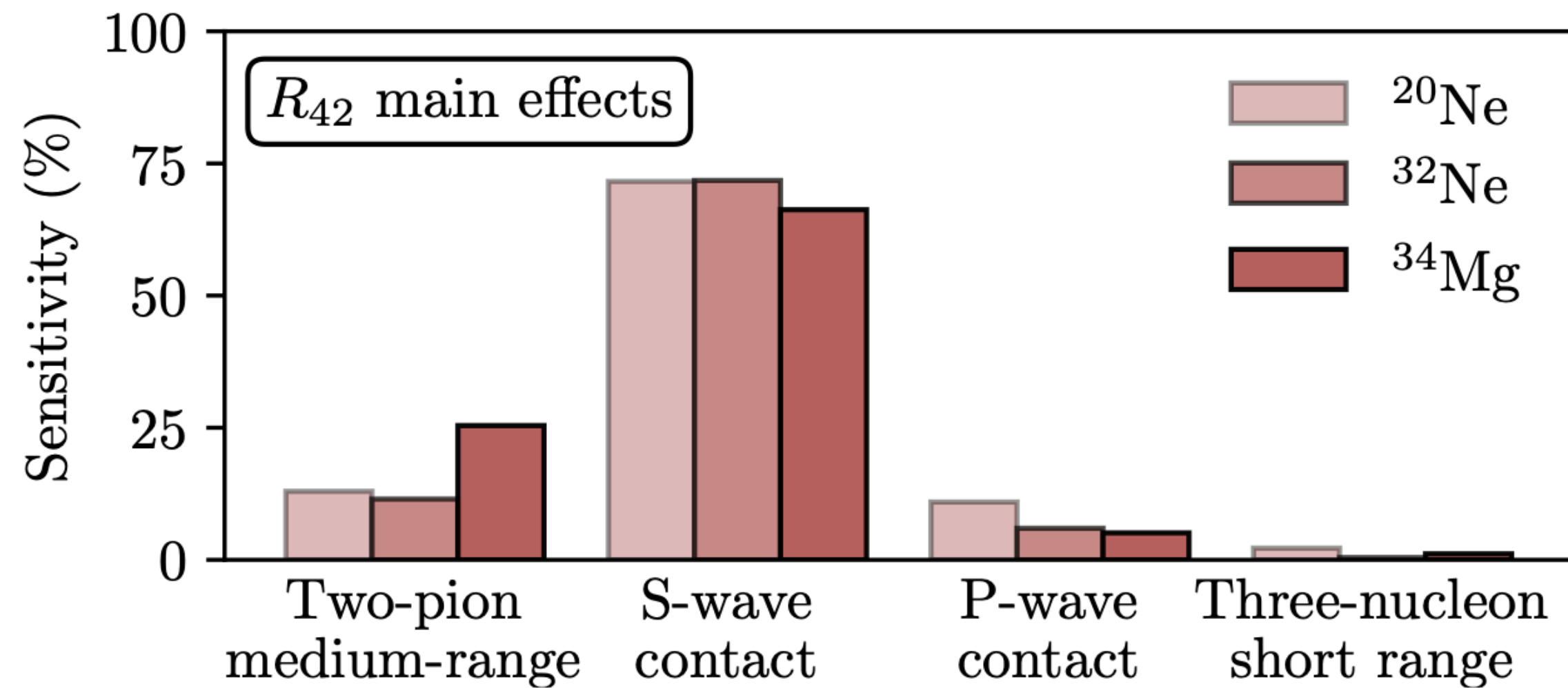
Ab initio theory reveals correlations, e.g., between L and R_{skin} previously indicated in mean-field models

Multiscale physics of atomic nuclei from first principles



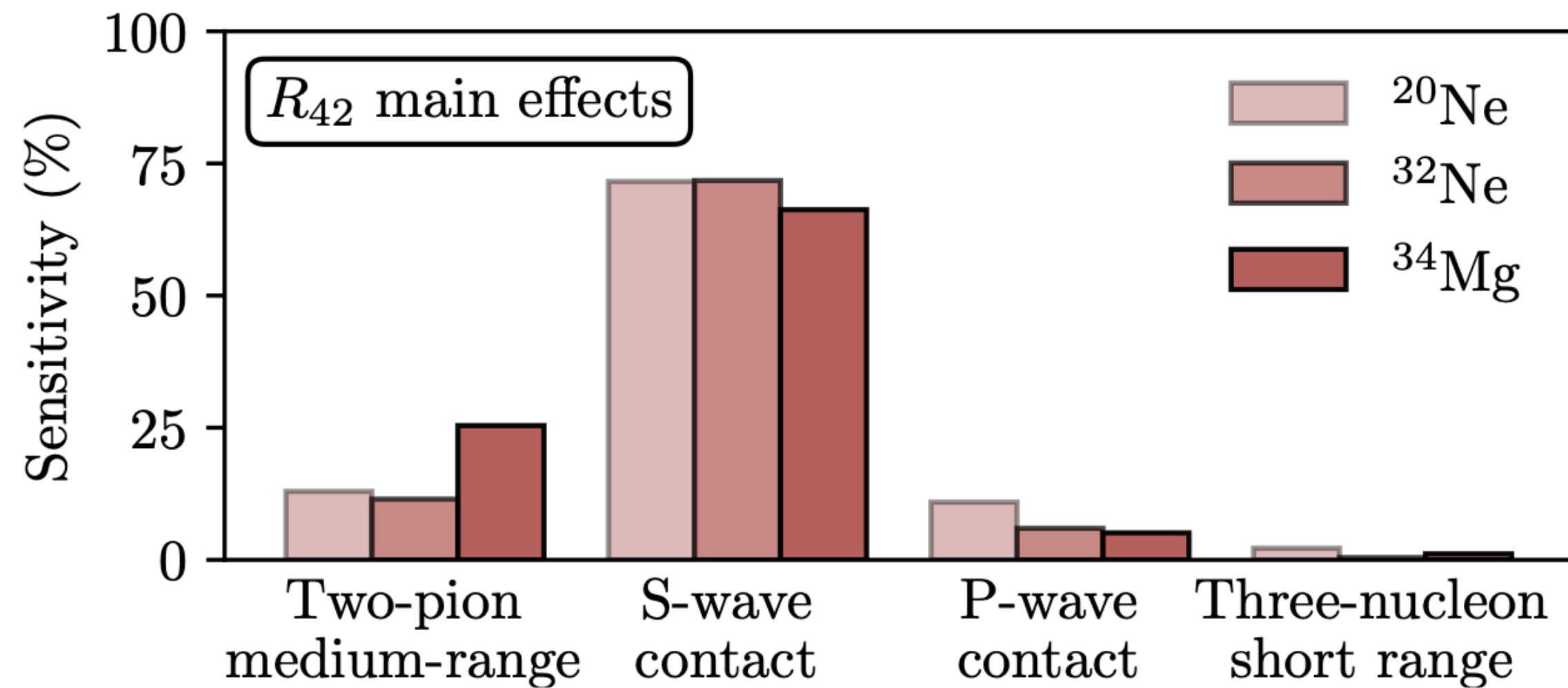
Quantifying sensitivities

What drives nuclear deformation in χ EFT?

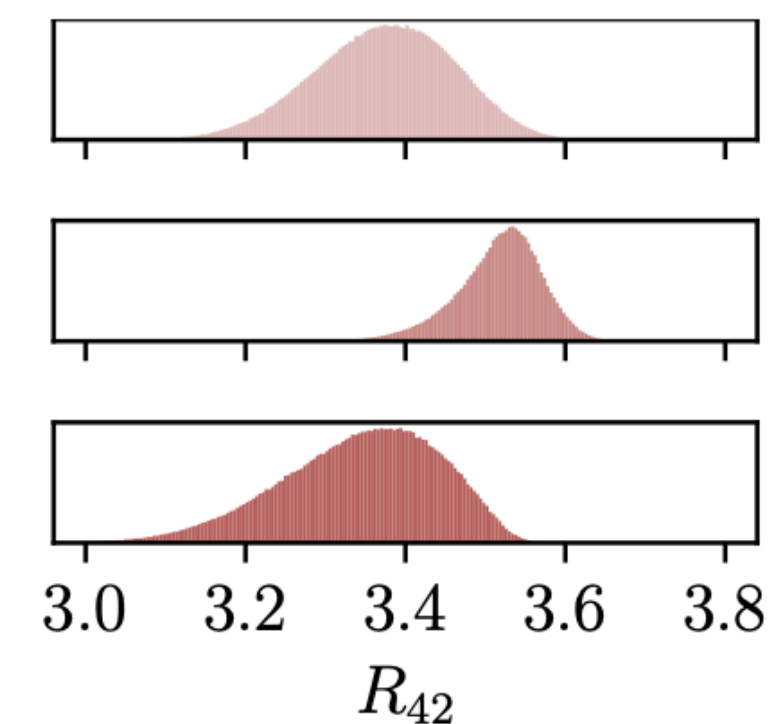
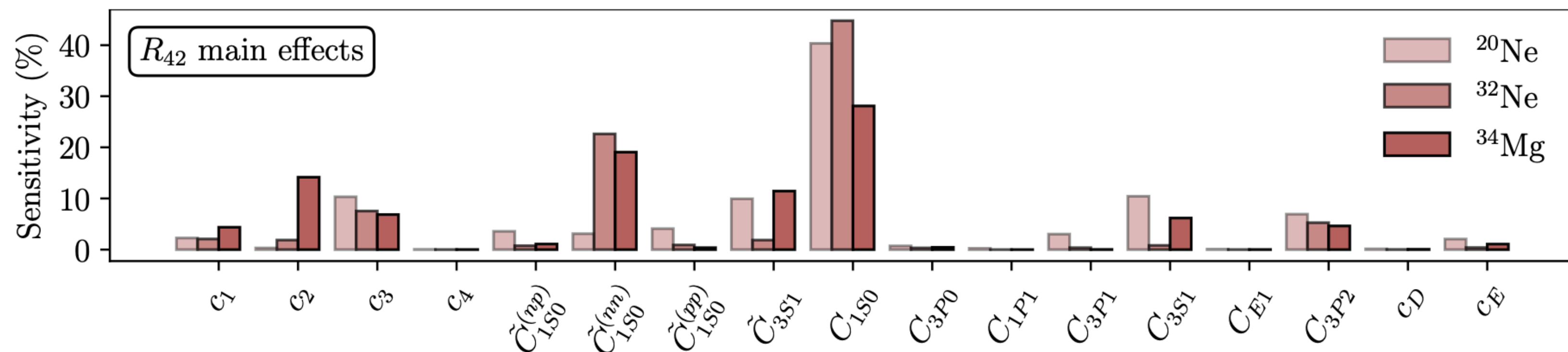


Quantifying sensitivities

What drives nuclear deformation in χ EFT?



Challenge: account for correlated LEC pdf and more complex domains for the variance integrals



RG-invariant χ EFT: proposal by Long & Yang

non-perturbative one-pion-exchange

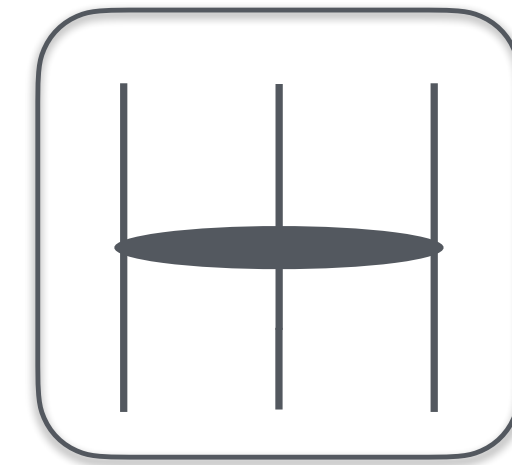
${}^3S_0, {}^3S_1 - {}^3D_1, {}^3P_{0,1}, {}^3P_2 - {}^3F_2, {}^1P_1$

amplitude expanded in (Q/Λ_χ)



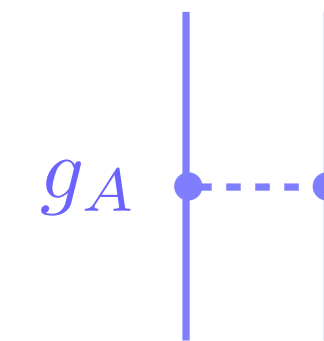
perturbative contributions

LO g_A  $C_{1S_0}, C_{3S_1}, D_{3P_0}, D_{3P_2}$



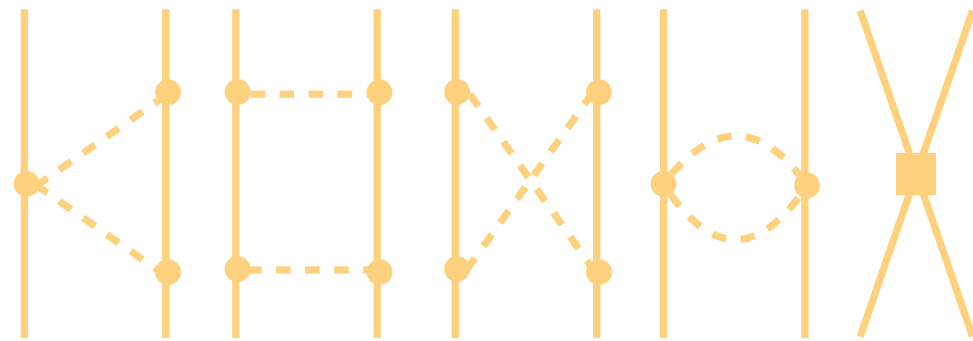
promote?

All other partial waves



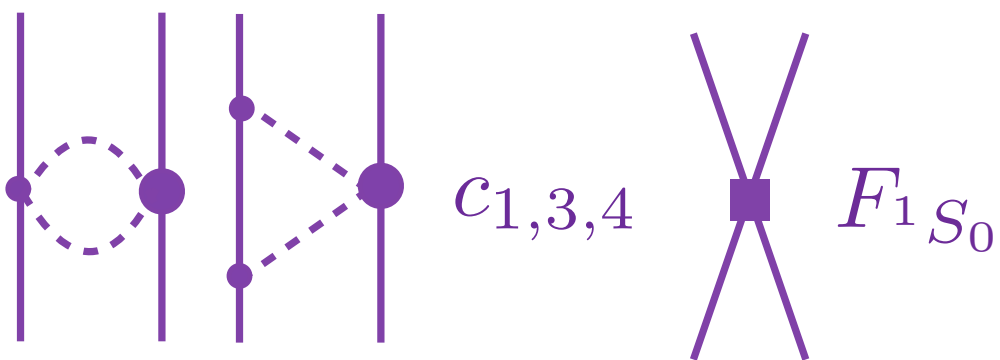
NLO  D_{1S_0}

N²LO

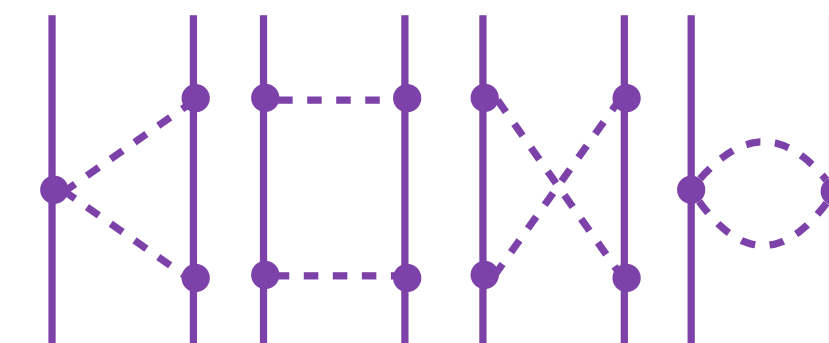


$E_{1S_0}, D_{3S_1}, D_{3S_1} - {}^3D_1, D_{1P_1},$
 $D_{3P_1}, E_{3P_0}, E_{3P_2}, E_{3P_2} - {}^3F_2$

N³LO



$c_{1,3,4}$ F_{1S_0}



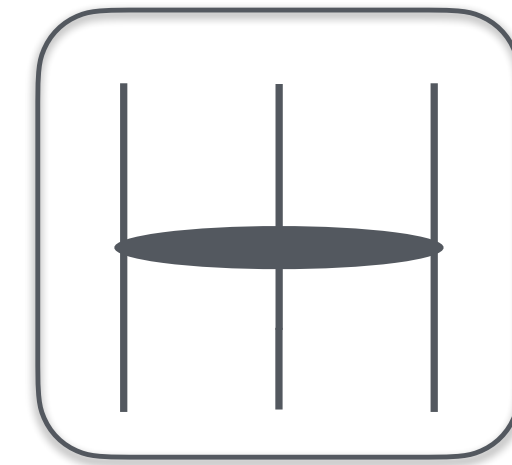
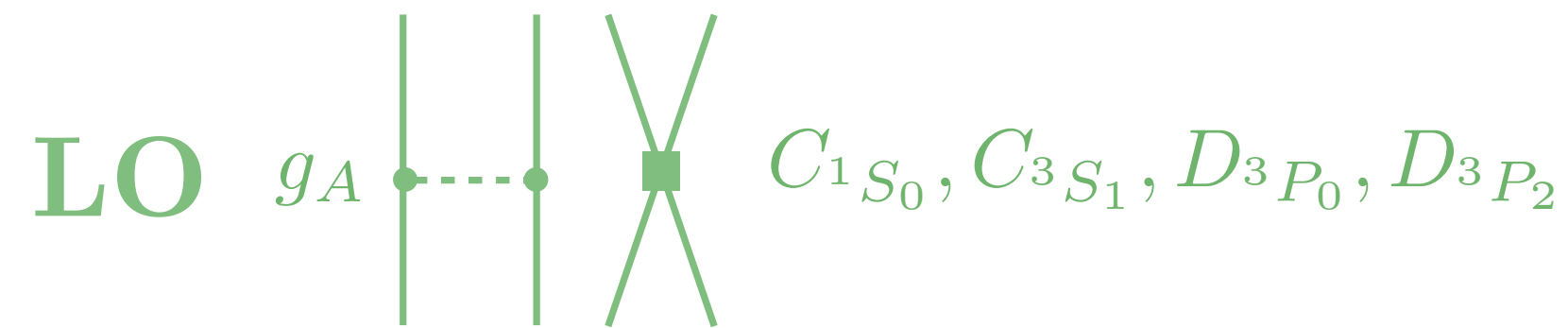
Several other RG-invariant PCs exist: Kolck, Kaplan, Savage, Wise, Long, Valderrama, Griesshammer, Yang, Birse, Arriola, Phillips, ...

RG-invariant χ EFT: proposal by Long & Yang

non-perturbative one-pion-exchange

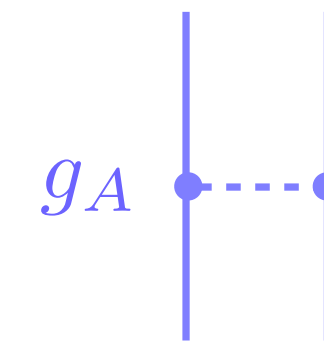
Challenge: analyze RG-invariance for $A \gtrsim 3$ systems

${}^3S_0, {}^3S_1 - {}^3D_1, {}^3P_{0,1}, {}^3P_2 - {}^3F_2, {}^1P_1$

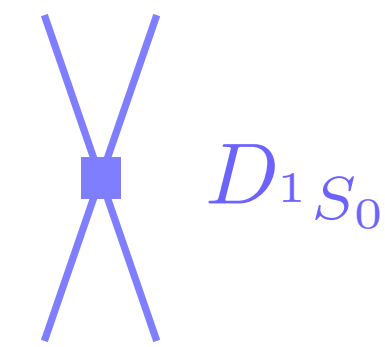


promote?

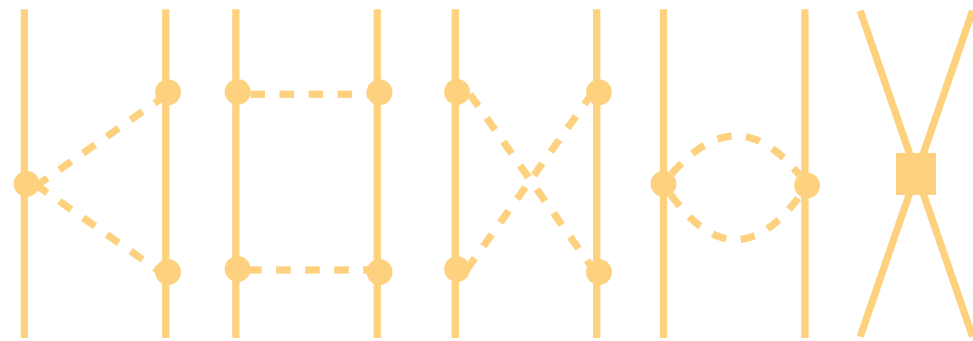
All other partial waves



NLO

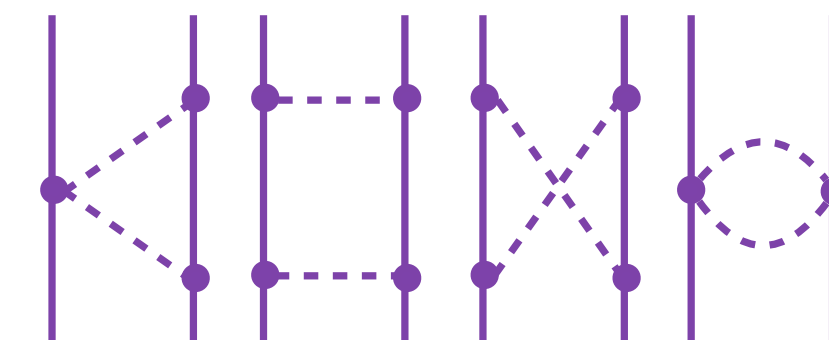
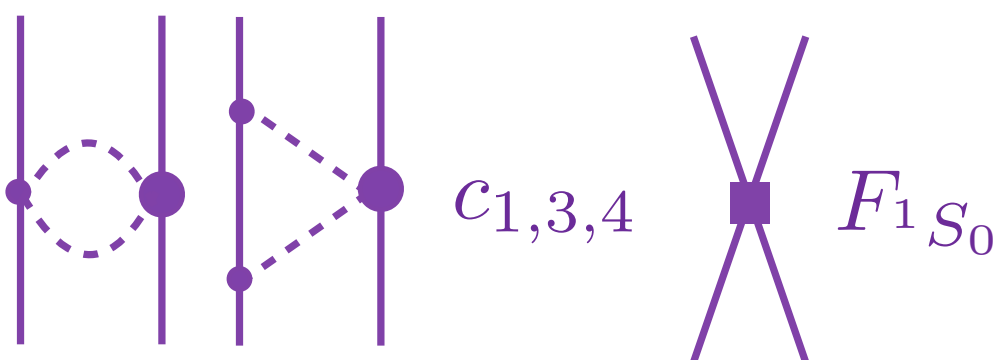


N²LO



$E_1S_0, D_3S_1, D_3S_1 - {}^3D_1, D_1P_1, D_3P_1, E_3P_0, E_3P_2, E_3P_2 - {}^3F_2$

N³LO



Several other RG-invariant PCs exist: Kolck, Kaplan, Savage, Wise, Long, Valderrama, Griesshammer, Yang, Birse, Arriola, Phillips, ...

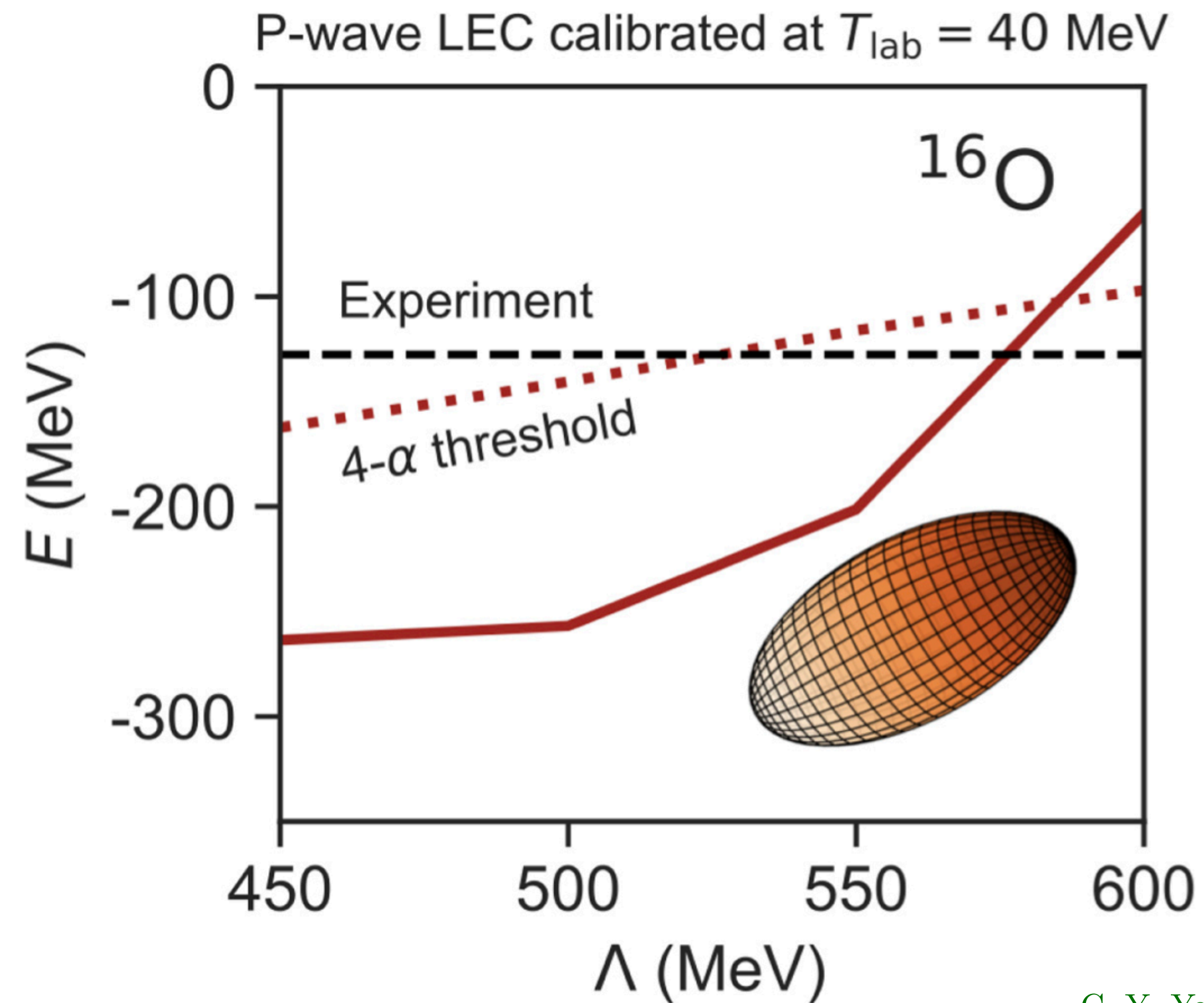
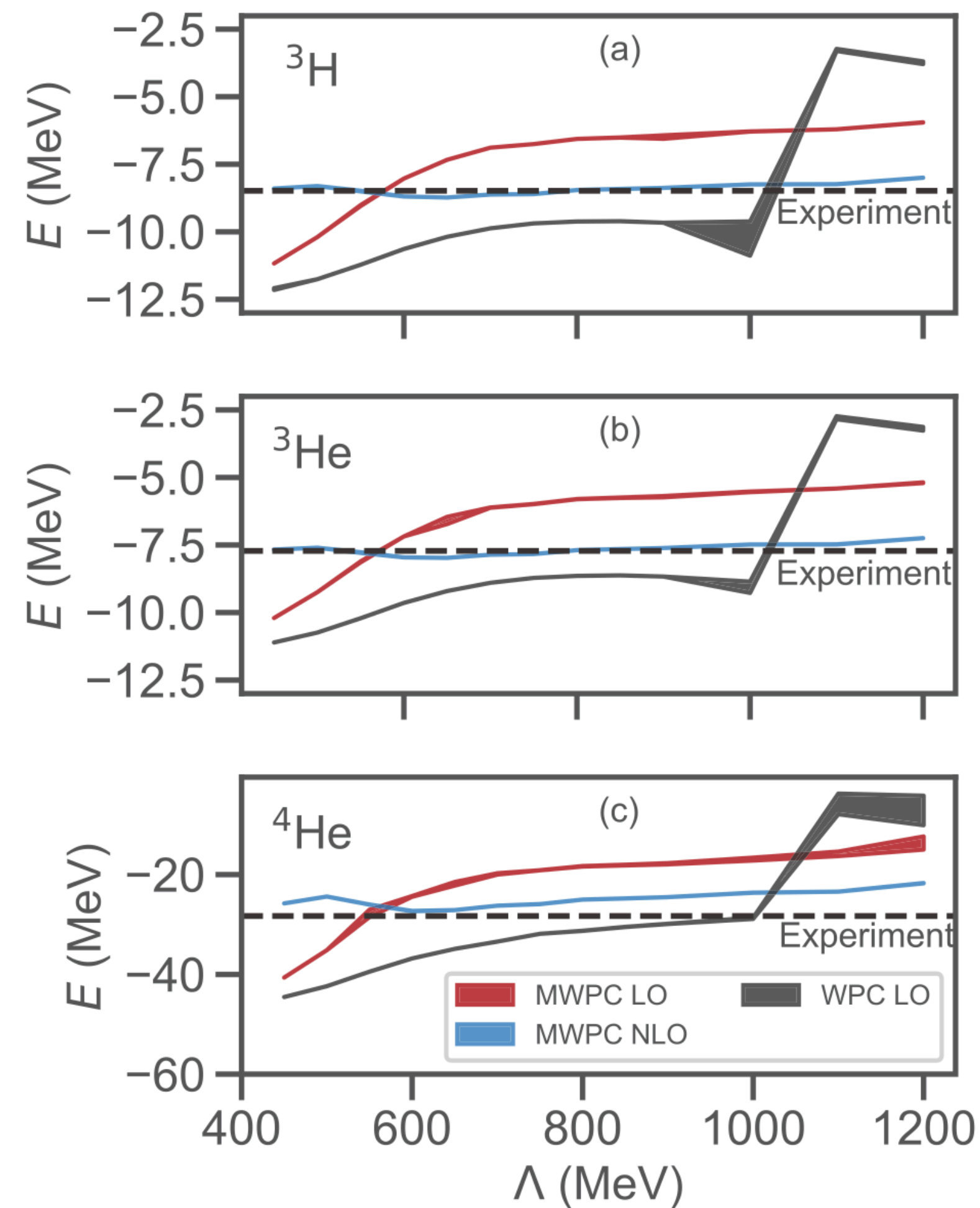
amplitude expanded in (Q/Λ_χ)

perturbative contributions



Problems at leading order in χ EFT

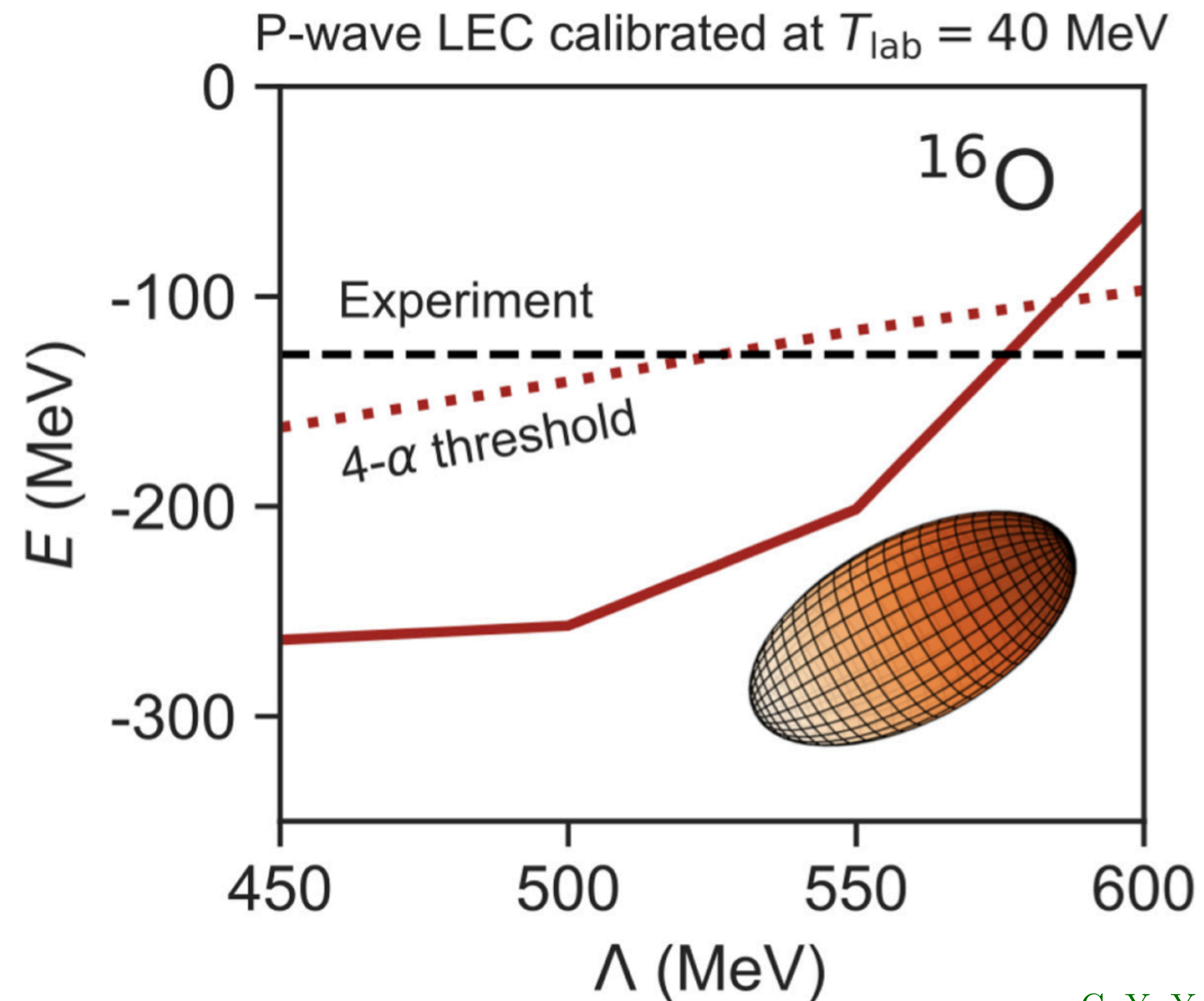
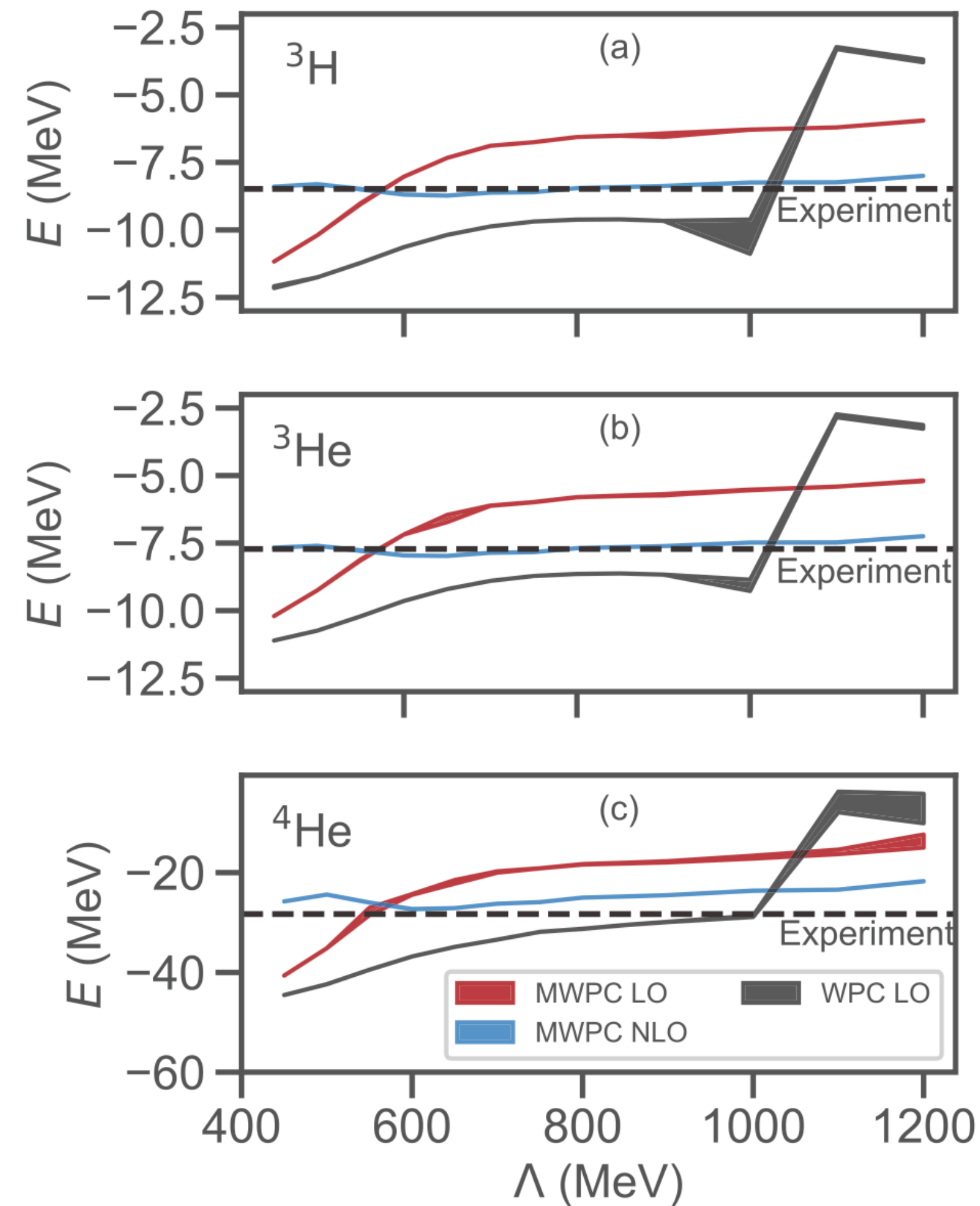
Atomic nuclei with $A > 4$ unstable



Problems at leading order in χ EFT

Atomic nuclei with $A > 4$ unstable

Challenge: possible fine tuning effects?
flawed power counting?



A possible solution?

Combinatorial enhancement of many-body forces

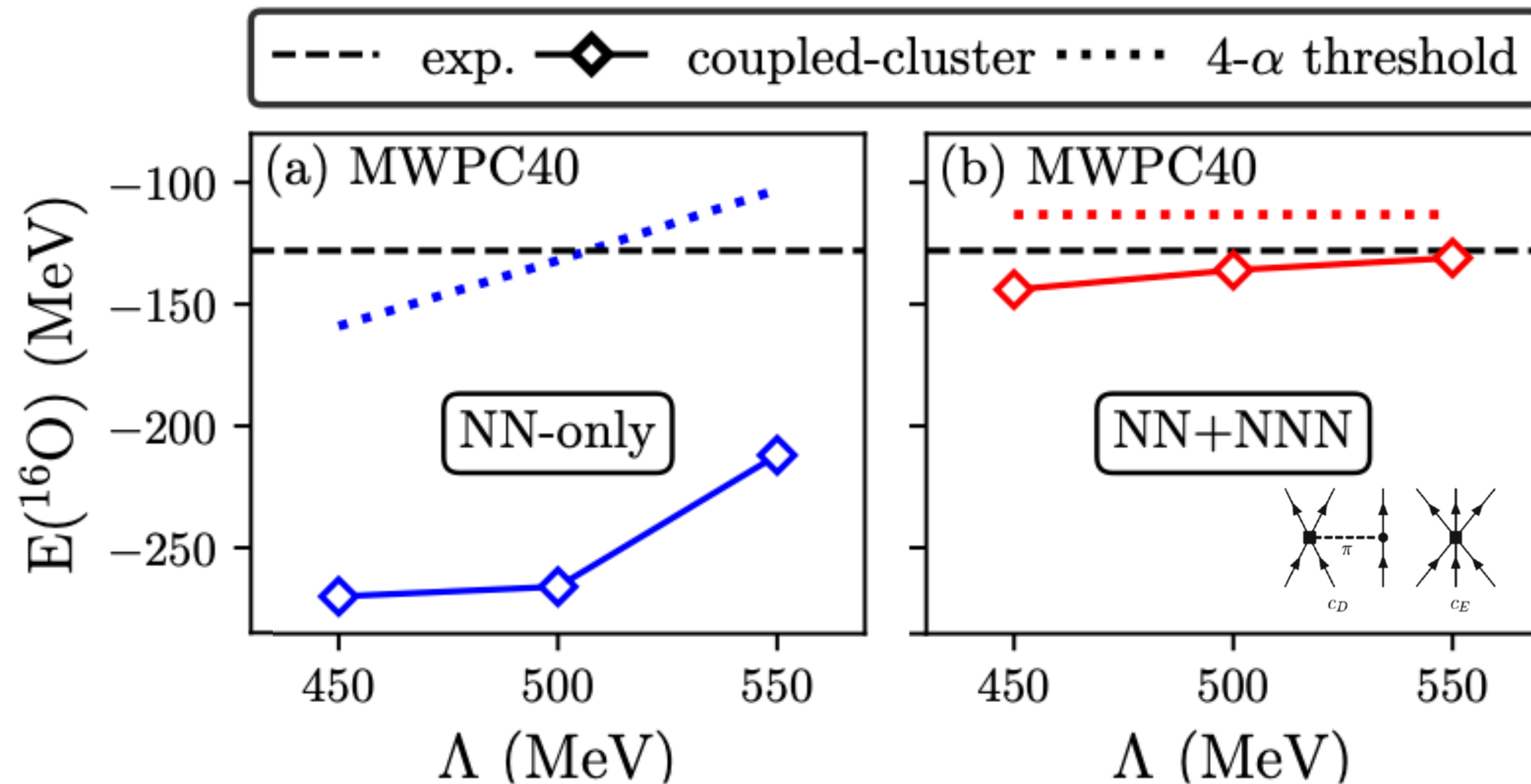


Table 1 Binding energy per nucleon (B_A/A) obtained with NN-only and NN+NNN interactions at LO. Here MWPC40 and $\Lambda=450$ MeV is adopted

B_A/A	^3H	^4He	^{16}O	^{40}Ca
NN-only	3.3	8	17.5	31.6
NN+NNN	3.3	8	8.2	9.4

A possible solution?

Combinatorial enhancement of many-body forces

Challenge: explore enhanced importance of 3-body forces for increasing mass number and quantify uncertainties

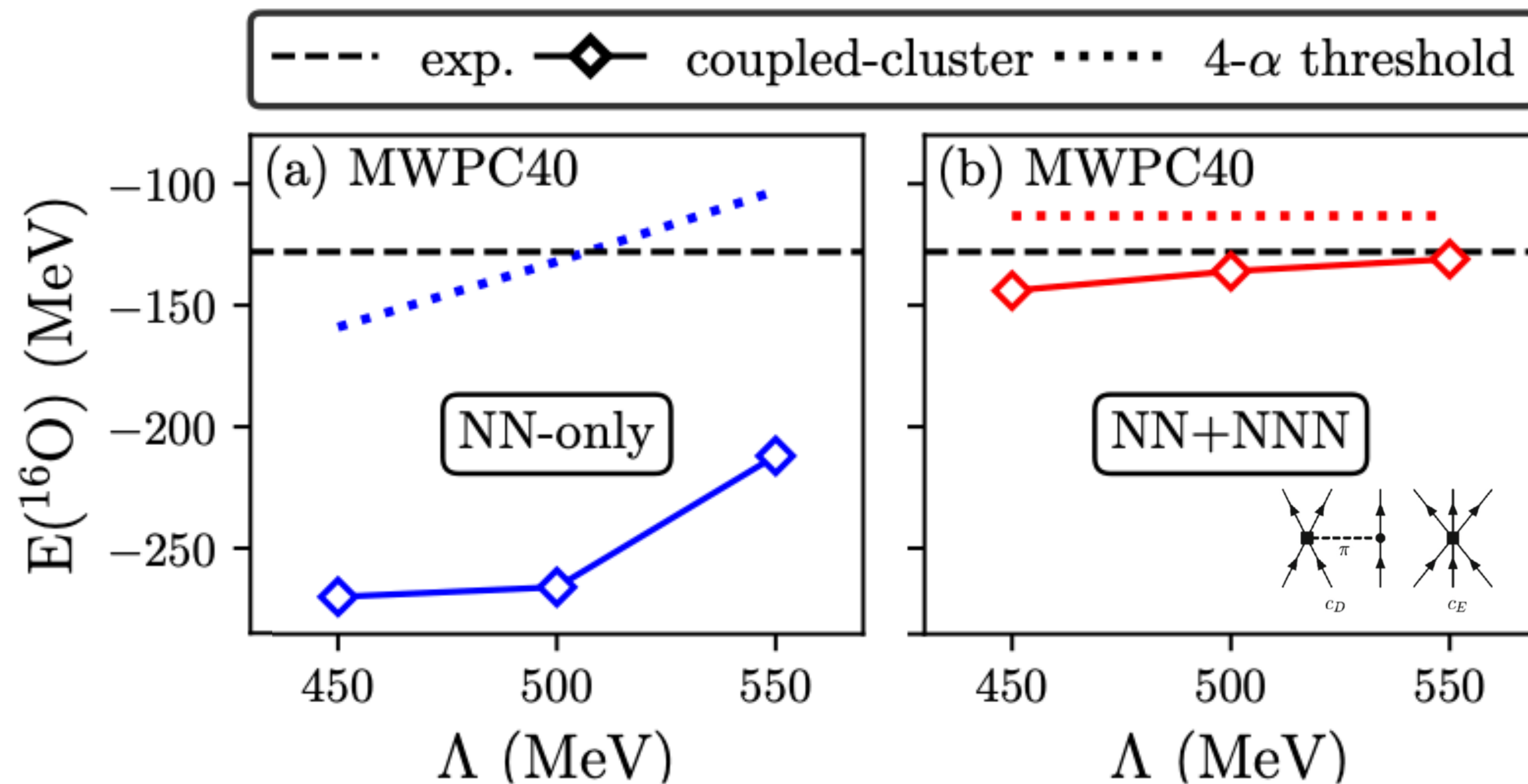


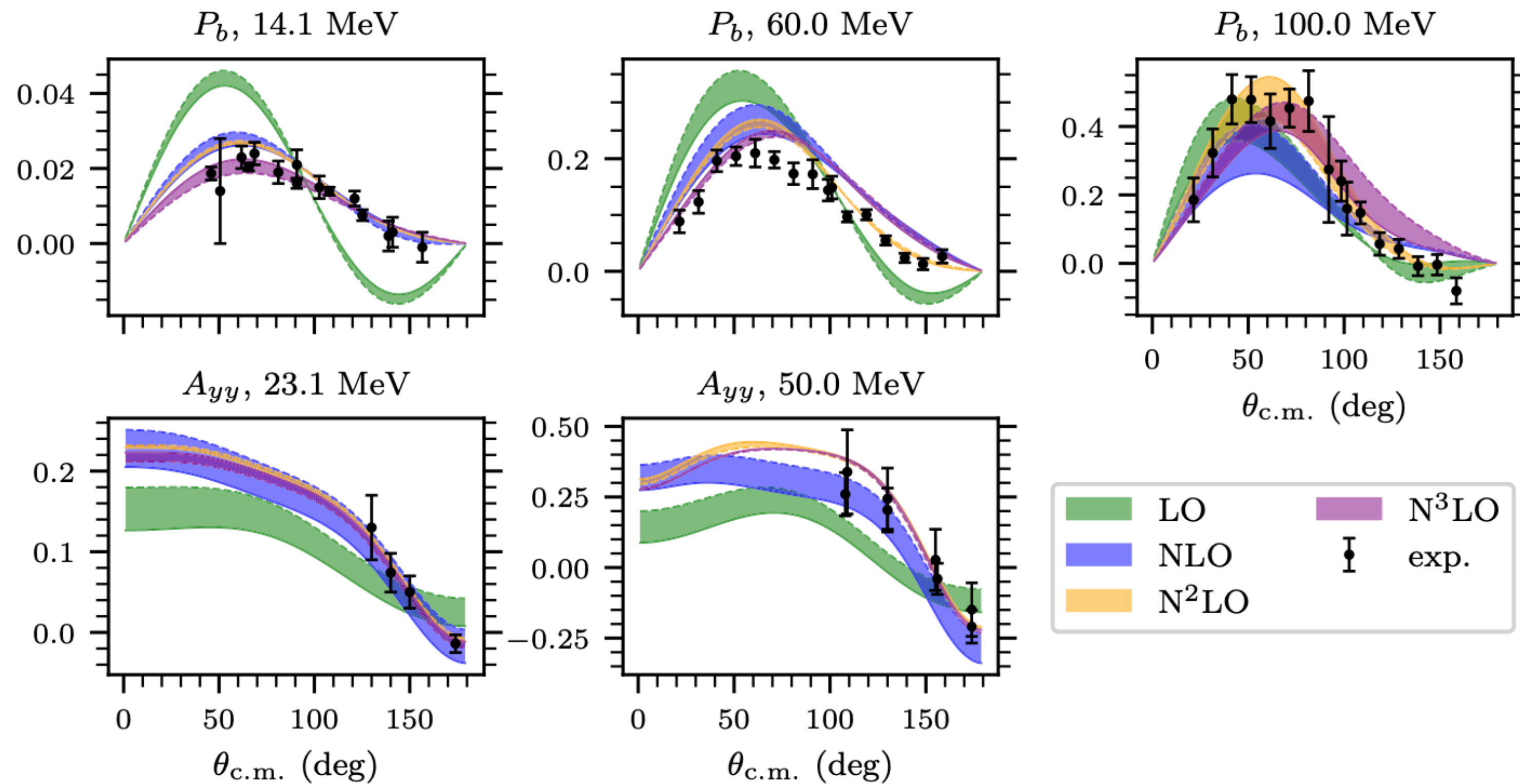
Table 1 Binding energy per nucleon (B_A/A) obtained with NN-only and NN+NNN interactions at LO. Here MWPC40 and $\Lambda=450$ MeV is adopted

B_A/A	^3H	^4He	^{16}O	^{40}Ca
NN-only	3.3	8	17.5	31.6
NN+NNN	3.3	8	8.2	9.4

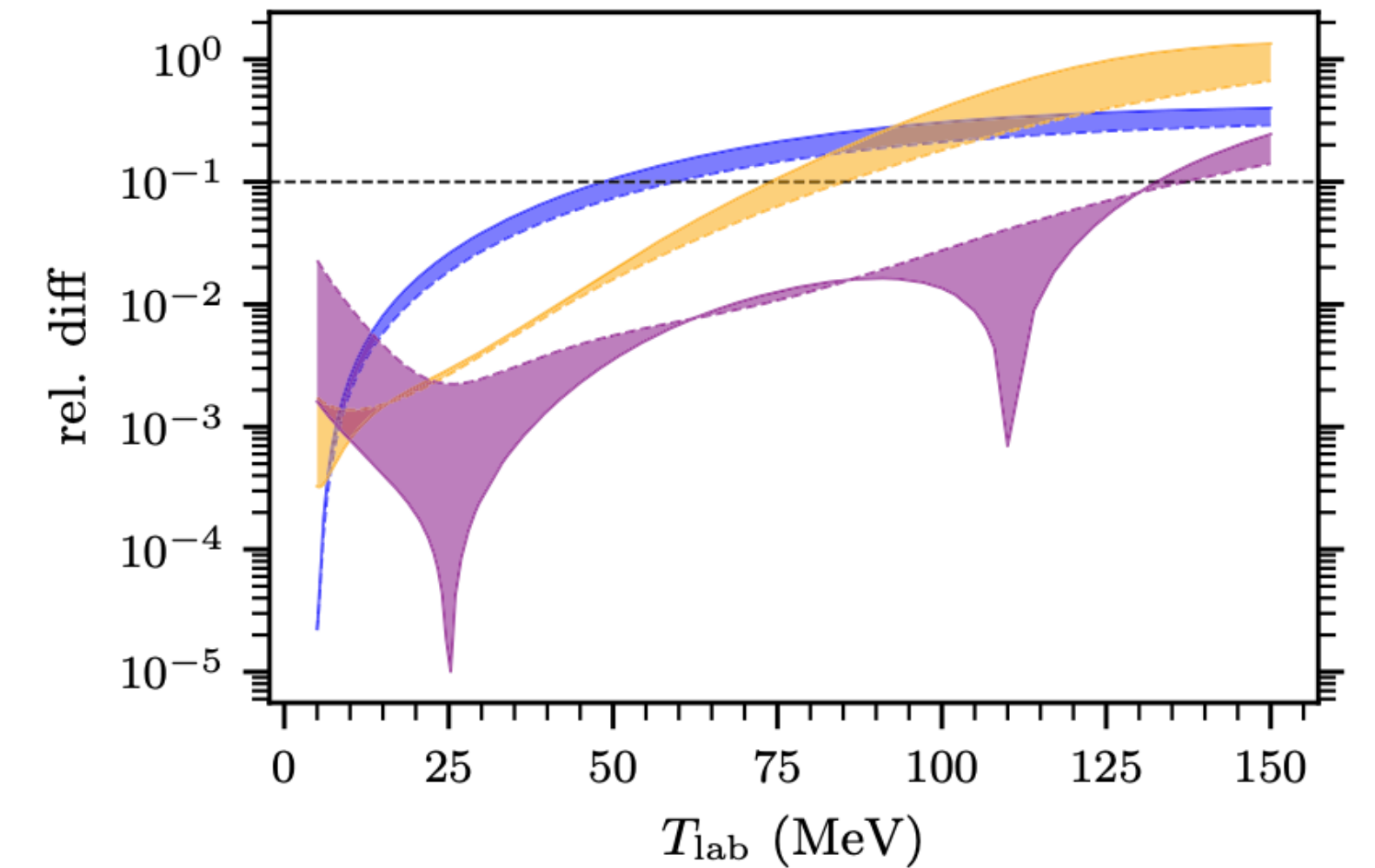
Over-fitted interaction / fine-tuning?

Preparing for Bayesian inference with modified Weinberg PC

Bands indicate $\Lambda = 500 - 2500$ MeV



Perturbative unitarity breaking in total cross section calculation



$$(S^{(\nu)})^\dagger S^{(\nu)} = 1 - \mathcal{C}(Q/\Lambda_\chi)^{\nu+1}$$

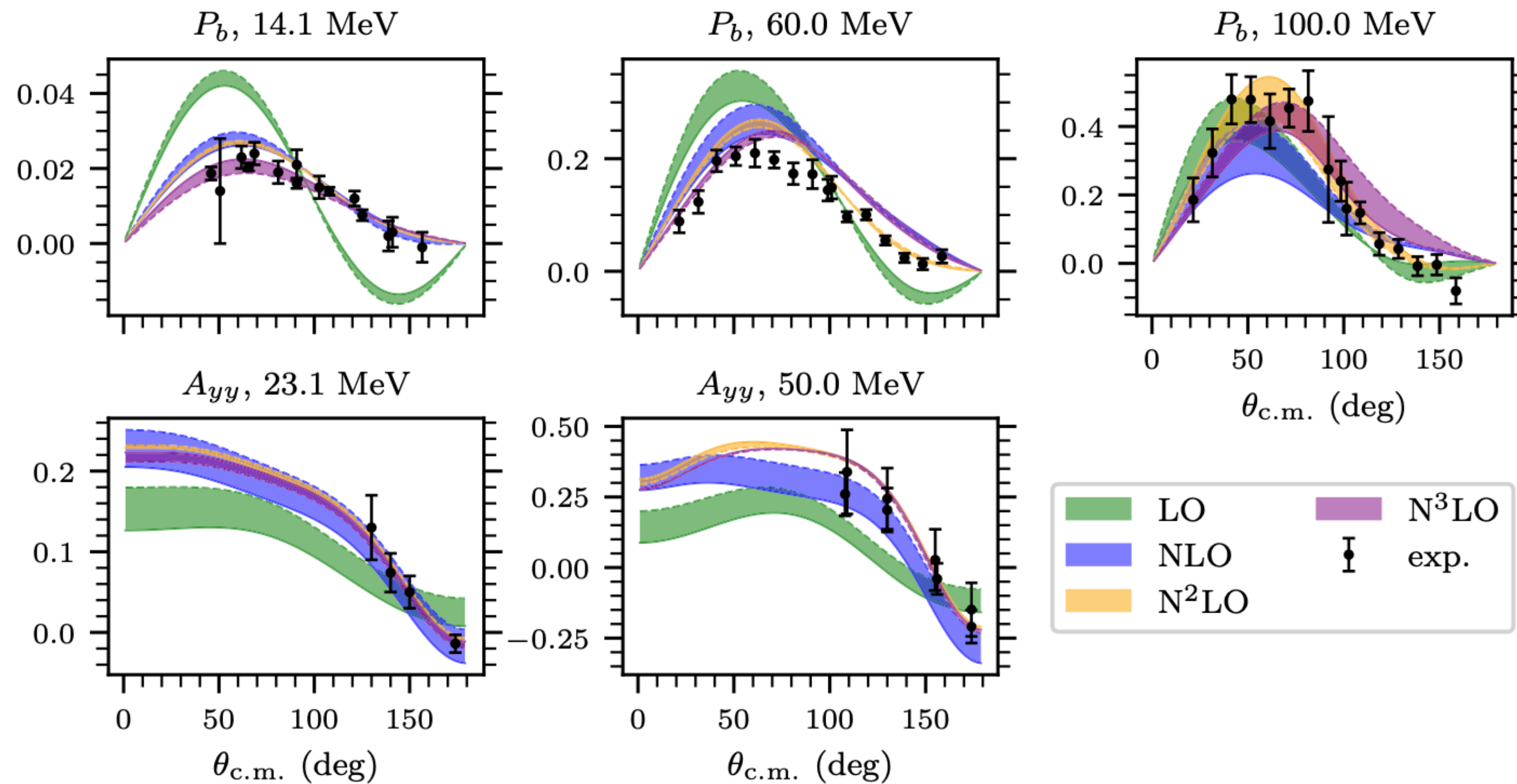
$$\Lambda_b \approx 220 \text{ MeV} \approx m_\Delta - m_N$$

$$p(\Lambda_b | y, I)?$$

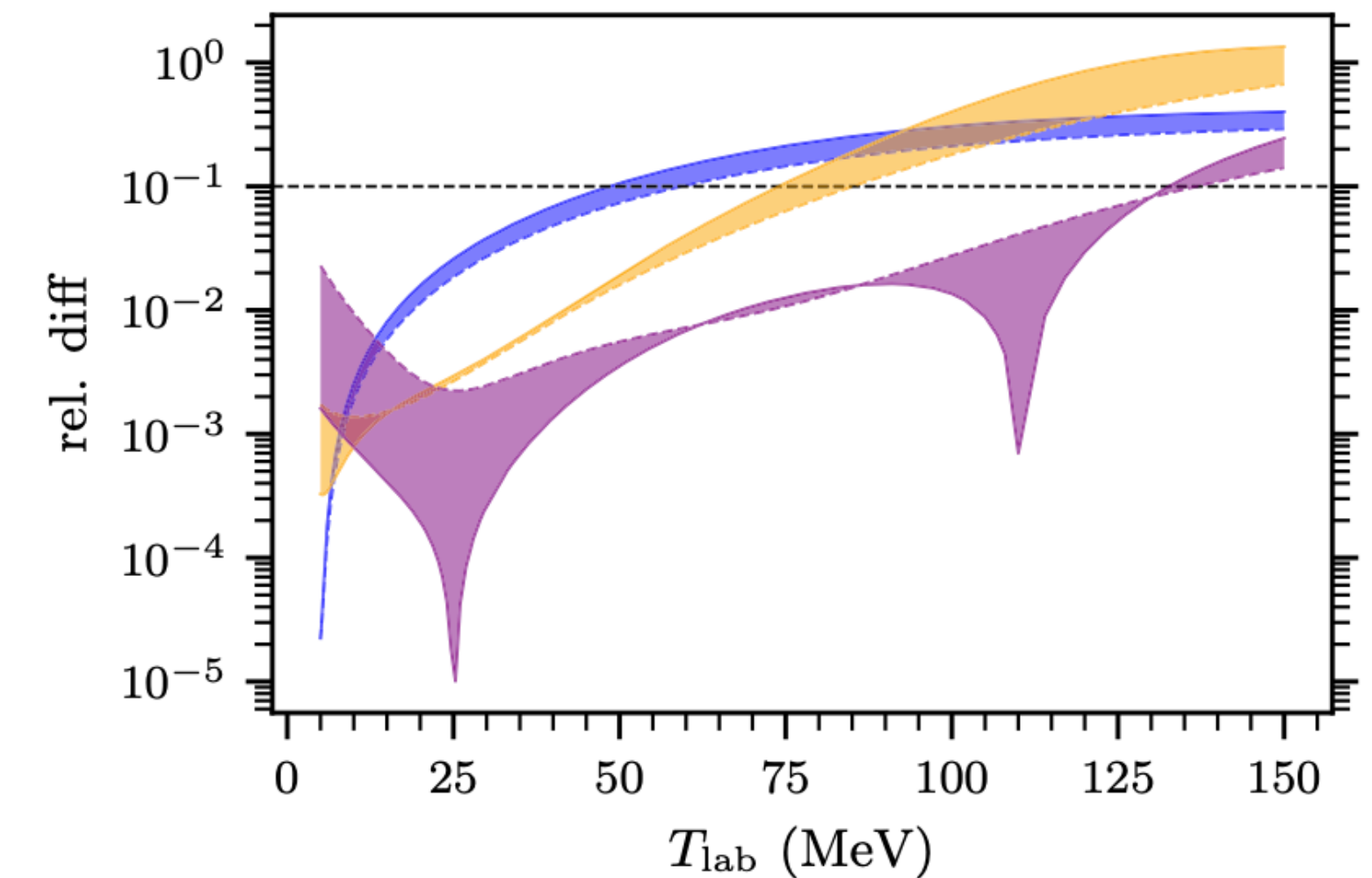
Over-fitted interaction / fine-tuning?

Preparing for Bayesian inference with modified Weinberg PC

Bands indicate $\Lambda = 500 - 2500$ MeV



Perturbative unitarity breaking in total cross section calculation



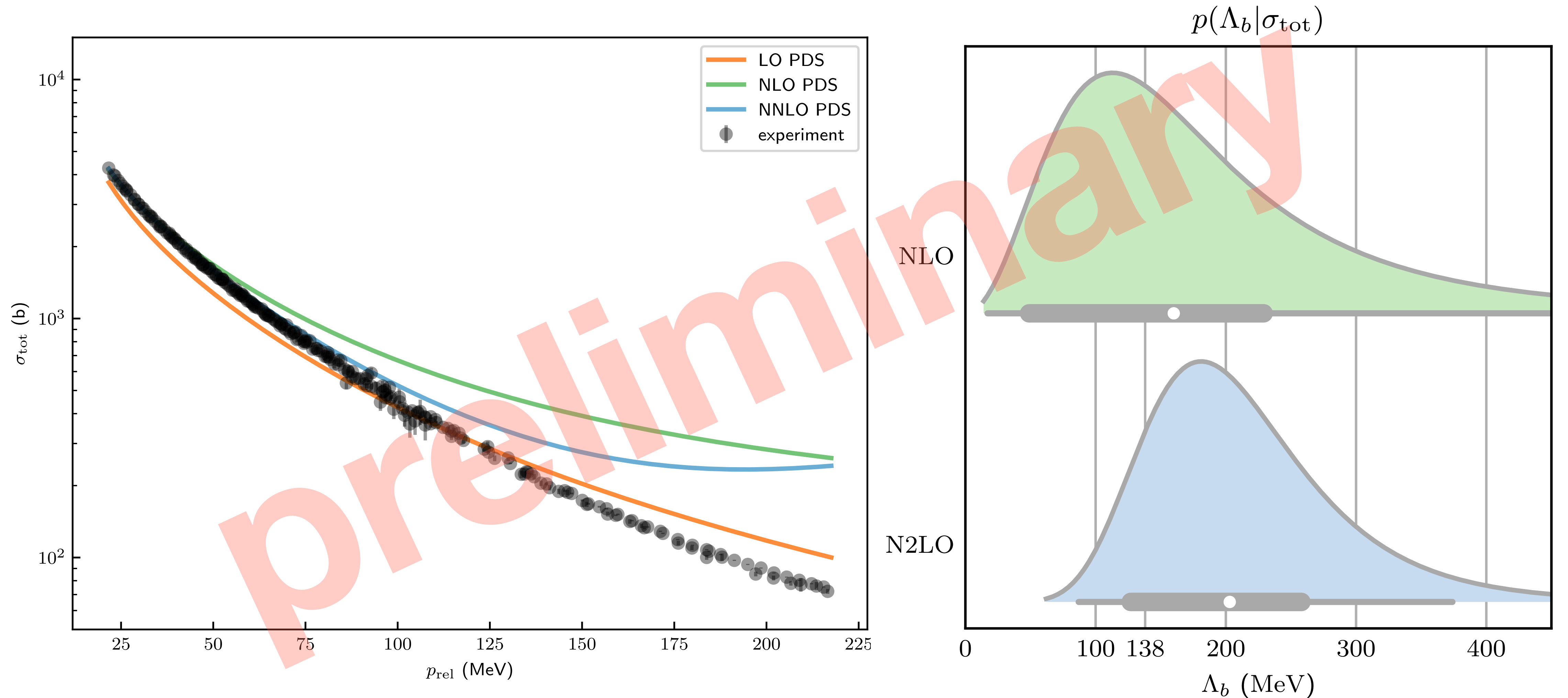
$$(S^{(\nu)})^\dagger S^{(\nu)} = 1 - \mathcal{C}(Q/\Lambda_\chi)^{\nu+1}$$

$$\Lambda_b \approx 220 \text{ MeV} \approx m_\Delta - m_N$$

$$p(\Lambda_b | y, I)?$$

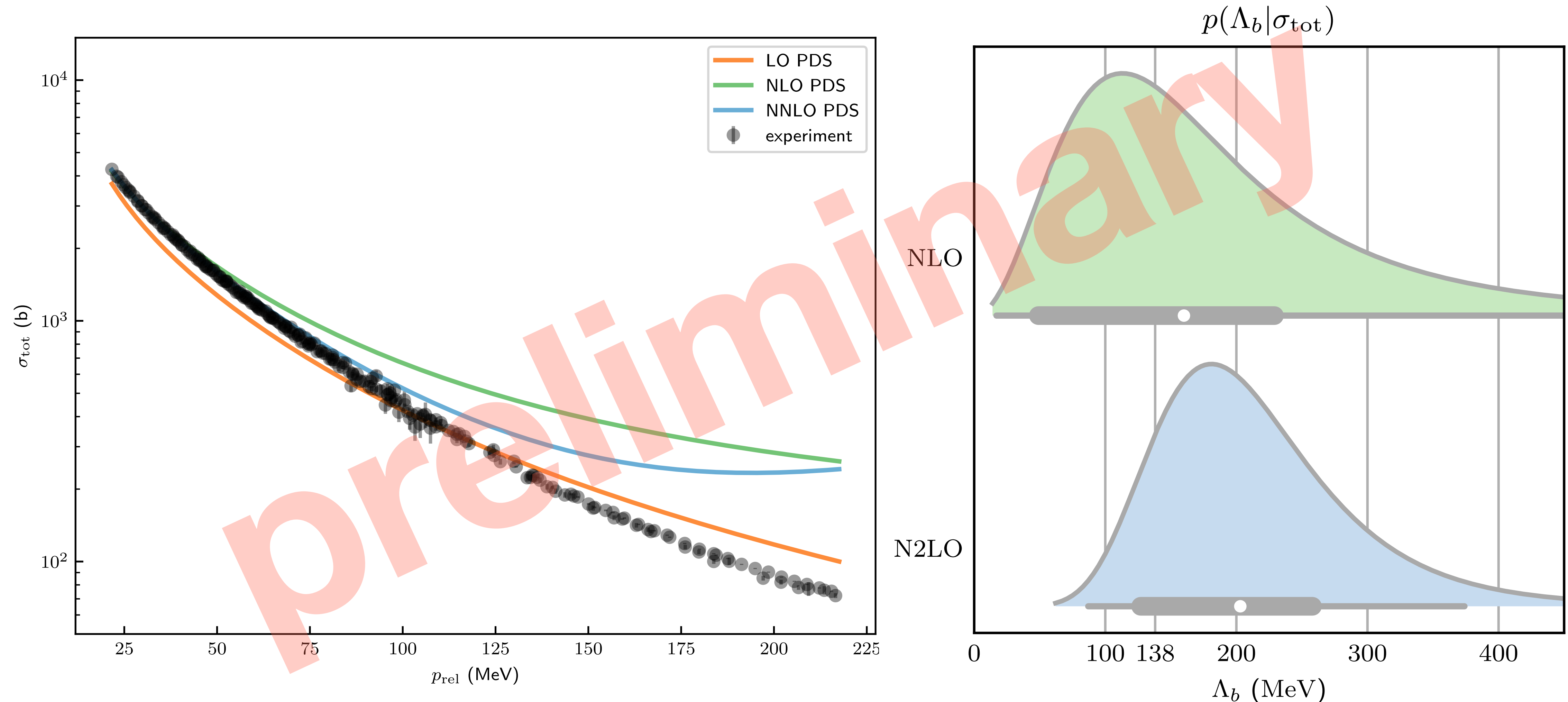
We estimate $\Lambda_b \approx 1.5m_\pi$ in π EFT

np scattering: total cross sections



We estimate $\Lambda_b \approx 1.5m_\pi$ in π EFT

np scattering: total cross sections



Summary

- Bayesian inference plays a critical role in nuclear physics
- We are witnessing tremendous progress in *ab initio* applications
- There are several important challenges and interesting future directions
 - important to improve uncertainty estimates of *ab initio* many-body computations.
 - develop (and share!) emulators for managing computational costs and facilitating model mixing for comprehensive inference and better predictive performance.
 - explore the predictive power of EFTs based on RG-invariant and modified power counting schemes.

Thanks to all my collaborators!

Thank you for your attention!



CHALMERS
UNIVERSITY OF TECHNOLOGY

Global sensitivity analysis (GSA)

A **sensitivity analysis** addresses the question *‘How much does each model parameter contribute to the variance in the prediction?’*

Variance-based methods for GSA decompose the variance of a certain model output in terms of each input and their combinations.

Global methods deal with the uncertainties of the outputs due to input variations over the whole domain.

Bottleneck: Converging the MC sampling of the variance integrals require approximately 10^6 samples

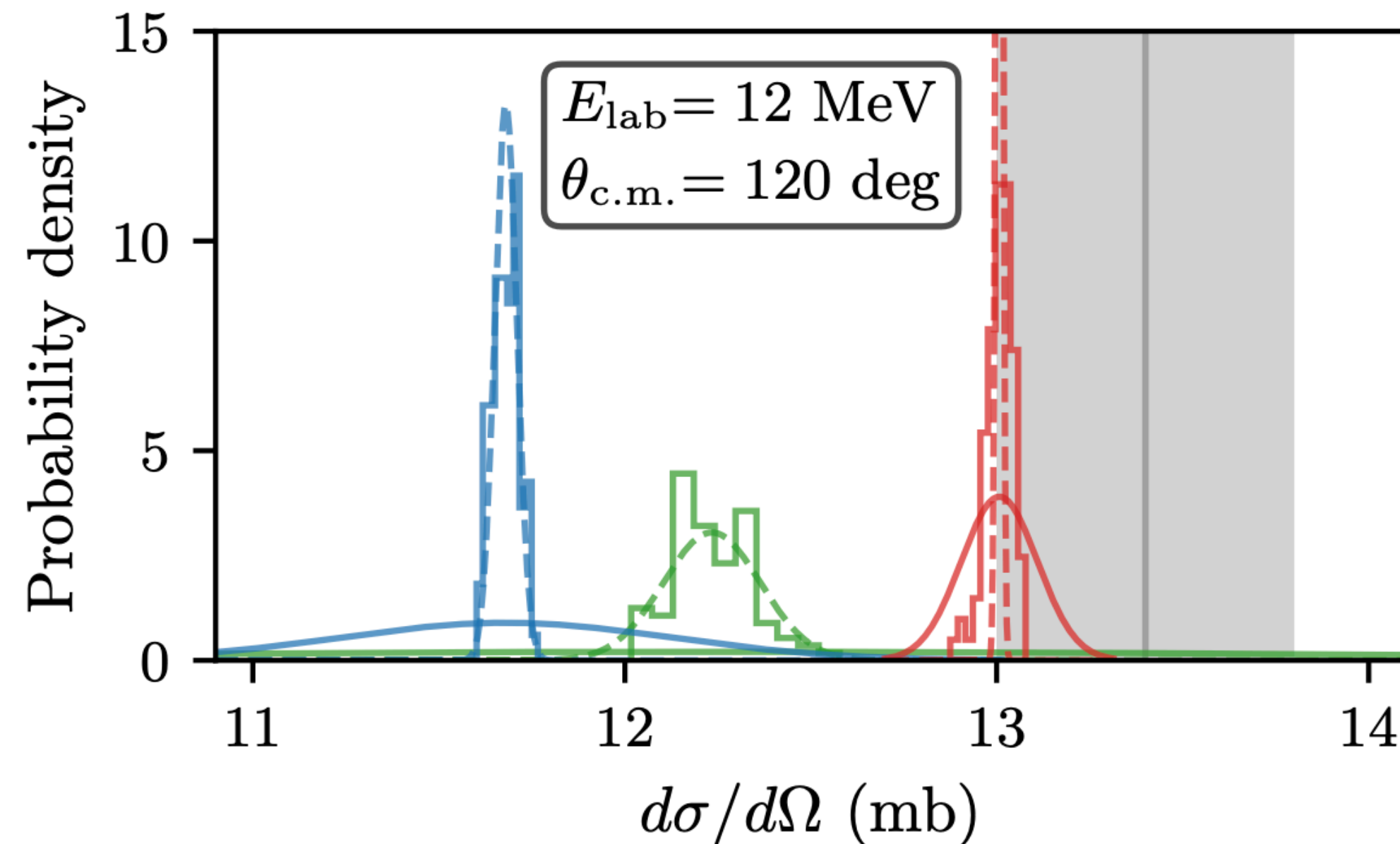


More PPDs

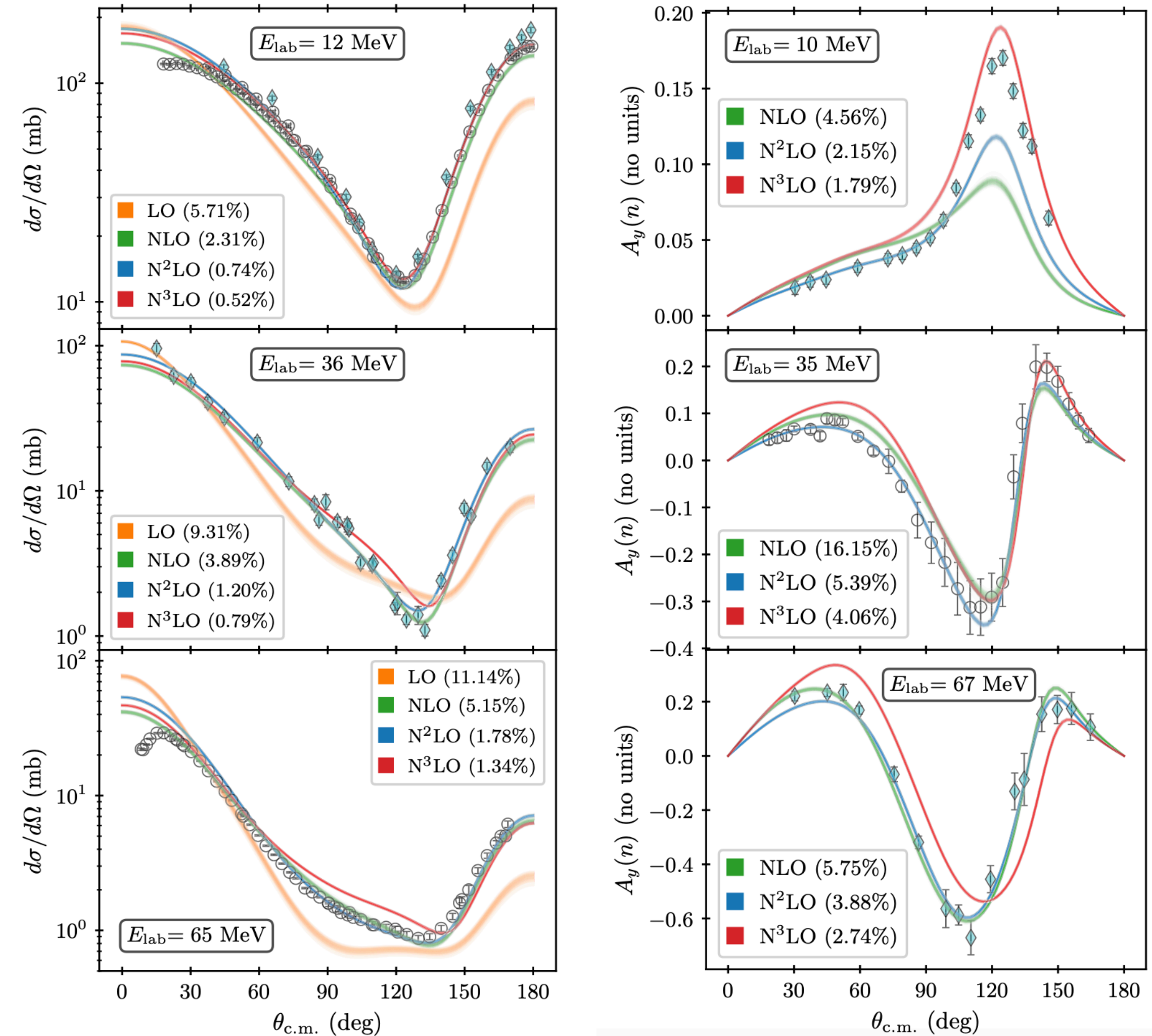
Low-energy nd scattering

100 samples from the LEC posteriors at LO, ..., N3LO sufficient to represent nd cross section ppd.

At low energy: N3LO truncation error is comparable to the LEC uncertainty and less than experiment (gray).



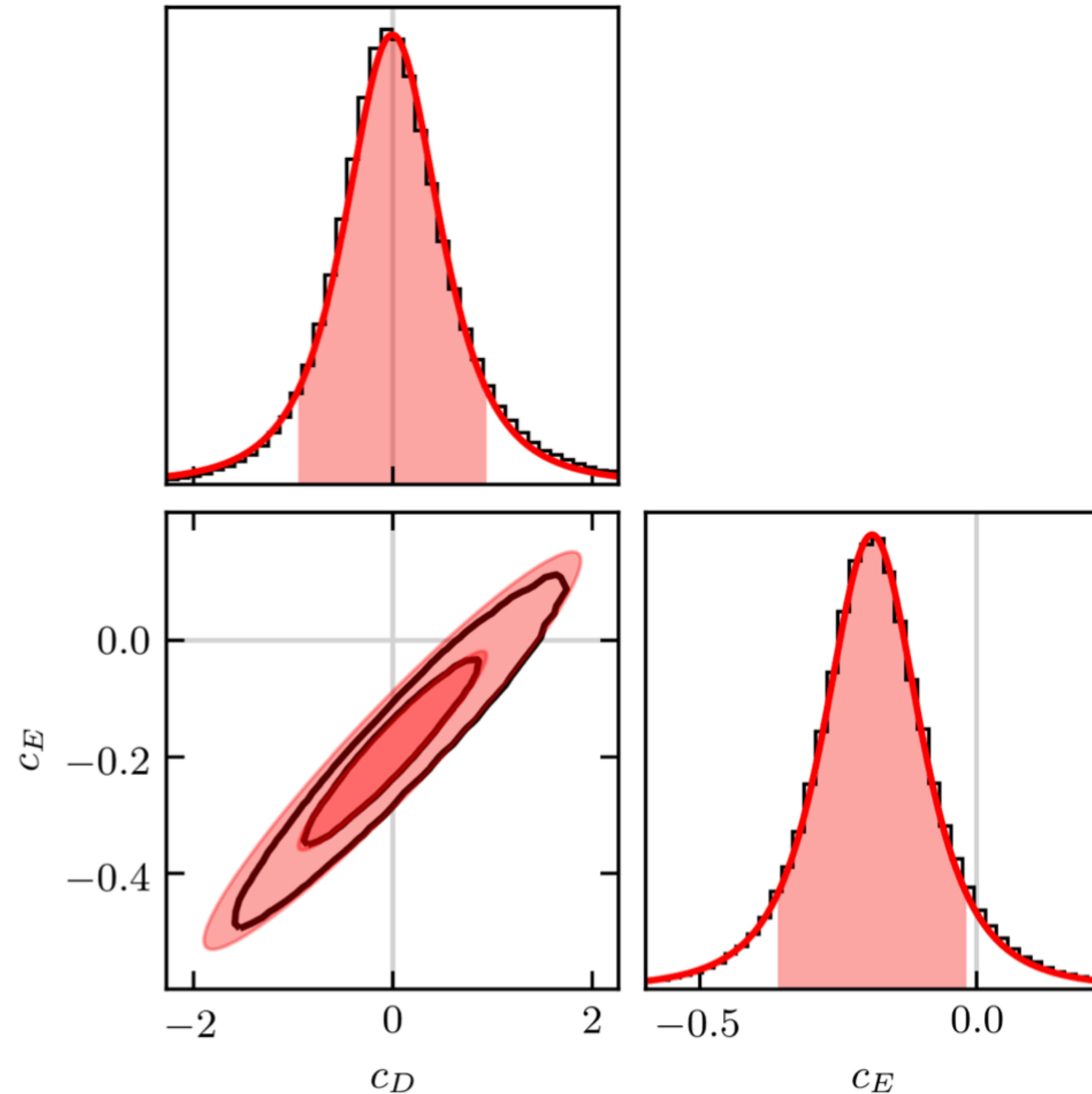
LEC uncertainty does not resolve the A_y puzzle



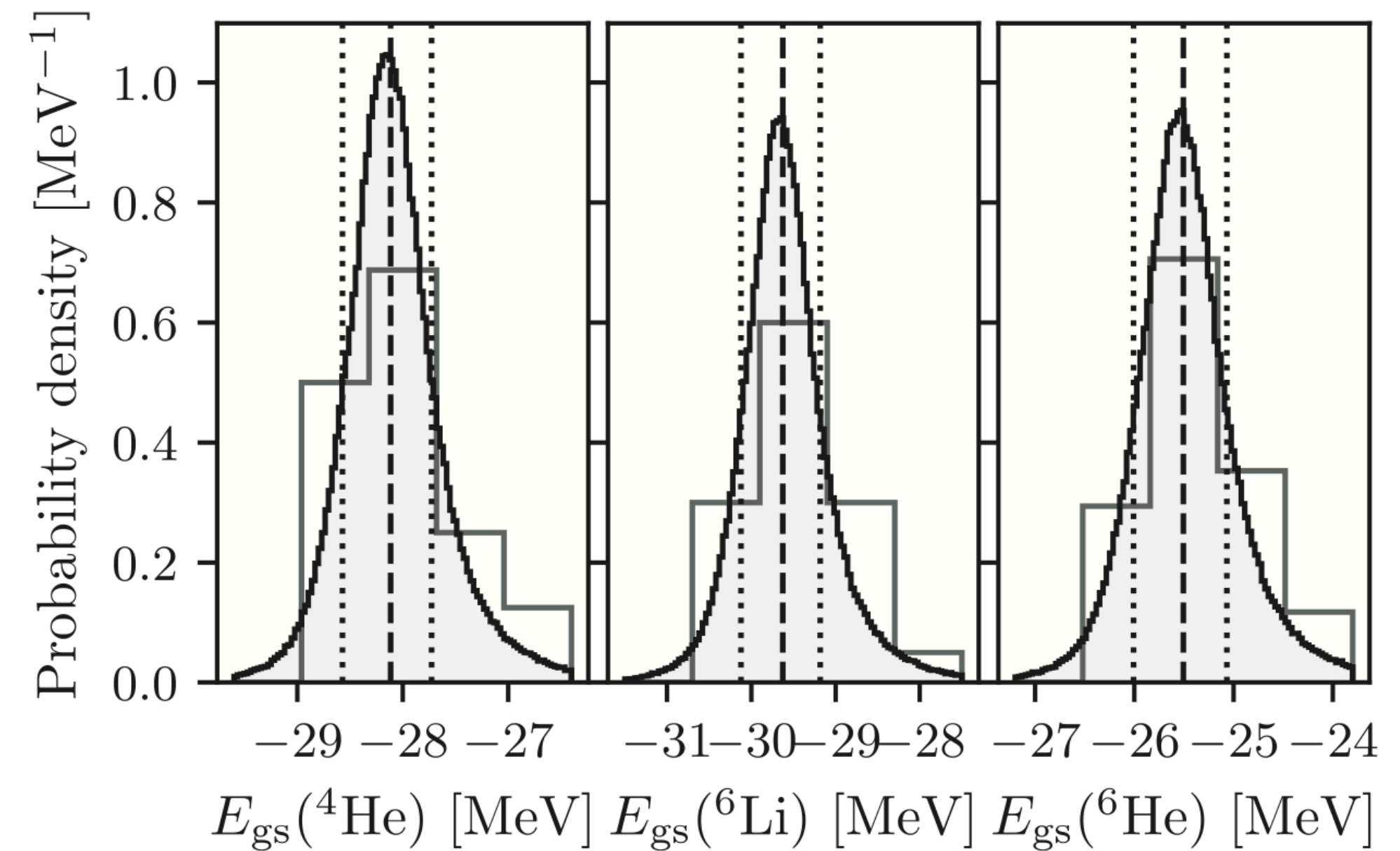


More PPDs

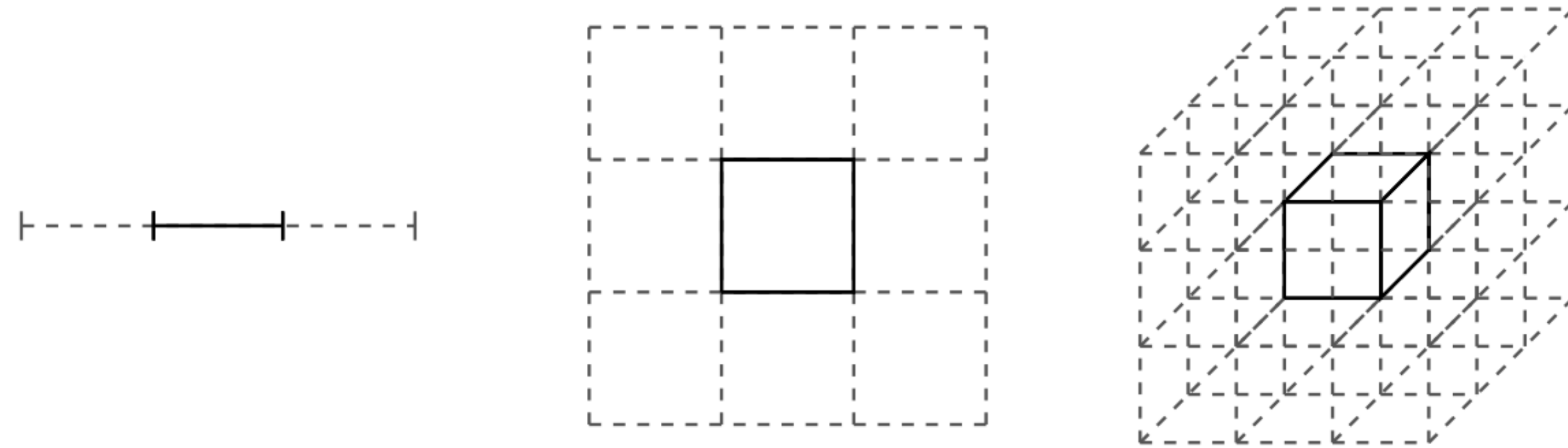
Low-sample representations can be useful



$$\begin{aligned} \text{pr}(\mathbf{y}_{\text{NCSM}} | \mathcal{D}, I) &= \int d\vec{a} \text{pr}(\mathbf{y}_{\text{NCSM}}, \vec{a} | \mathcal{D}, I) \\ &= \int d\vec{a} \text{pr}(\mathbf{y}_{\text{NCSM}} | \vec{a}, \mathcal{D}, I) \text{pr}(\vec{a} | \mathcal{D}, I), \\ \text{pr}(\vec{a} | \mathcal{D}, I) &= \delta(\vec{a}_{\text{NN}} - \vec{a}_{\text{NN}}^*) \delta(\vec{a}_{\pi\text{N}} - \vec{a}_{\pi\text{N}}^*) \text{pr}(c_D, c_E) \end{aligned}$$

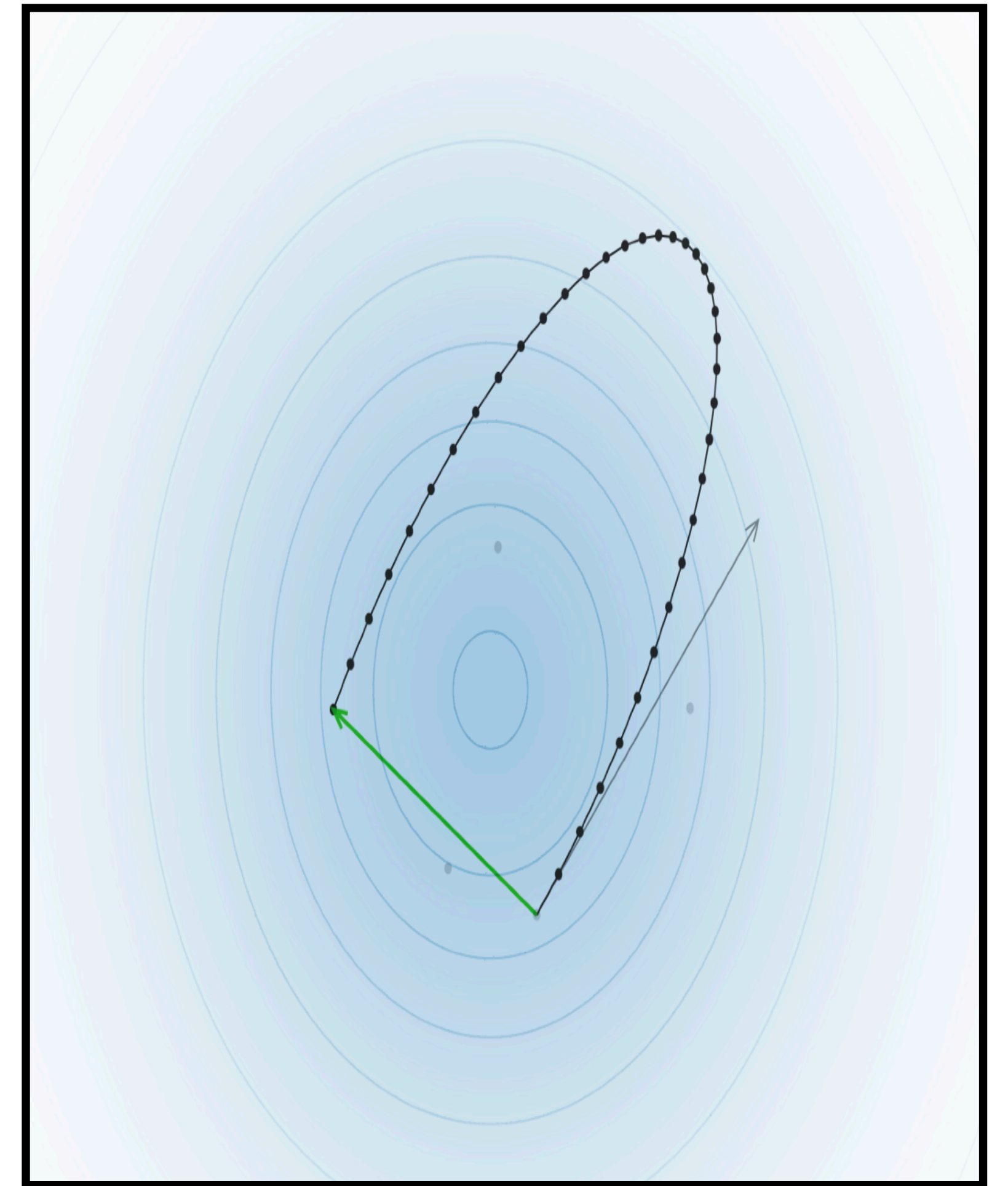


Hamiltonian Monte Carlo for high-dim spaces



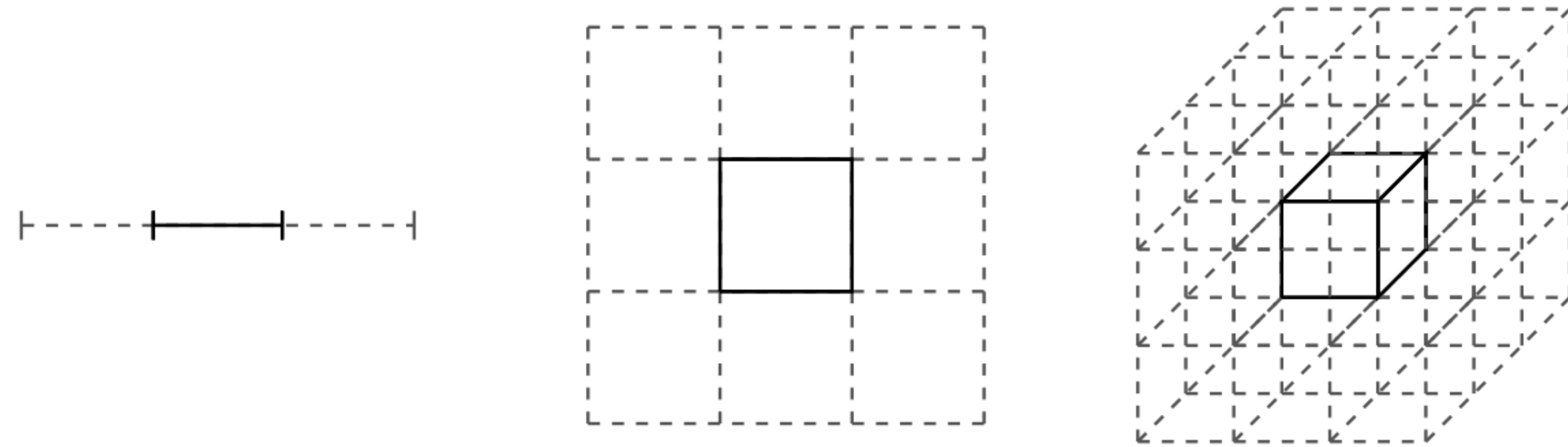
credit: M. Betancourt arXiv:1701.02434

The LEC posterior is often multivariate (30 np/pp LECs at N3LO). Naive “guess and check” (random walk metropolis) will fail exponentially. We use Hamiltonian Monte Carlo (HMC) to take long jumps in parameter space while staying in regions with high probability mass.



credit: <https://chi-feng.github.io/mcmc-demo/>

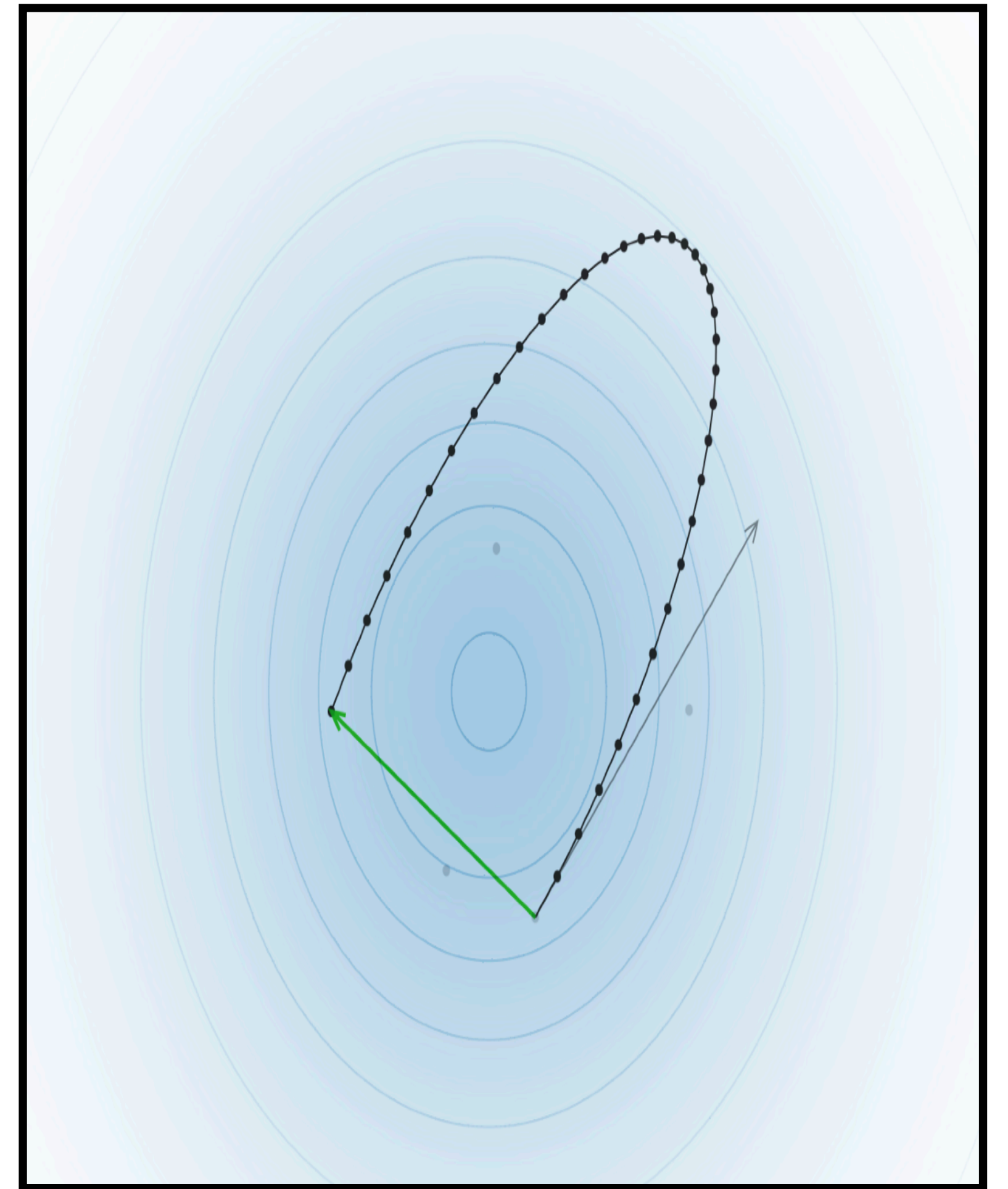
Hamiltonian Monte Carlo for high-dim spaces



credit: M. Betancourt arXiv:1701.02434

With 10^4 posterior samples per chain, and 10 chains, at each order the HMC sampling passes all convergence tests.

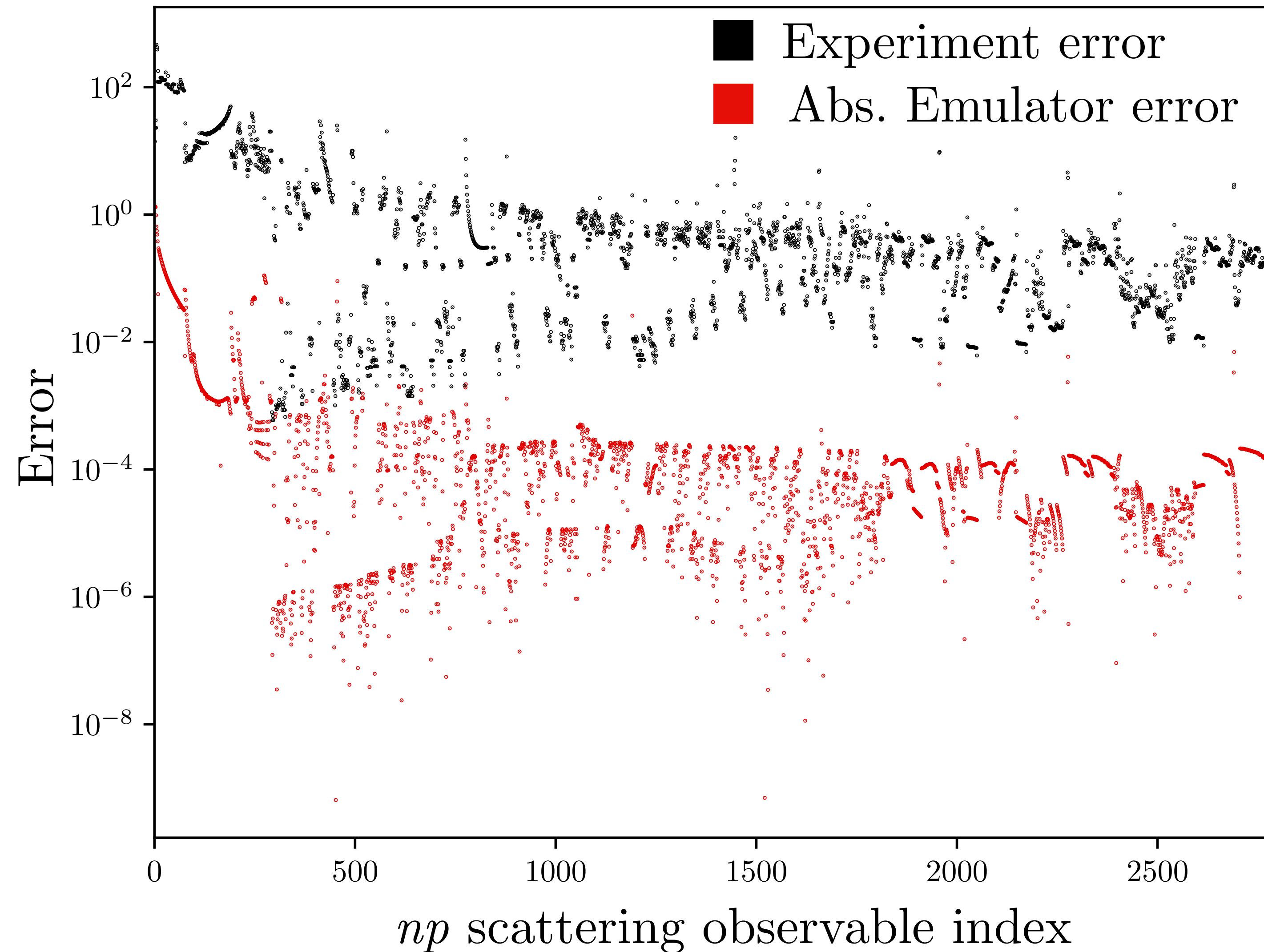
Although we have to compute derivatives and integrate Hamilton's equations at ~ 20 (time) steps for each HMC step, each posterior sample is very informative. This leads to an overall advantage of using HMC.




credit: <https://chi-feng.github.io/mcmc-demo/>

Benchmarking the NN scattering emulator

Deltafull NNLO np sector, 8 training points

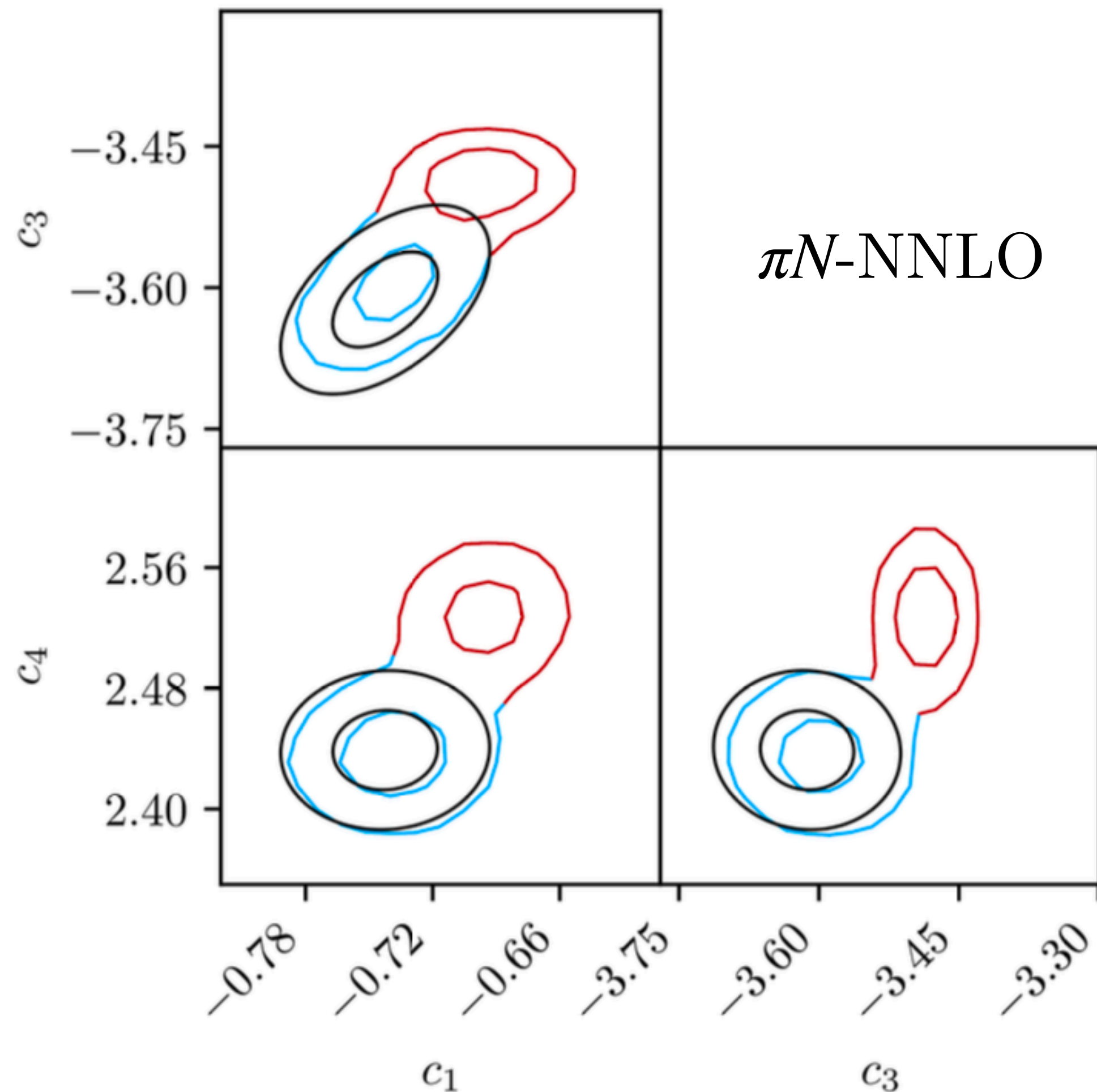


It takes **0.4 seconds** to evaluate the entire likelihood.

Python implementation accelerated by Google  jit-compilation. Provides derivatives via AD as well. (*overhead x2*)

In progress: LEC inference with correlated EFT truncation error.

Inferring LECs up to 4th order in χ EFT



Black ellipse: Roy-Steiner prior

Blue ellipse: πN posterior when conditioning on low-energy NN data ($p_{rel} < m_\pi$)

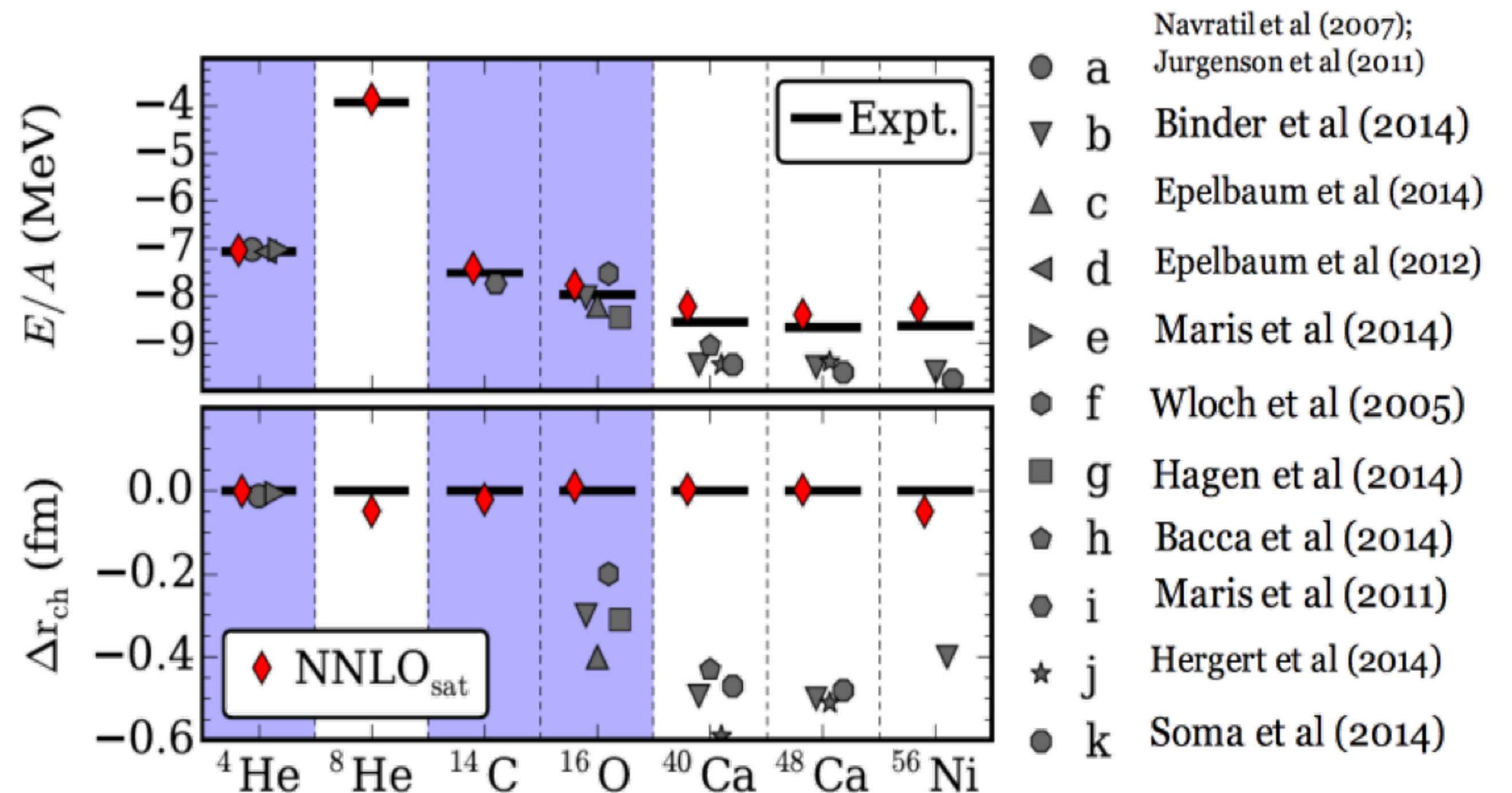
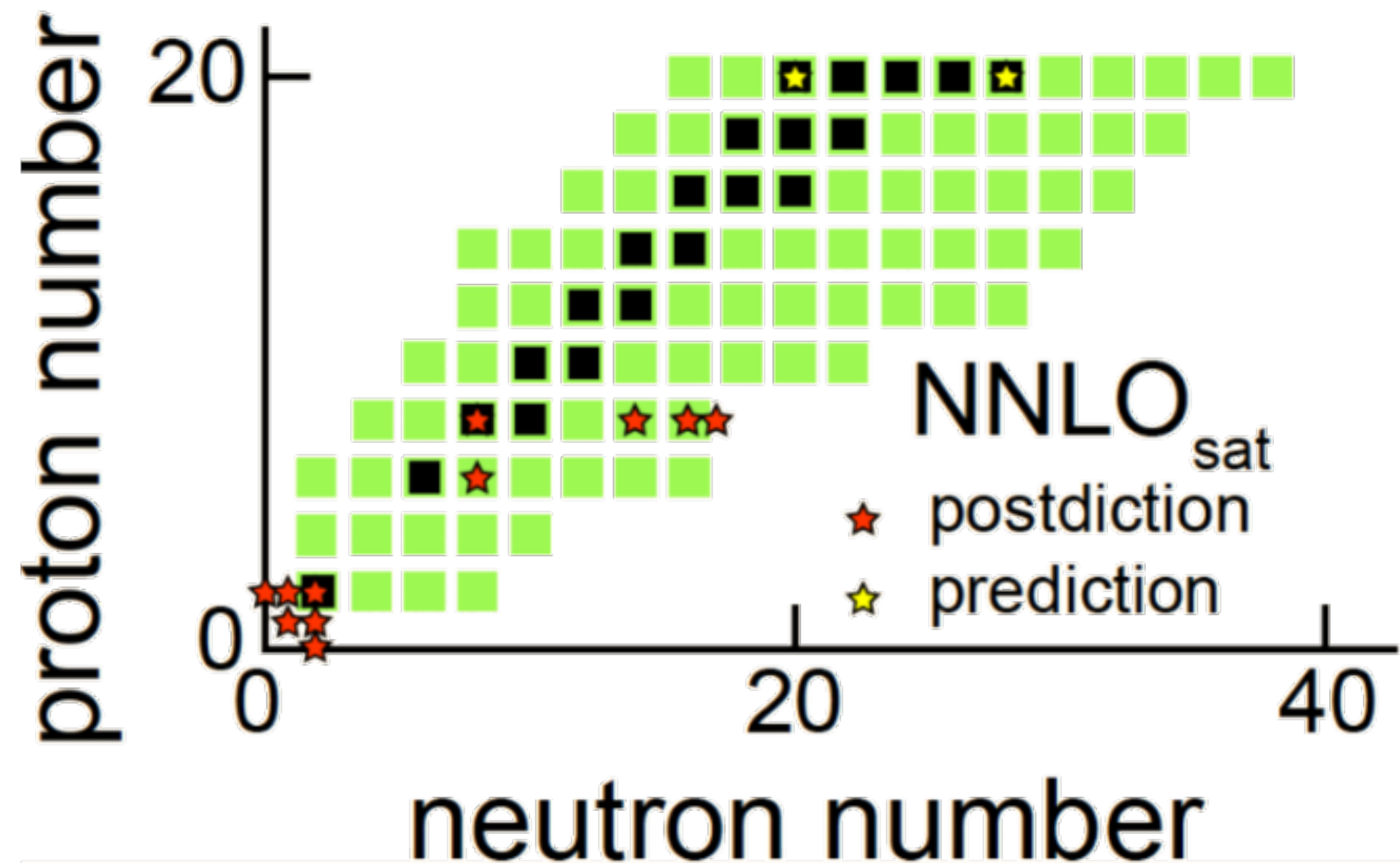
Red ellipse: πN posterior when conditioning on all NN data with $T_{lab} < 290$ MeV

We observe the same behaviour at N3LO.

UQ to prevent overfitting in model calibration

$$y_{\text{exp}}(\vec{x}) = \underbrace{y_{\text{th}}(\vec{\alpha}; \vec{x}) + \delta y_{\text{th}}(\vec{\alpha}; \vec{x})}_{\text{'Model'}} + \delta y_{\text{exp}}(\vec{x})$$

Heavy-mass data is important in nuclear physics calibration.
Priors and model discrepancy are key to inhibit overfitting



Inference under model misspecification

We consider our *ab initio* **model** as a function $y = f(\theta)$, $\theta \in \Omega \subset \mathbb{R}^d$ where Ω is some specified input parameter space of interest.

We seek a **posterior predictive**
 $p(\tilde{y} | y, M, I)$


$$M = \{f(\theta) : \theta \in \Omega\}$$

Inference under model misspecification

We consider our *ab initio* model as a function $y = f(\theta)$, $\theta \in \Omega \subset \mathbb{R}^d$ where Ω is some specified input parameter space of interest.

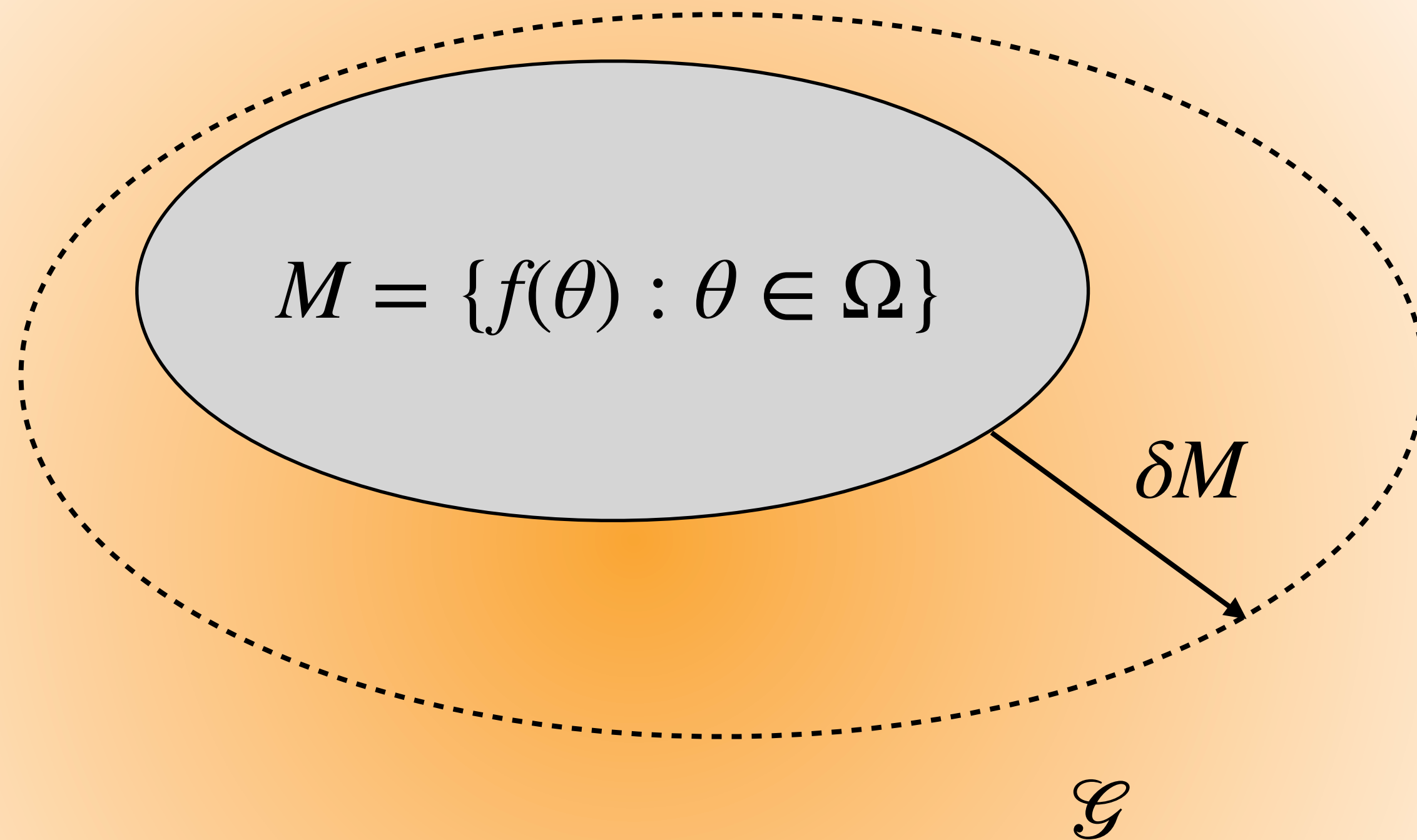
We seek a **posterior predictive**

$$p(\tilde{y} | y, M, I)$$

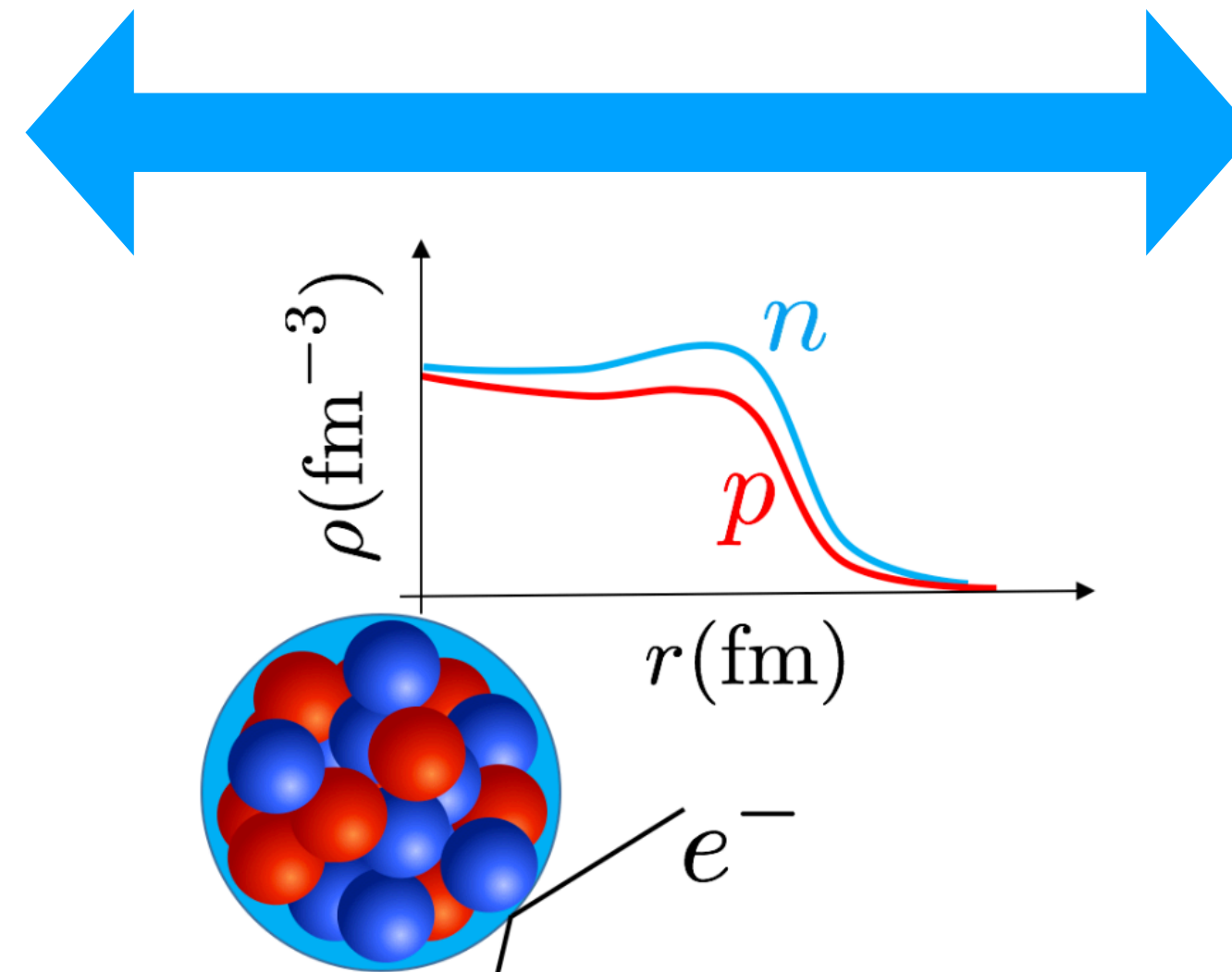
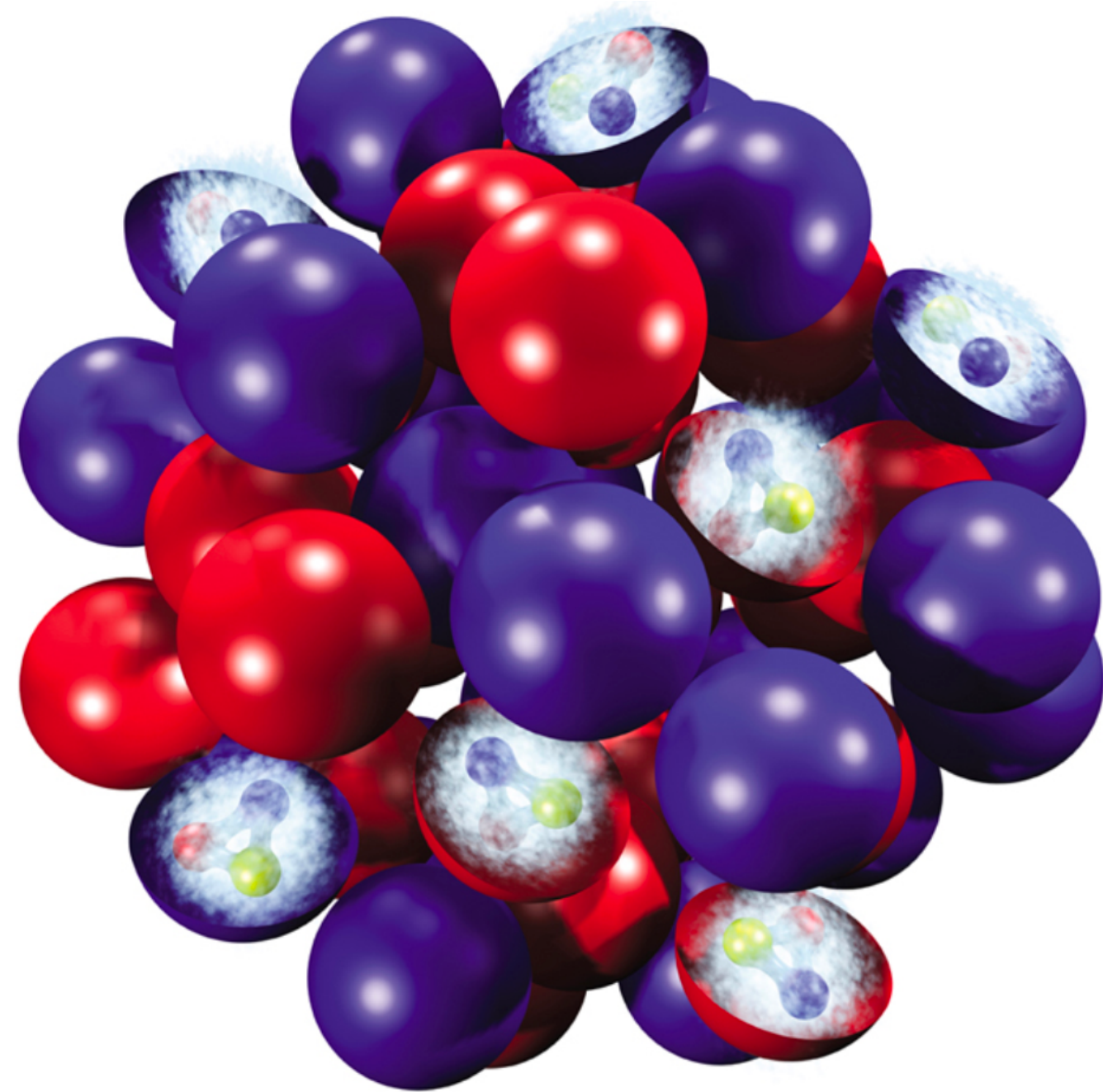
“All models are wrong”

i.e., data $y \sim \mathcal{G}$ where $\mathcal{G} \notin M$

Estimate the model discrepancy δM and improve our model(s) to make meaningful inferences and predictions.



Linking nuclei and nuclear matter through χ EFT

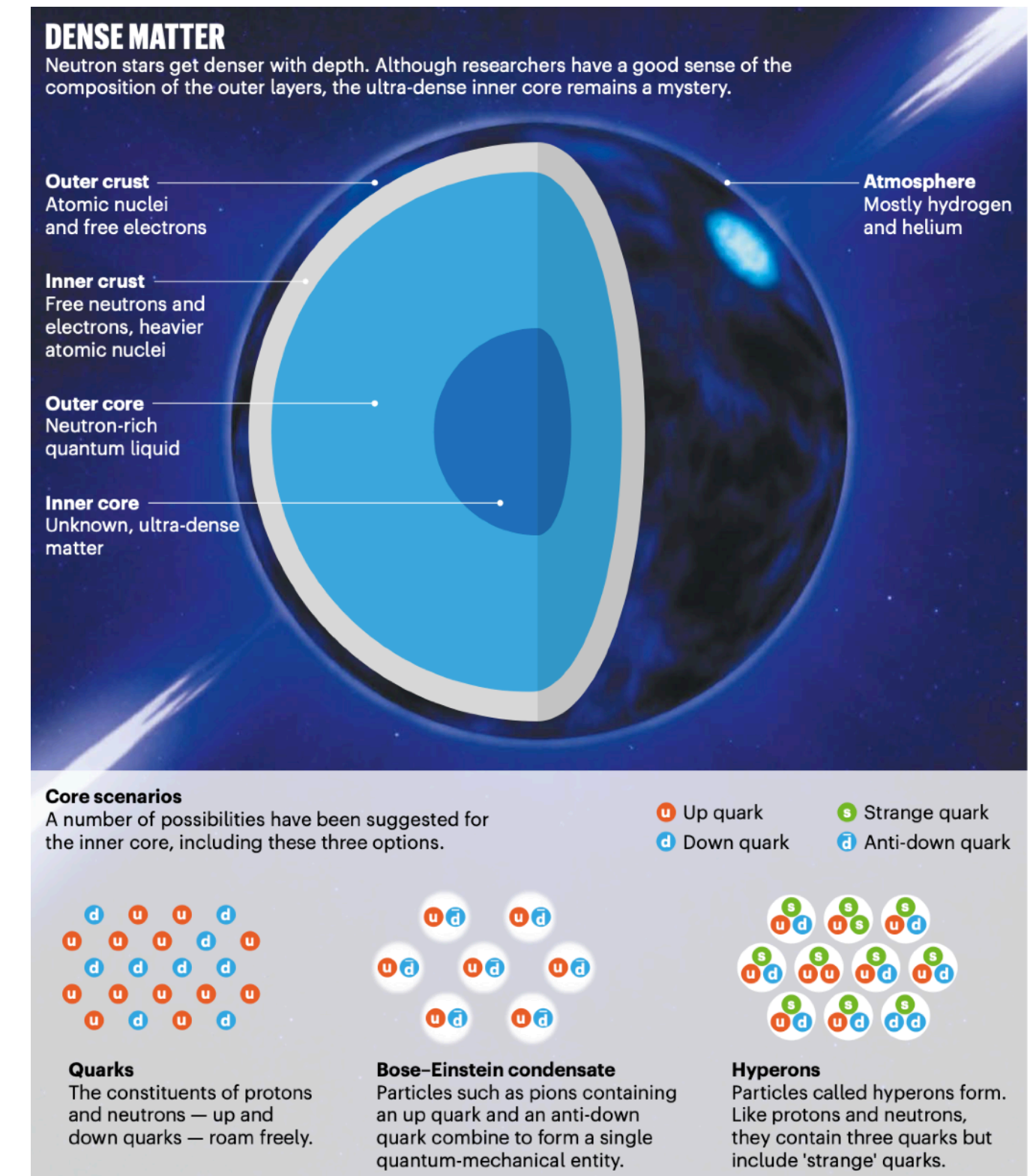


(1) Challenging to find a “terrestrial slab” of pure neutron matter to probe its EOS.

$$P \approx \frac{L\rho_0}{3}$$

- (2) Instead: measure the skin thickness.
 (3) Use a theoretical model to analyze correlation between PNM pressure and the skin thickness.

The thickness of the neutron skin depends on the pressure (P) of neutron-rich matter: the greater the pressure, the thicker the skin as neutrons are pushed out against surface tension.

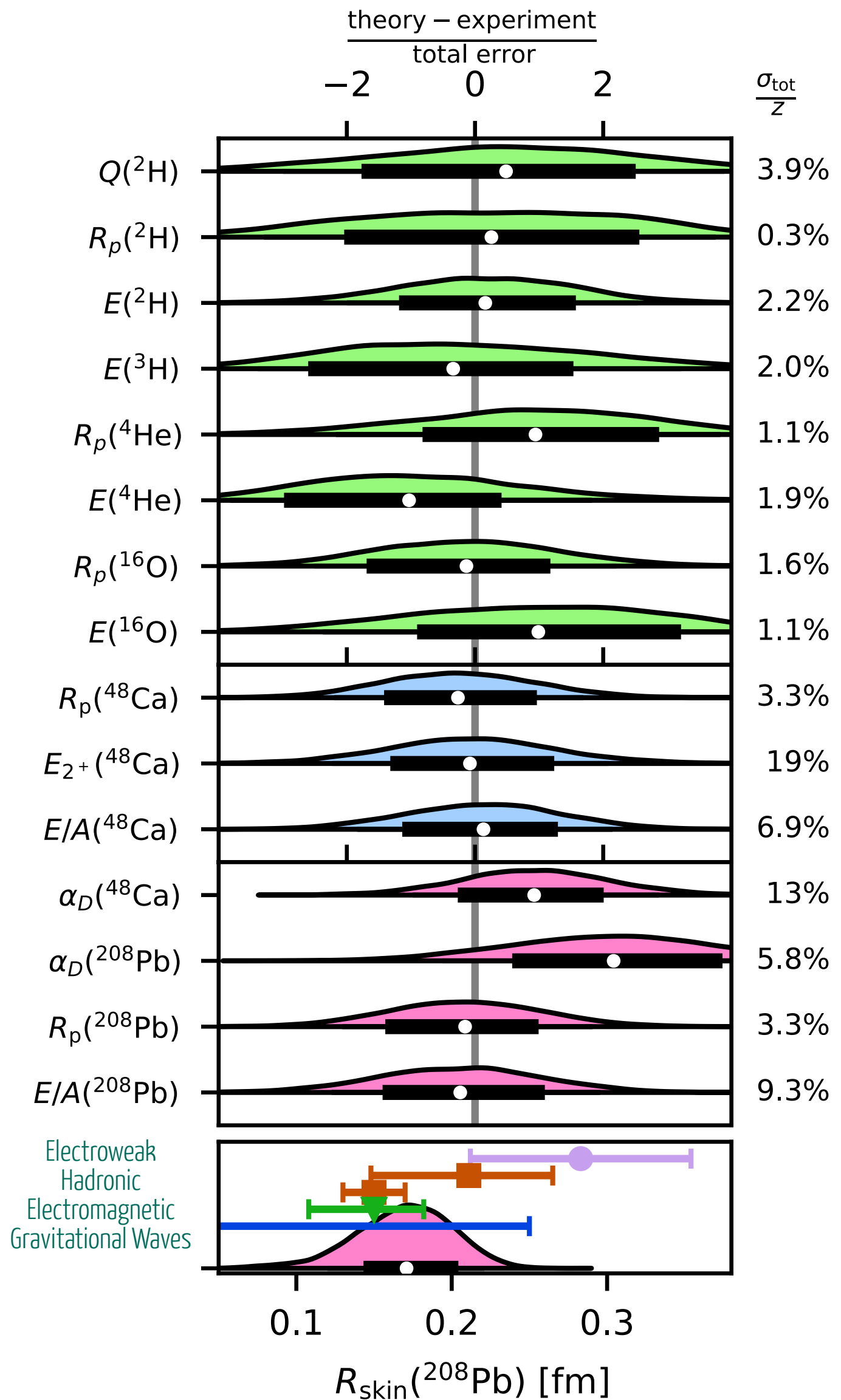


The same pressure supports a neutron star against gravity. Thus models with thicker neutron skins often produce neutron stars with larger radii.

B. A. Brown Phys. Rev. Lett. 85, 5296 (2000)

C. J. Horowitz and J. Piekarewicz Phys. Rev. Lett. 86, 5647 (2001)

Predicting the skin thickness of ^{208}Pb



History Matching

We explore 10^9 different interaction parameterizations. Confronted with $A=2-16$ data + NN scattering information. Find 34 non-implausible interactions

Calibration

Likelihood weighting

Validation

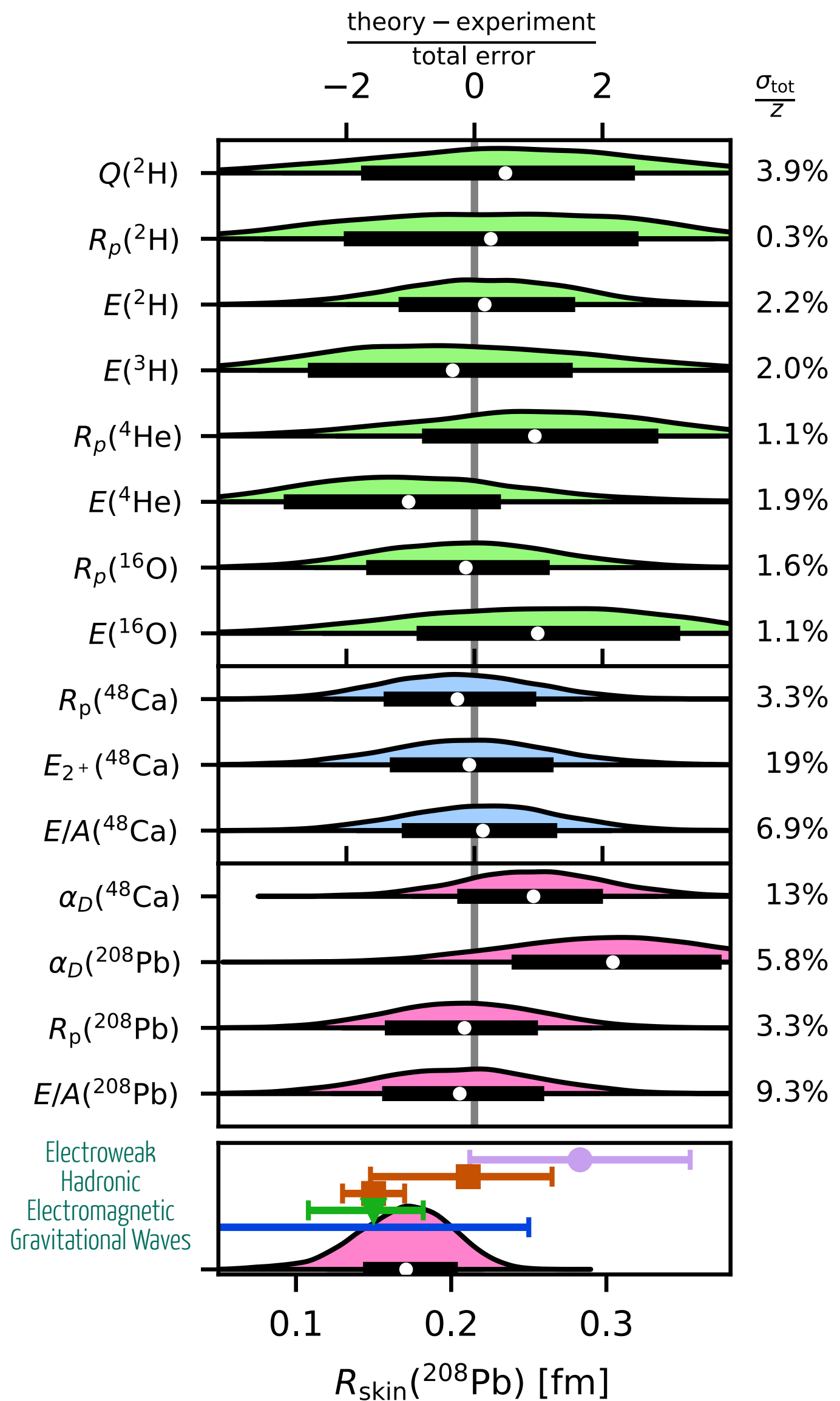
Inspect ab initio model and error estimates

Prediction: small skin thickness 0.14-0.20 fm in mild (1.5sigma) tension with PREX.

History-matching observables						
Observable	z	ϵ_{exp}	ϵ_{model}	ϵ_{method}	ϵ_{em}	PPD
$E(^2\text{H})$	-2.2246	0.0	0.05	0.0005	0.001%	$-2.22^{+0.07}_{-0.07}$
$R_p(^2\text{H})$	1.976	0.0	0.005	0.0002	0.0005%	$1.98^{+0.01}_{-0.01}$
$Q(^2\text{H})$	0.27	0.01	0.003	0.0005	0.001%	$0.28^{+0.02}_{-0.02}$
$E(^3\text{H})$	-8.4821	0.0	0.17	0.0005	0.01%	$-8.54^{+0.34}_{-0.37}$
$E(^4\text{He})$	-28.2957	0.0	0.55	0.0005	0.01%	$-28.86^{+0.86}_{-1.01}$
$R_p(^4\text{He})$	1.455	0.0	0.016	0.0002	0.003%	$1.47^{+0.03}_{-0.03}$
$E(^{16}\text{O})$	127.62	0.0	1.0	0.75	0.5%	$-126.2^{+3.0}_{-2.8}$
$R_p(^{16}\text{O})$	2.58	0.0	0.03	0.01	0.5%	$2.57^{+0.06}_{-0.06}$
Calibration observables						
Observable	z	ϵ_{exp}	ϵ_{model}	ϵ_{method}	ϵ_{em}	PPD
$E/A(^{48}\text{Ca})$	-8.667	0.0	0.54	0.25	—	$-8.58^{+0.72}_{-0.72}$
$E_{2+}(^{48}\text{Ca})$	3.83	0.0	0.5	0.5	—	$3.79^{+0.86}_{-0.96}$
$R_p(^{48}\text{Ca})$	3.39	0.0	0.11	0.03	—	$3.36^{+0.14}_{-0.13}$
Validation observables						
Observable	z	ϵ_{exp}	ϵ_{model}	ϵ_{method}	ϵ_{em}	PPD
$E/A(^{208}\text{Pb})$	-7.867	0.0	0.54	0.5	—	$-8.06^{+0.99}_{-0.88}$
$R_p(^{208}\text{Pb})$	5.45	0.0	0.17	0.05	—	$5.43^{+0.21}_{-0.23}$
$\alpha_D(^{48}\text{Ca})$	2.07	0.22	0.06	0.1	—	$2.30^{+0.31}_{-0.26}$
$\alpha_D(^{208}\text{Pb})$	20.1	0.6	0.59	0.8	—	$22.6^{+2.1}_{-1.8}$

Predicting the skin thickness of ^{208}Pb

Challenge: cutoff variation and N3LO predictions



History Matching

We explore 10^9 different interaction parameterizations. Confronted with $A=2-16$ data + NN scattering information. Find 34 non-implausible interactions

Calibration

Likelihood weighting

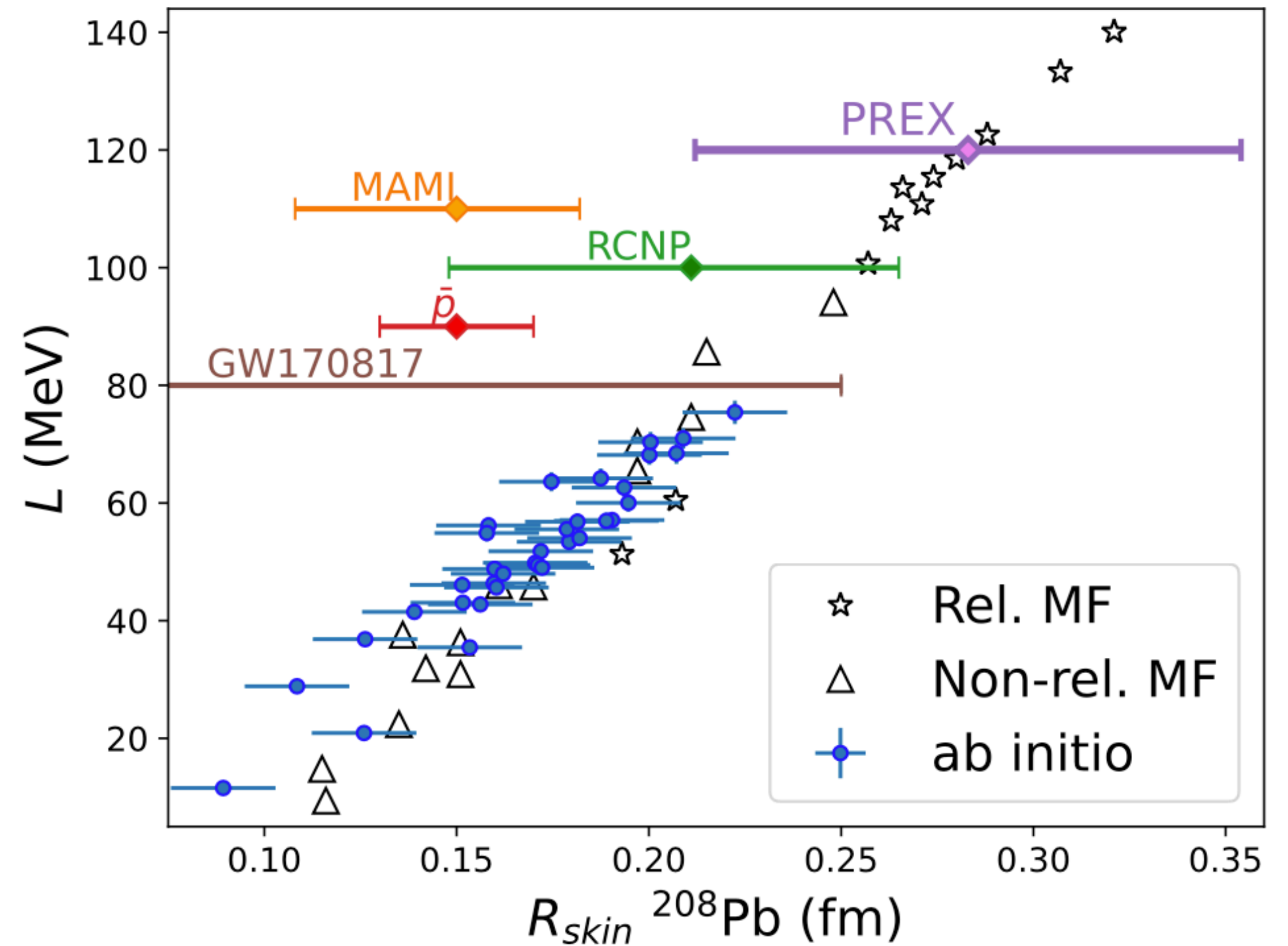
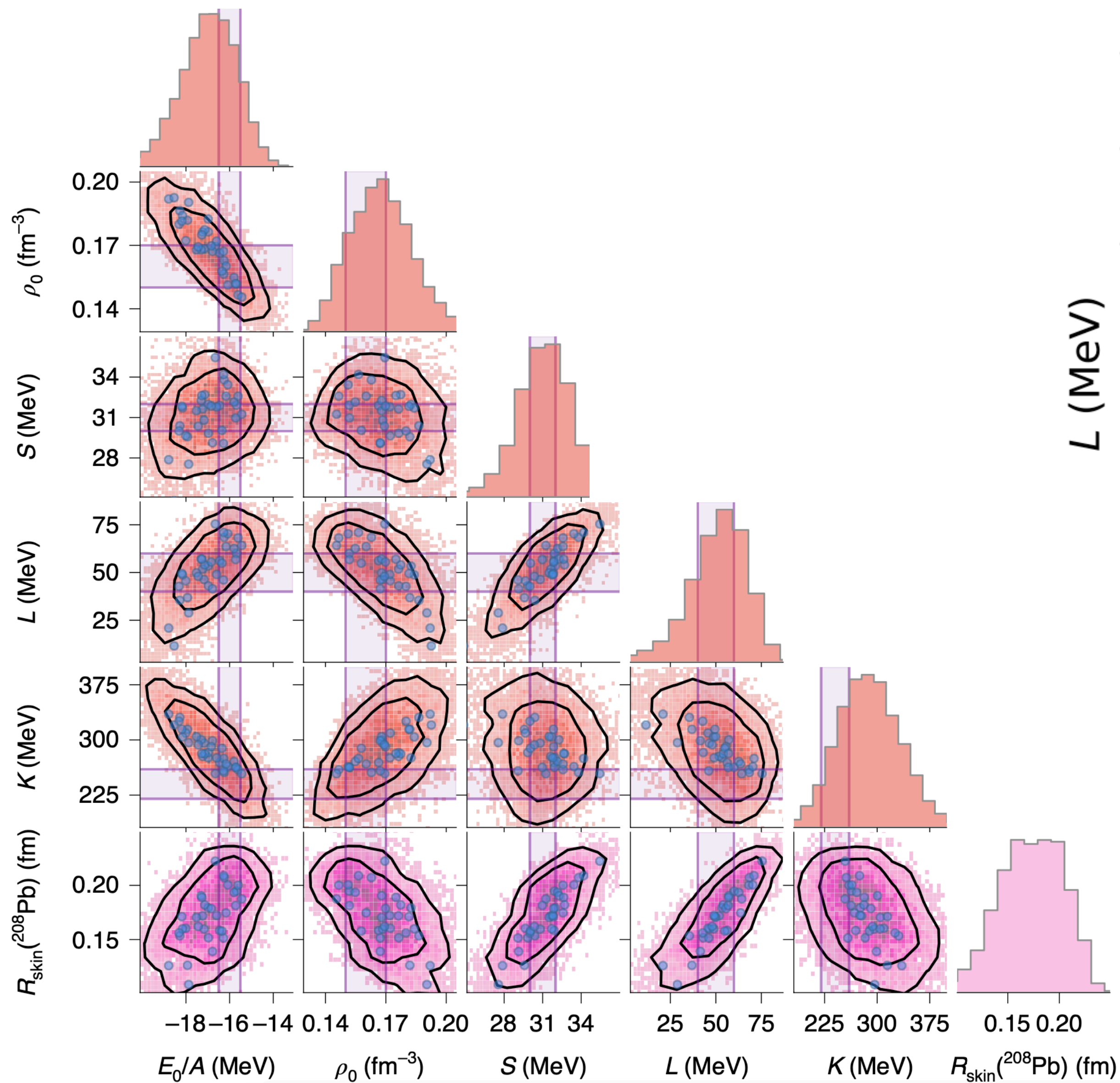
Validation

Inspect ab initio model and error estimates

Prediction: small skin thickness 0.14-0.20 fm in mild (1.5sigma) tension with PREX.

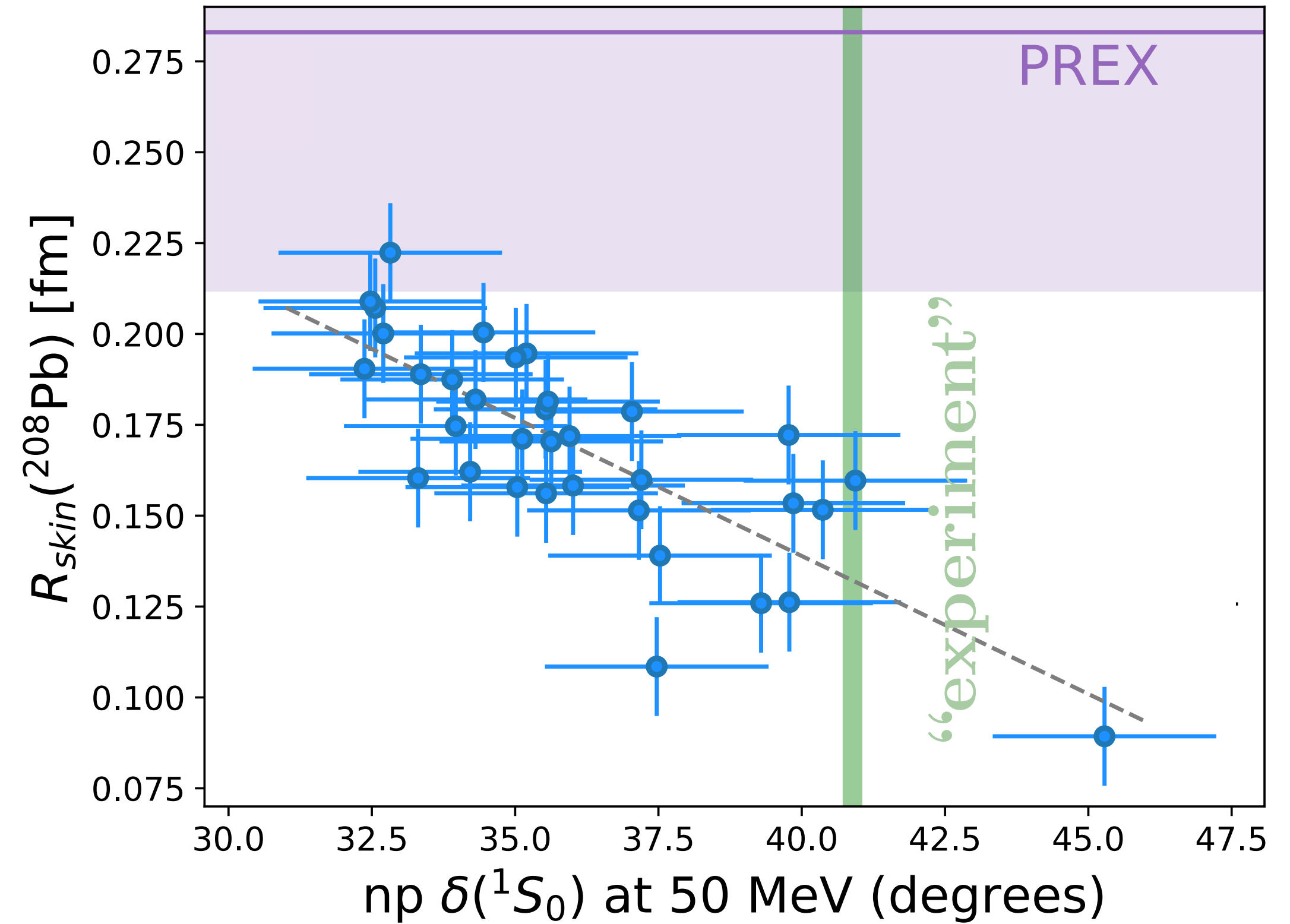
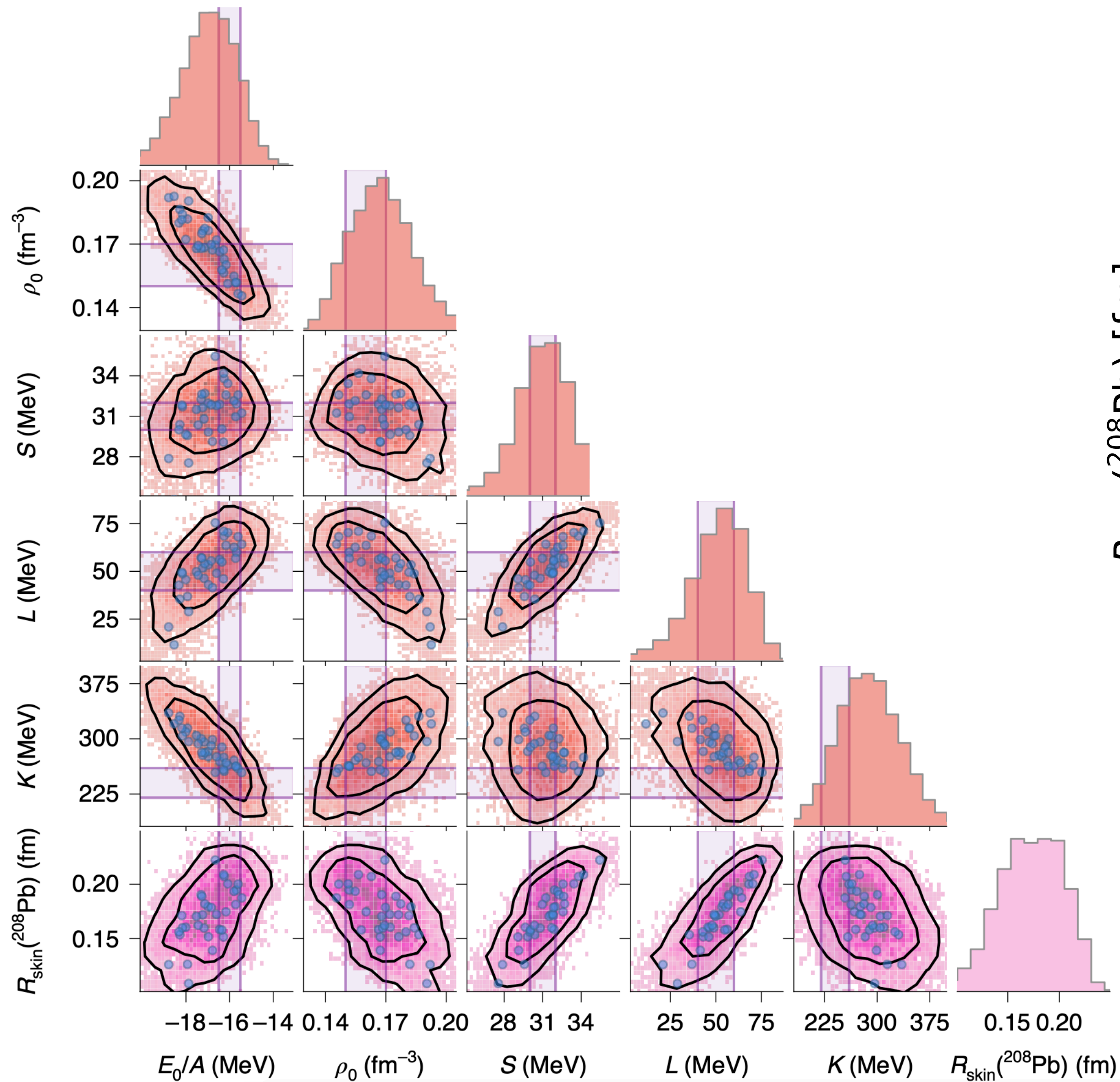
History-matching observables						
Observable	z	ϵ_{exp}	ϵ_{model}	ϵ_{method}	ϵ_{em}	PPD
$E(^2\text{H})$	-2.2246	0.0	0.05	0.0005	0.001%	$-2.22^{+0.07}_{-0.07}$
$R_p(^2\text{H})$	1.976	0.0	0.005	0.0002	0.0005%	$1.98^{+0.01}_{-0.01}$
$Q(^2\text{H})$	0.27	0.01	0.003	0.0005	0.001%	$0.28^{+0.02}_{-0.02}$
$E(^3\text{H})$	-8.4821	0.0	0.17	0.0005	0.01%	$-8.54^{+0.34}_{-0.37}$
$E(^4\text{He})$	-28.2957	0.0	0.55	0.0005	0.01%	$-28.86^{+0.86}_{-1.01}$
$R_p(^4\text{He})$	1.455	0.0	0.016	0.0002	0.003%	$1.47^{+0.03}_{-0.03}$
$E(^{16}\text{O})$	127.62	0.0	1.0	0.75	0.5%	$-126.2^{+3.0}_{-2.8}$
$R_p(^{16}\text{O})$	2.58	0.0	0.03	0.01	0.5%	$2.57^{+0.06}_{-0.06}$
Calibration observables						
Observable	z	ϵ_{exp}	ϵ_{model}	ϵ_{method}	ϵ_{em}	PPD
$E/A(^{48}\text{Ca})$	-8.667	0.0	0.54	0.25	—	$-8.58^{+0.72}_{-0.72}$
$E_{2+}(^{48}\text{Ca})$	3.83	0.0	0.5	0.5	—	$3.79^{+0.86}_{-0.96}$
$R_p(^{48}\text{Ca})$	3.39	0.0	0.11	0.03	—	$3.36^{+0.14}_{-0.13}$
Validation observables						
Observable	z	ϵ_{exp}	ϵ_{model}	ϵ_{method}	ϵ_{em}	PPD
$E/A(^{208}\text{Pb})$	-7.867	0.0	0.54	0.5	—	$-8.06^{+0.99}_{-0.88}$
$R_p(^{208}\text{Pb})$	5.45	0.0	0.17	0.05	—	$5.43^{+0.21}_{-0.23}$
$\alpha_D(^{48}\text{Ca})$	2.07	0.22	0.06	0.1	—	$2.30^{+0.31}_{-0.26}$
$\alpha_D(^{208}\text{Pb})$	20.1	0.6	0.59	0.8	—	$22.6^{+2.1}_{-1.8}$

Predictions for the skin thickness and nuclear matter

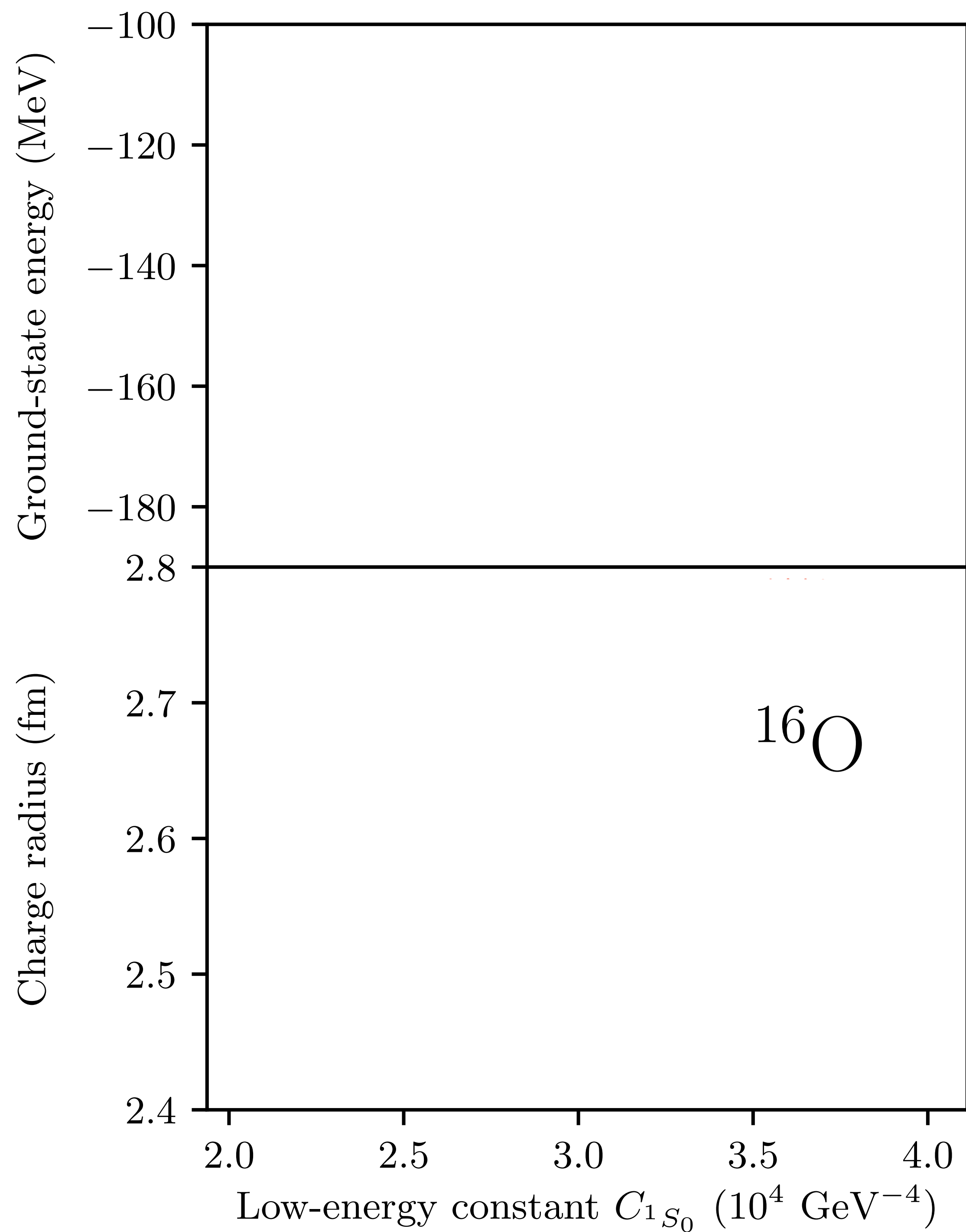


Mean-field models can accommodate very thick skins while reproducing binding energies and charge radii along the nuclear chart.

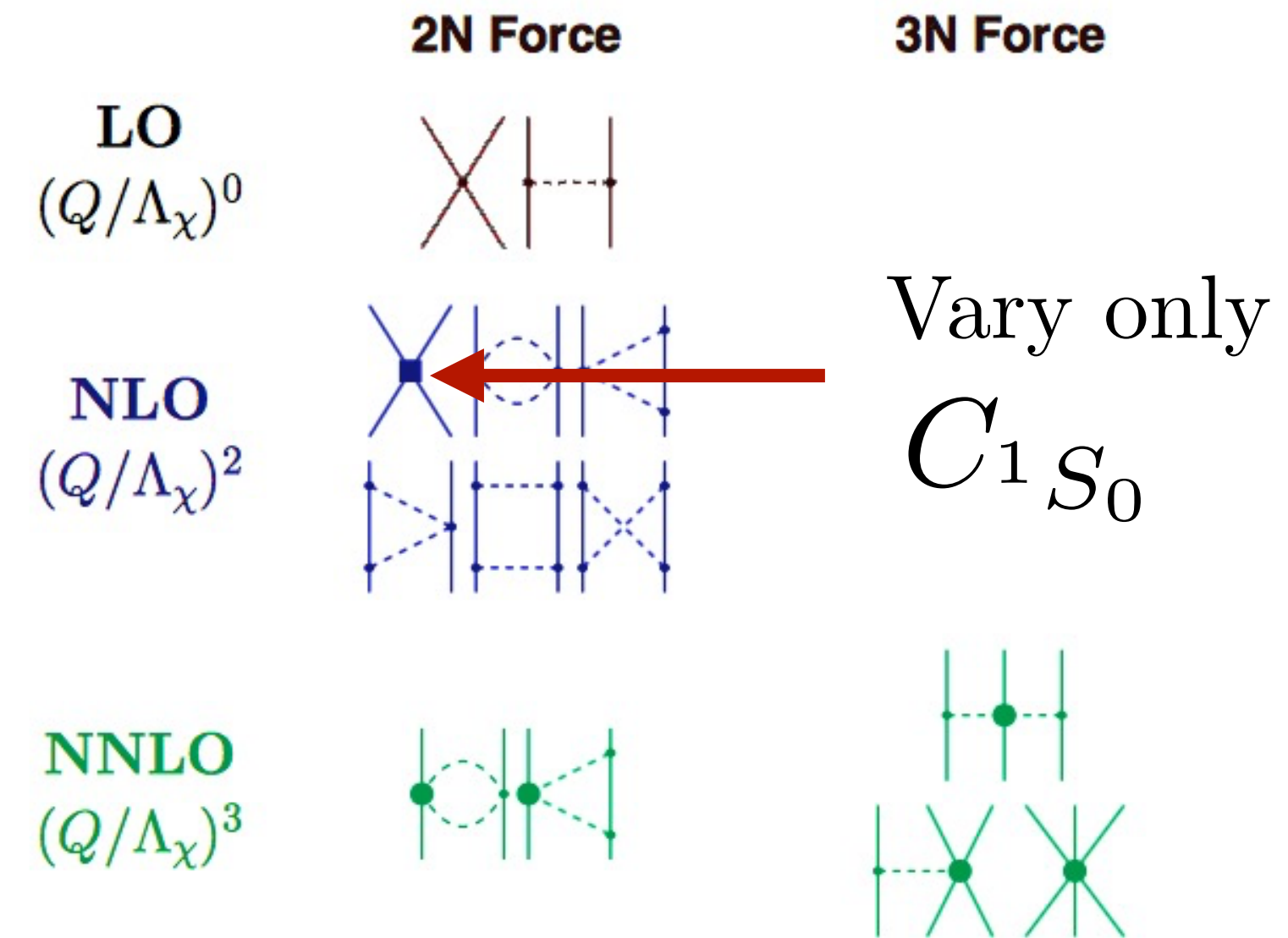
Predictions for the skin thickness and nuclear matter

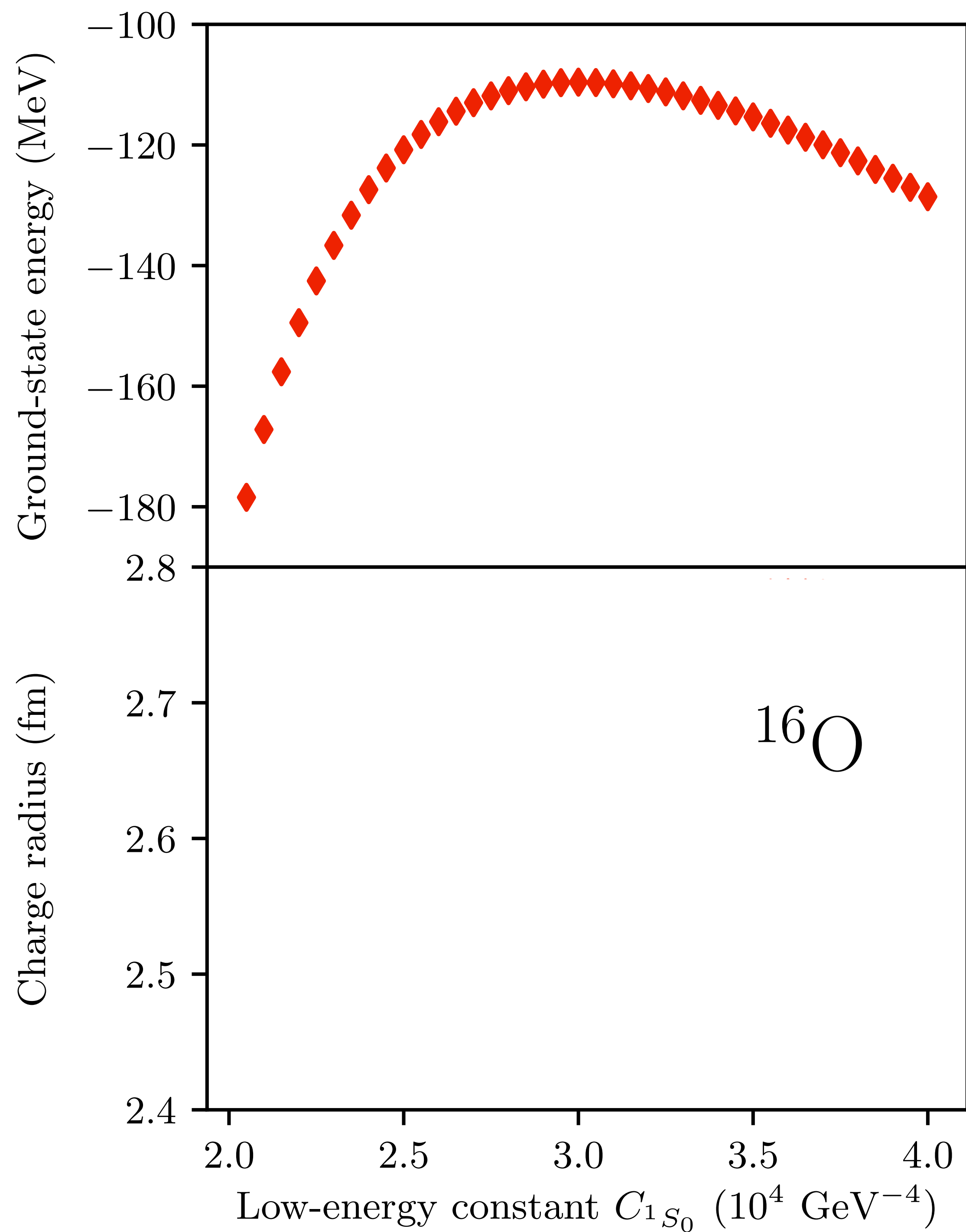


The skin thickness, and the slope L of the symmetry energy, is correlated with the $1S_0$ phase shift.

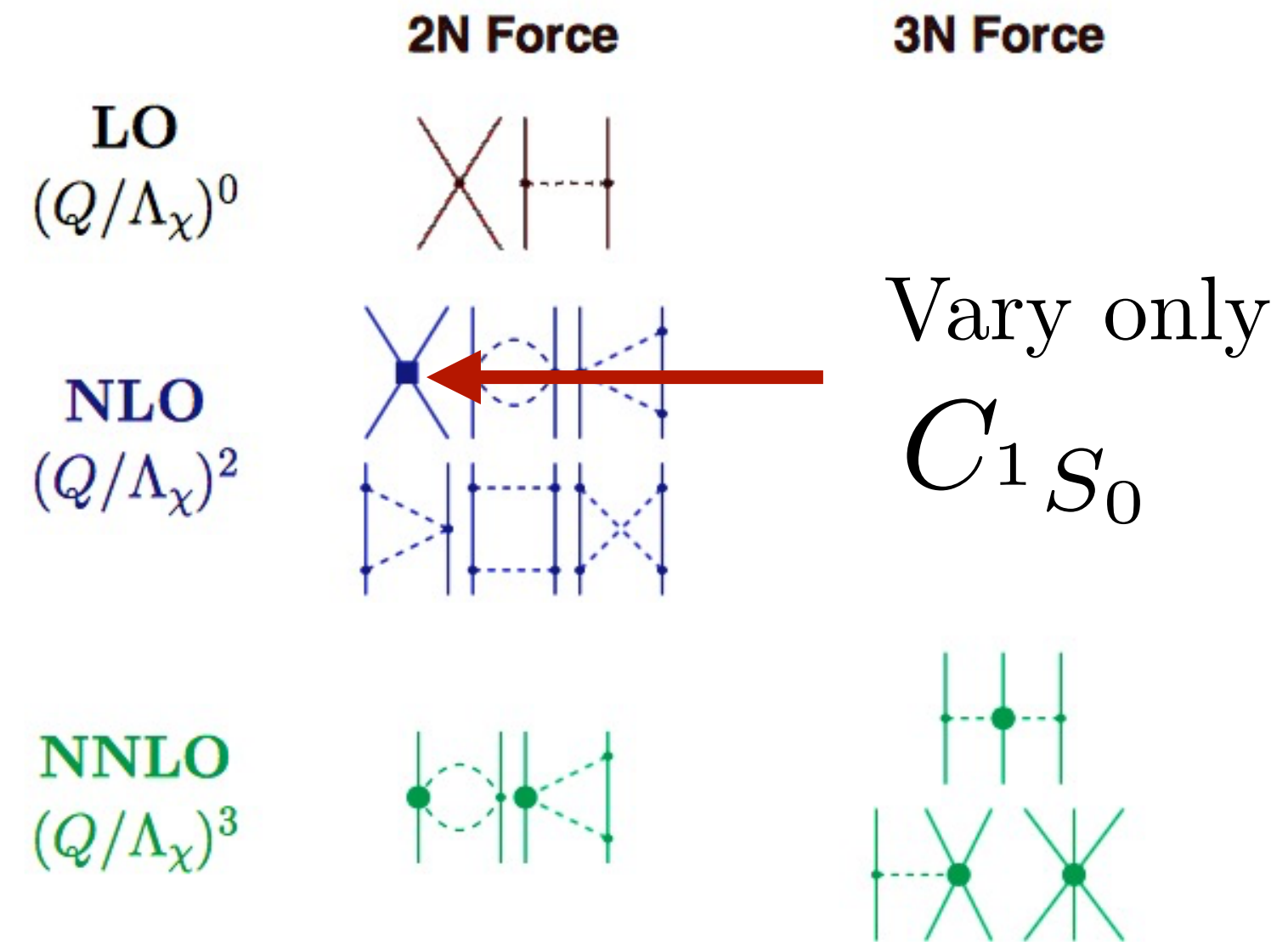


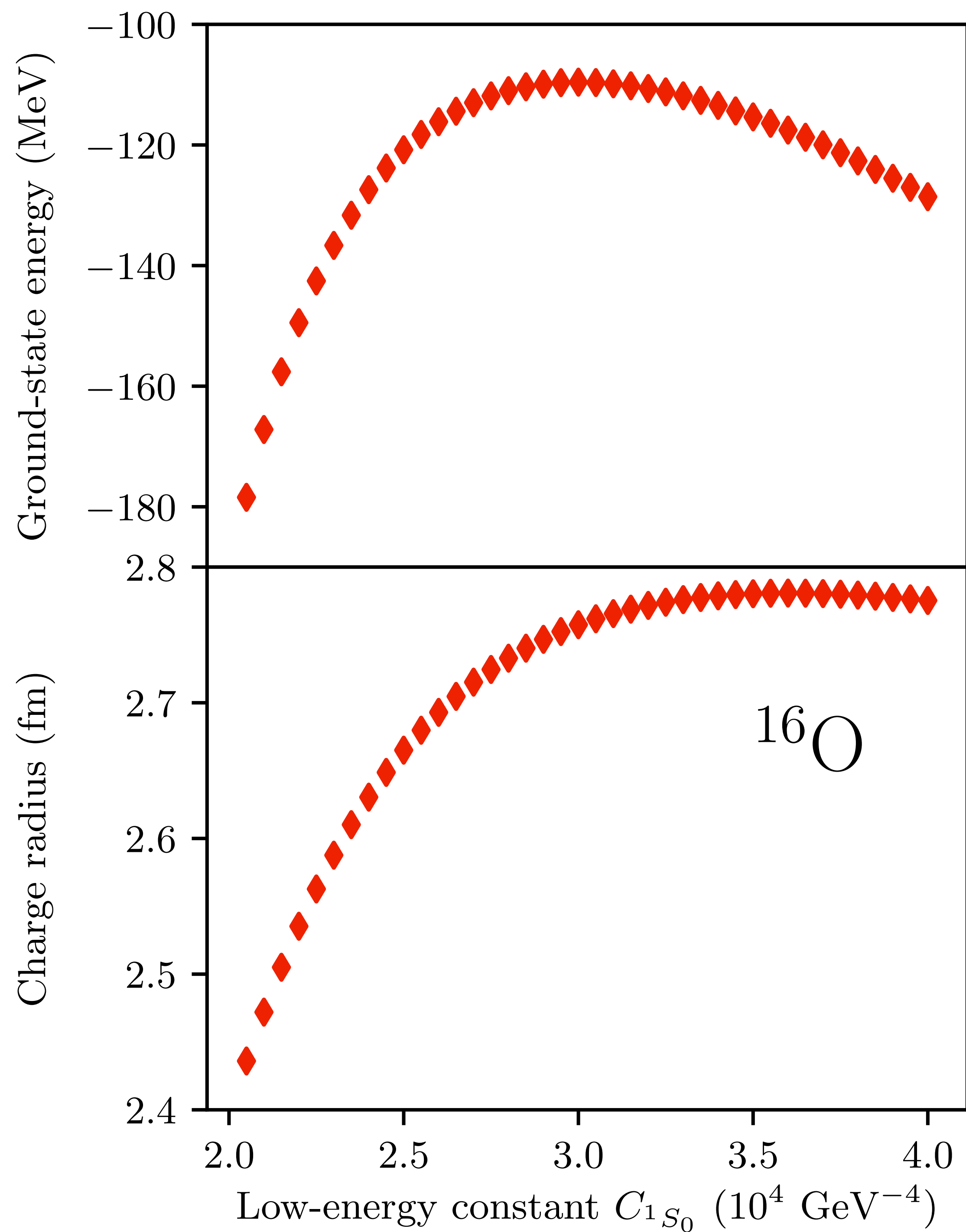
 Exact coupled cluster calculations at the singles and doubles level



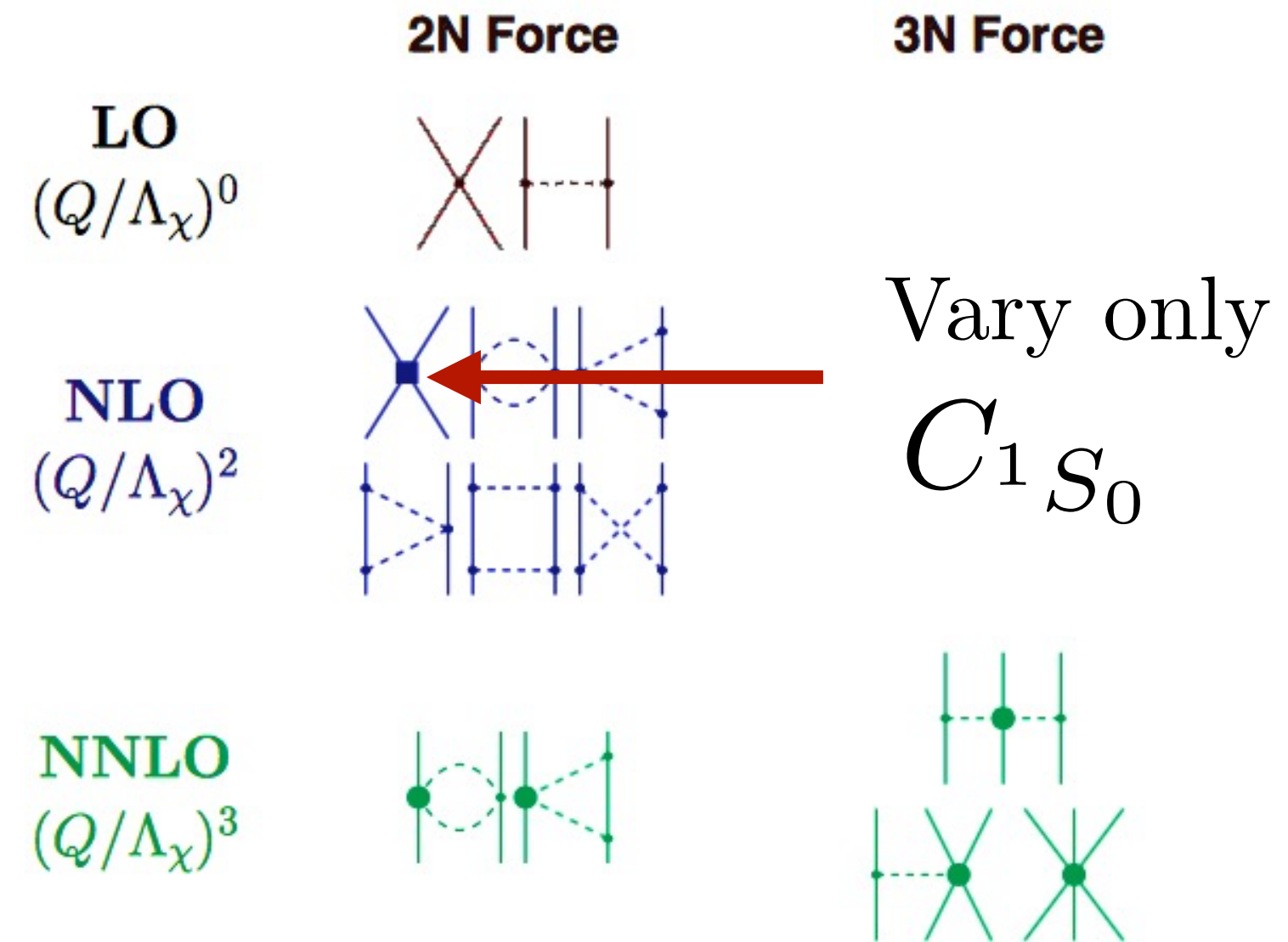


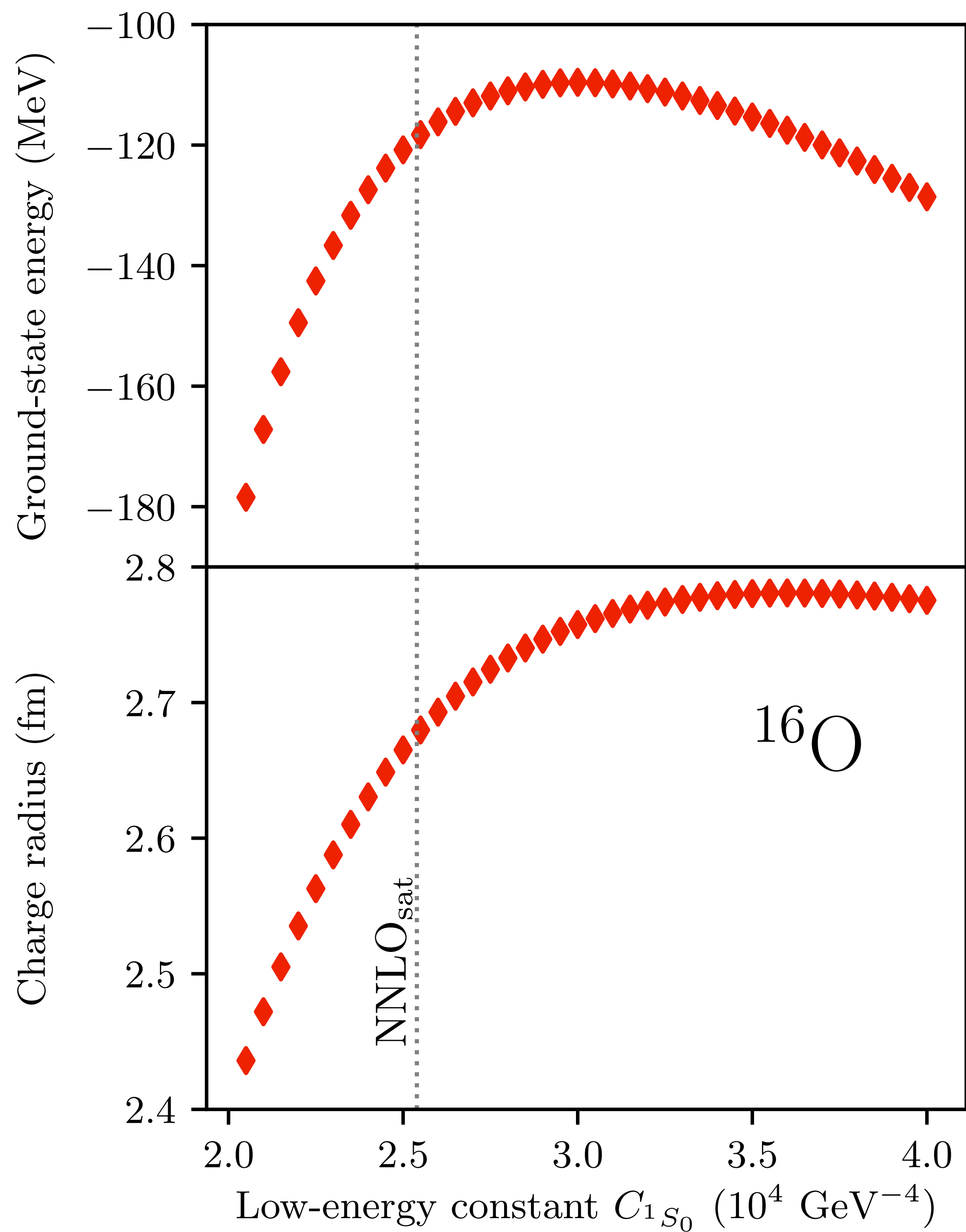
Exact coupled cluster calculations at the singles and doubles level



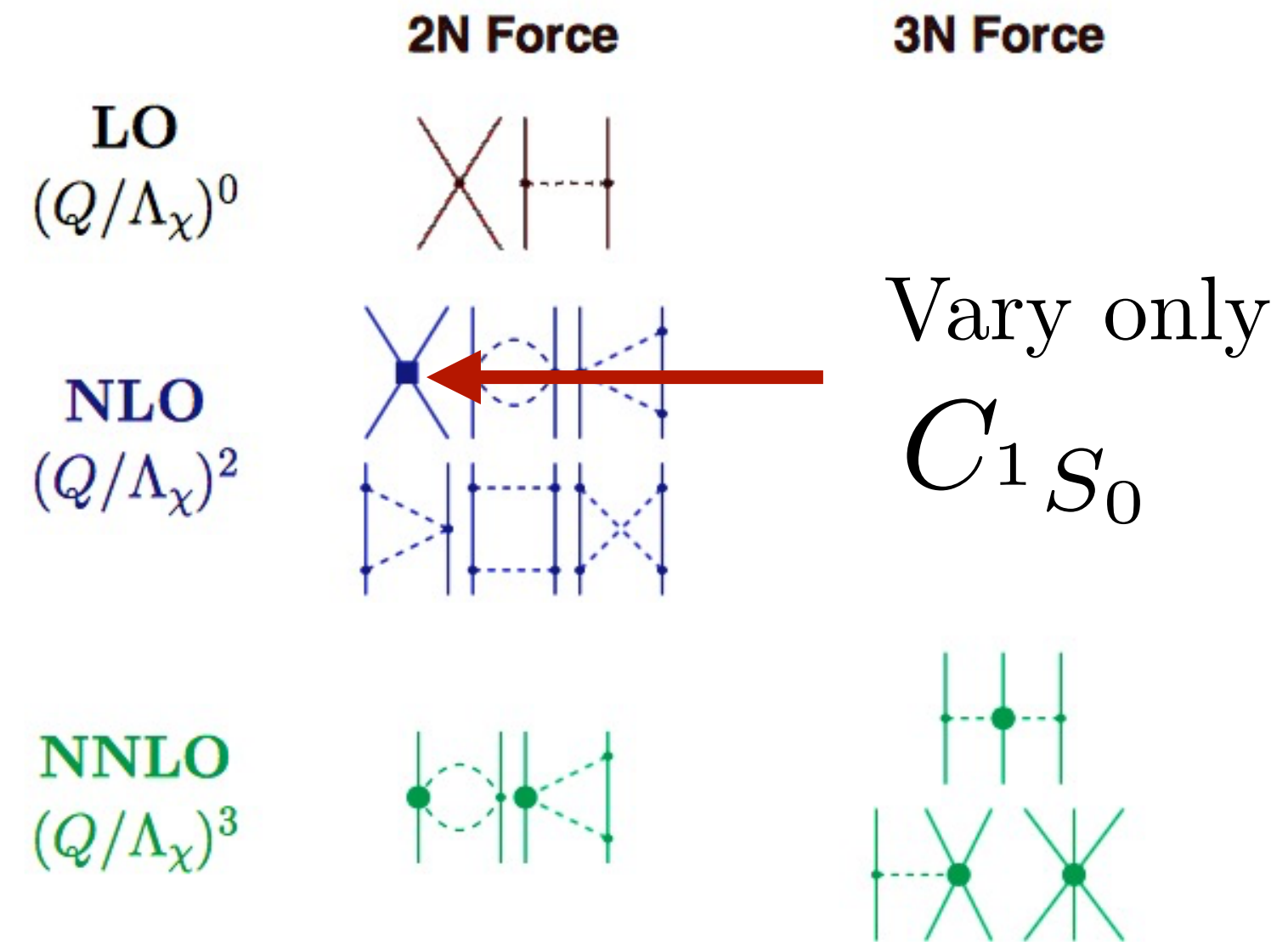


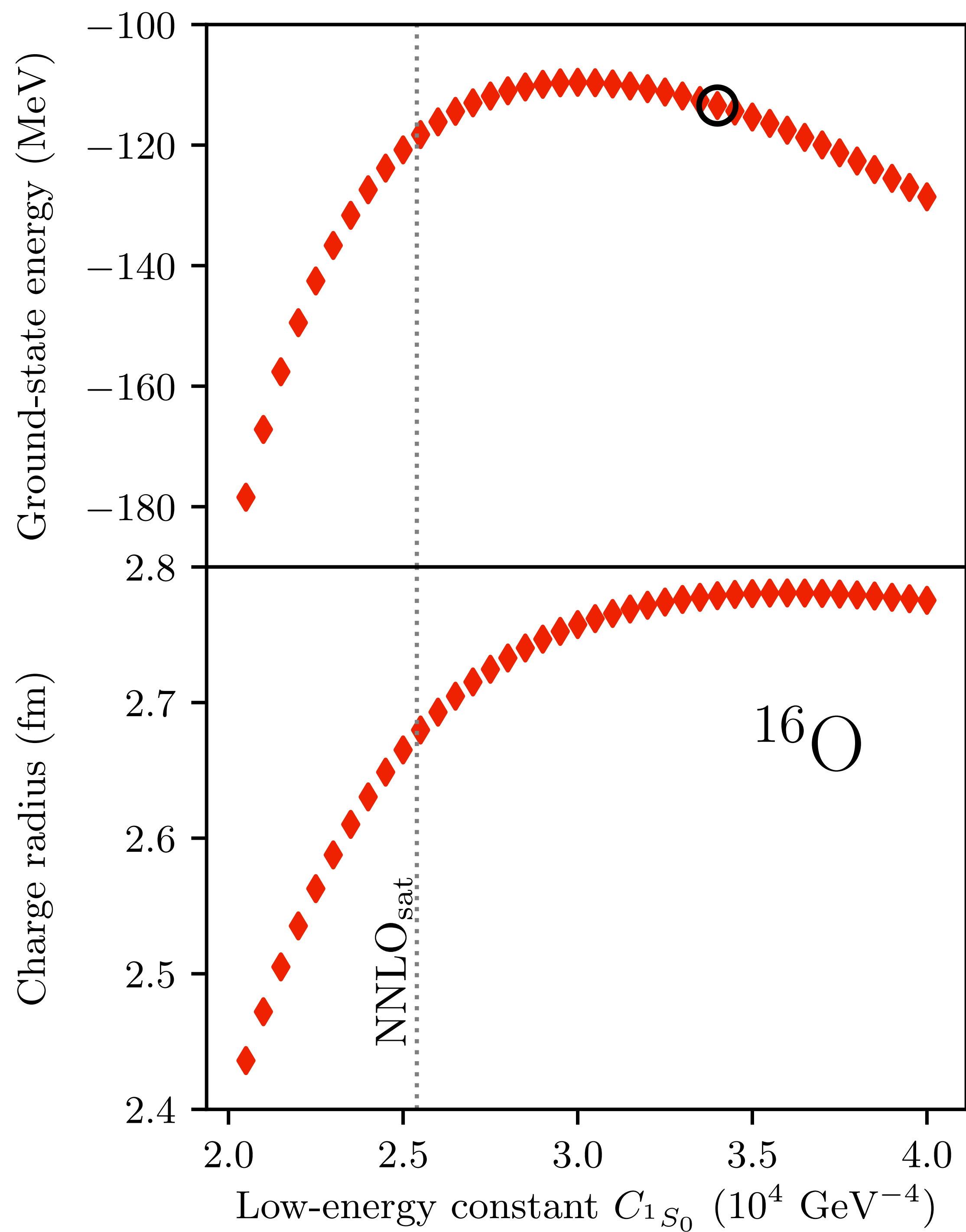
Exact coupled cluster calculations at the singles and doubles level



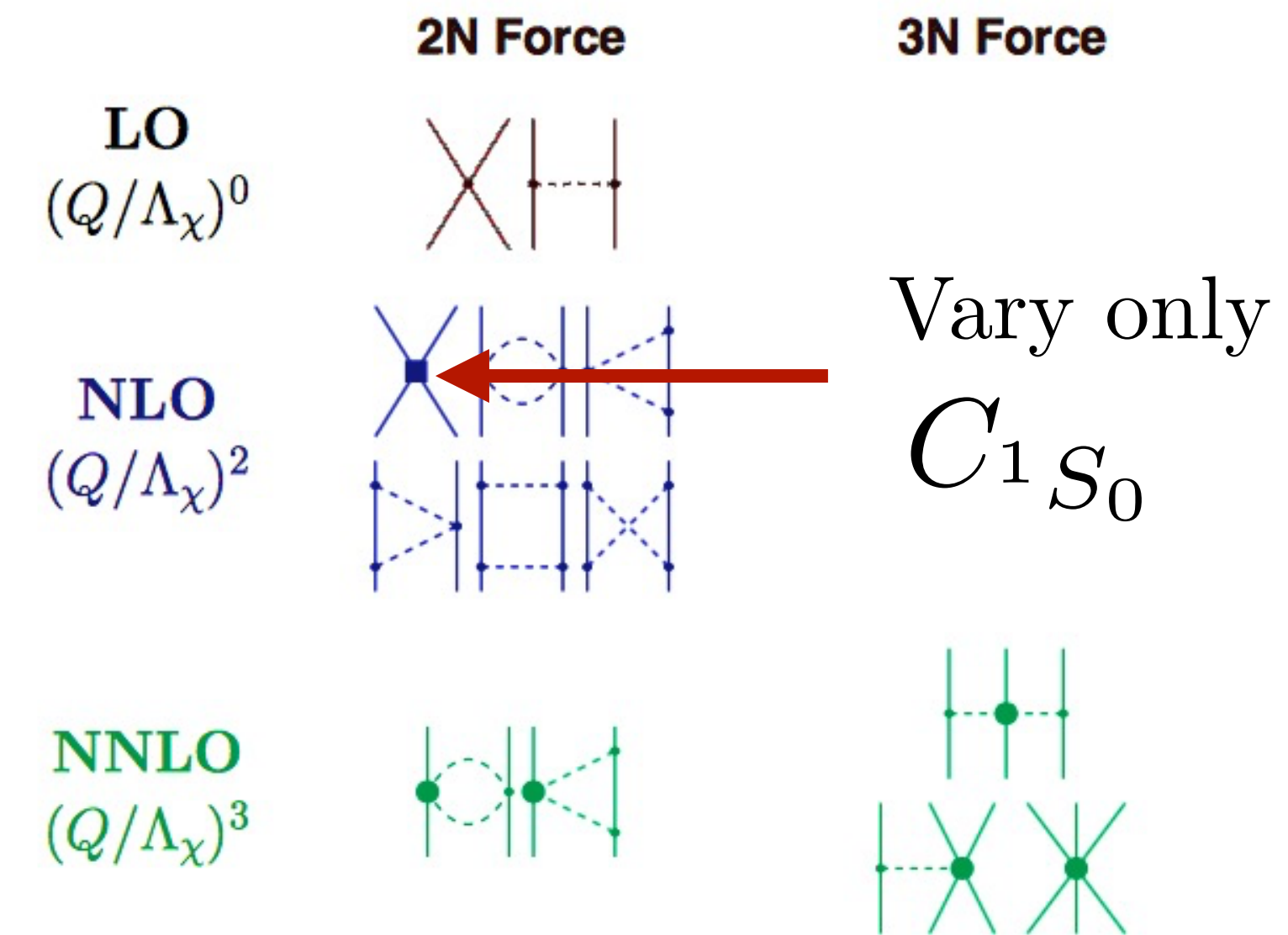


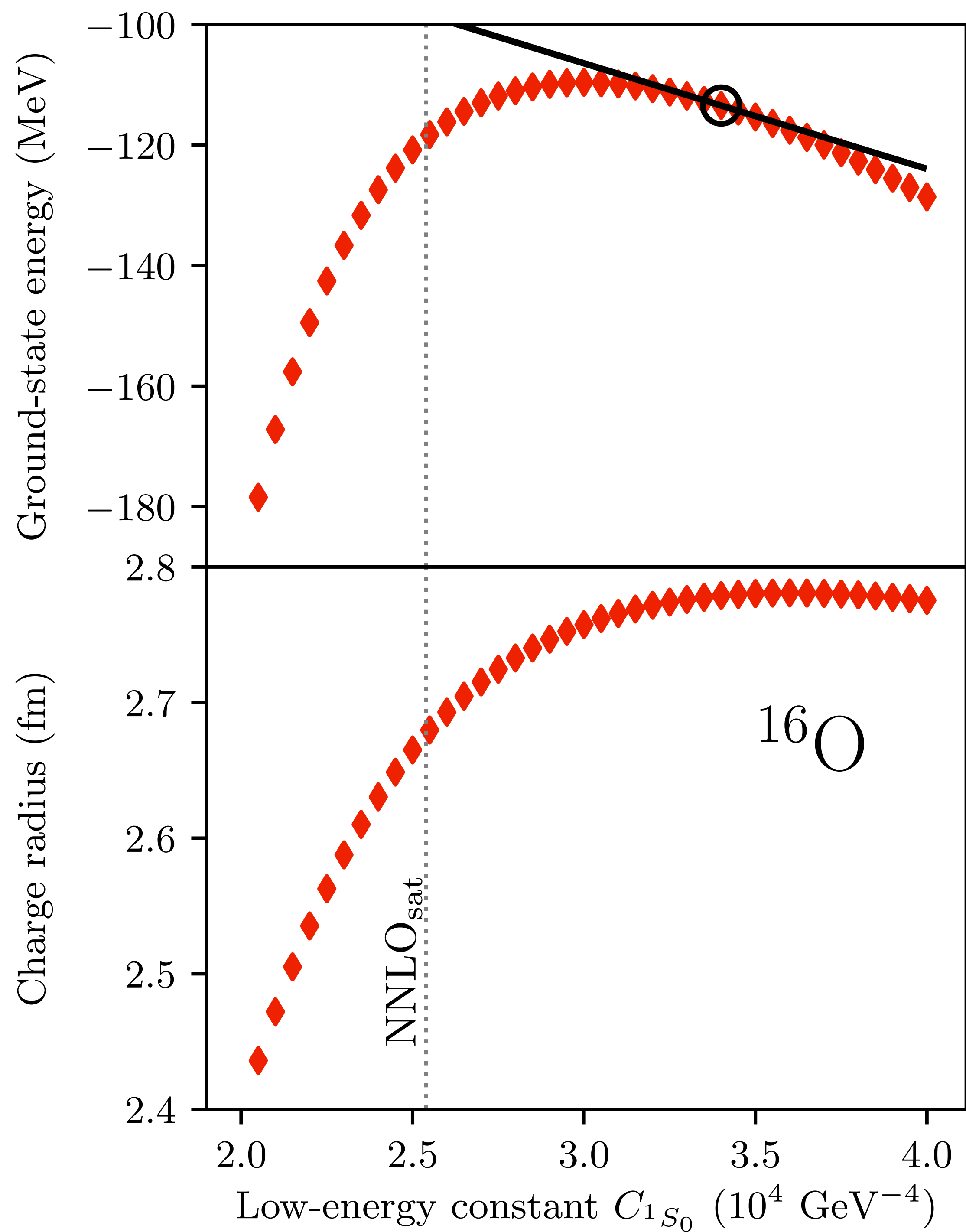
Exact coupled cluster calculations
at the singles and doubles level



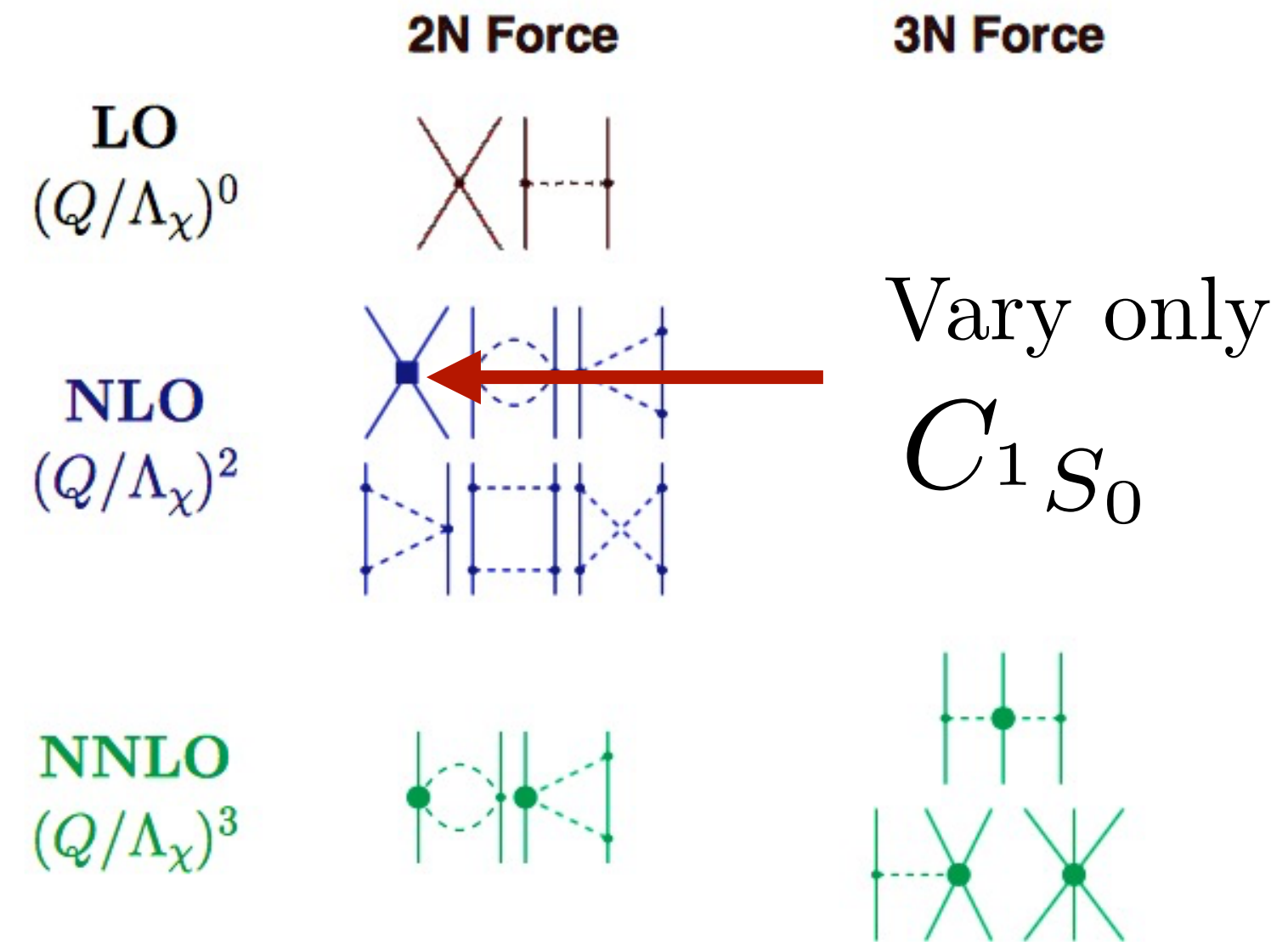


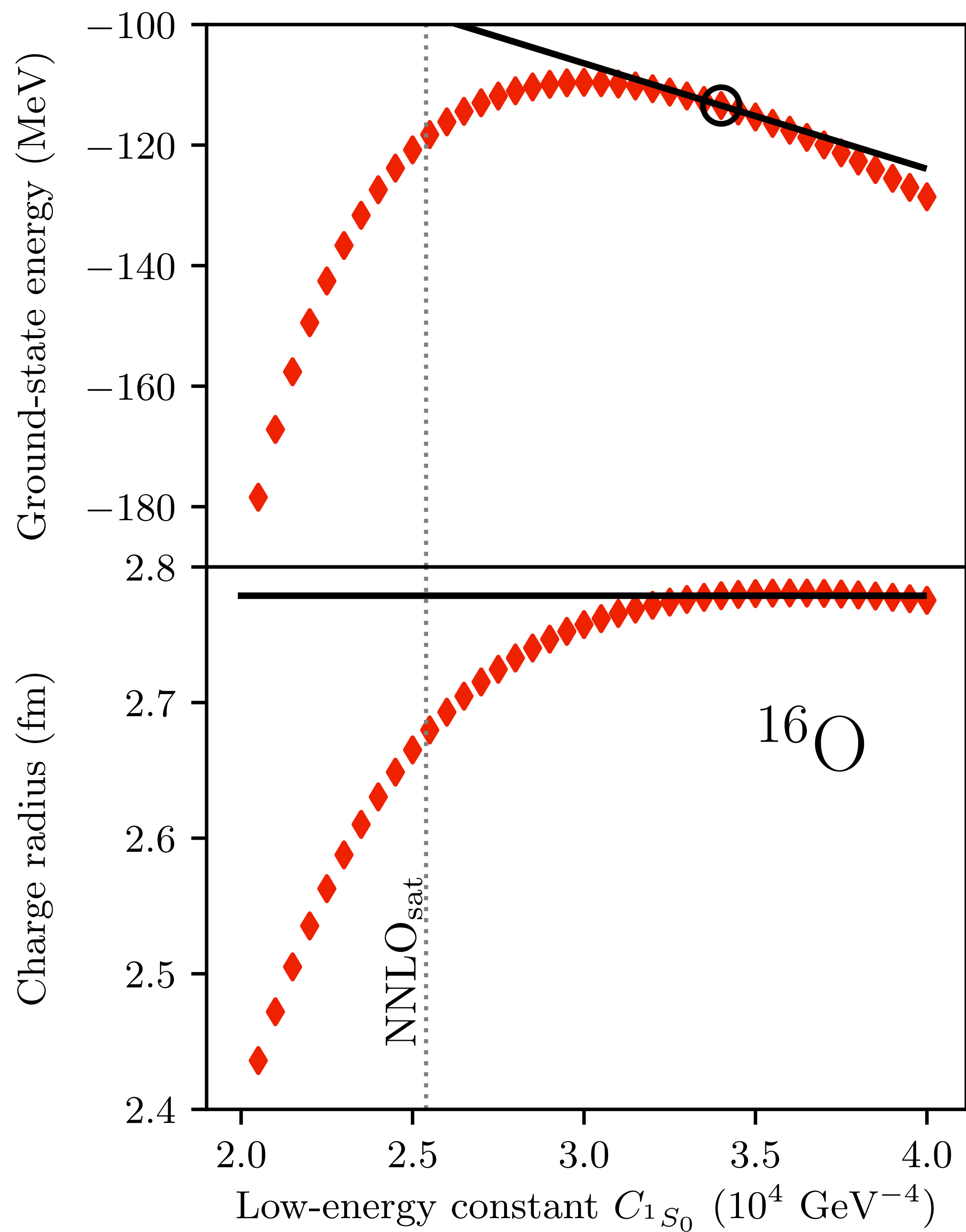
Exact coupled cluster calculations at the singles and doubles level



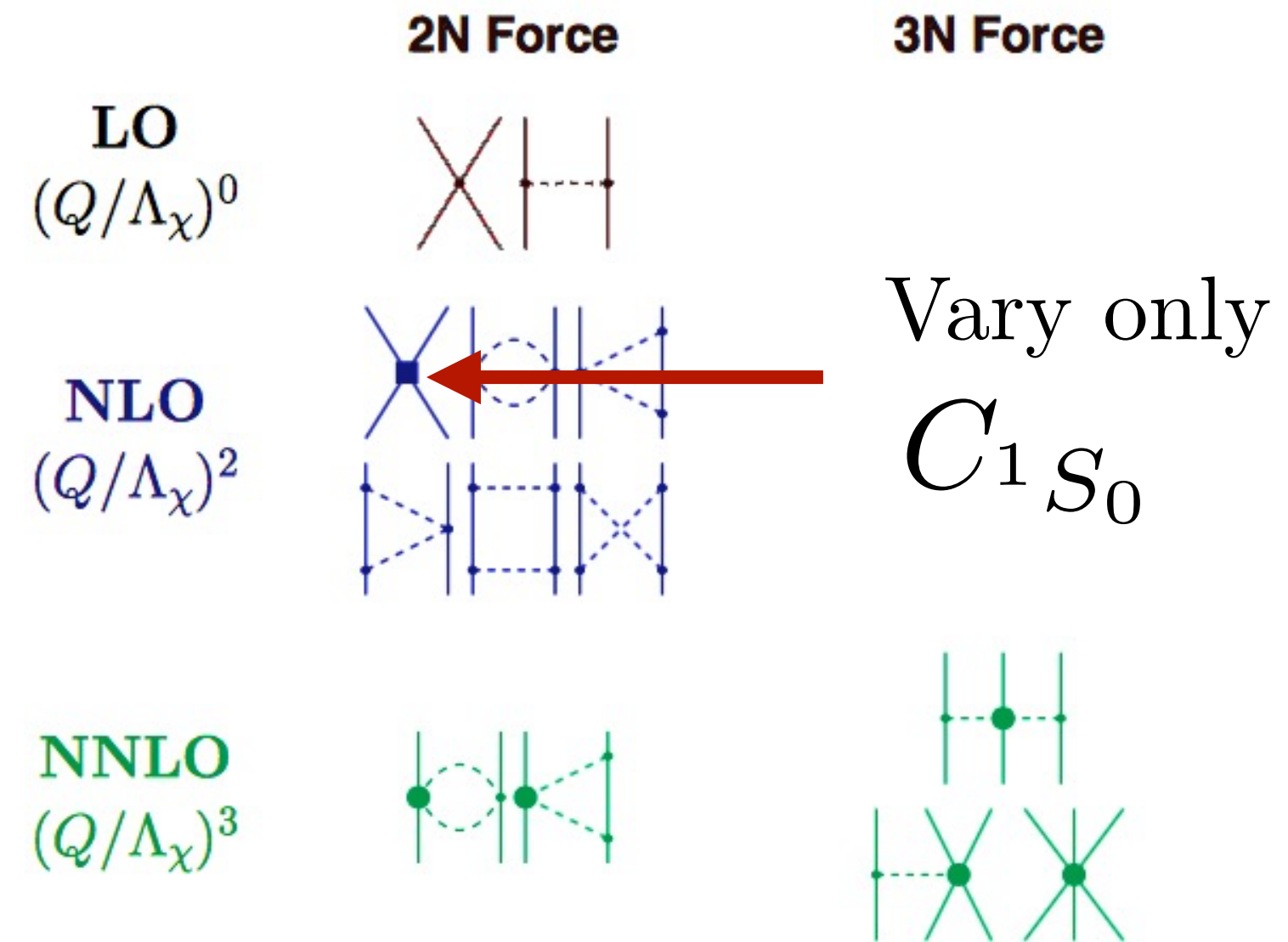


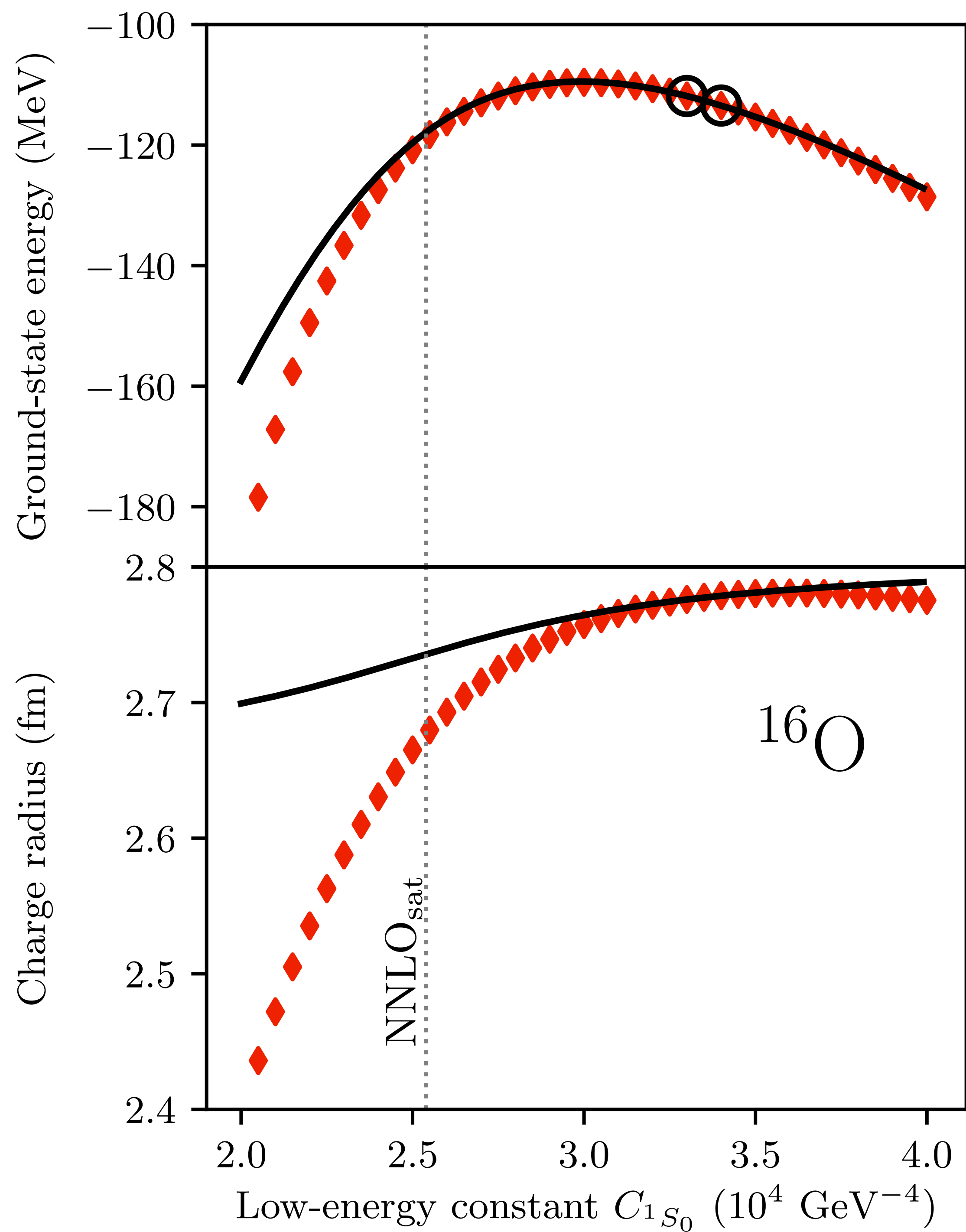
Exact coupled cluster calculations at the singles and doubles level



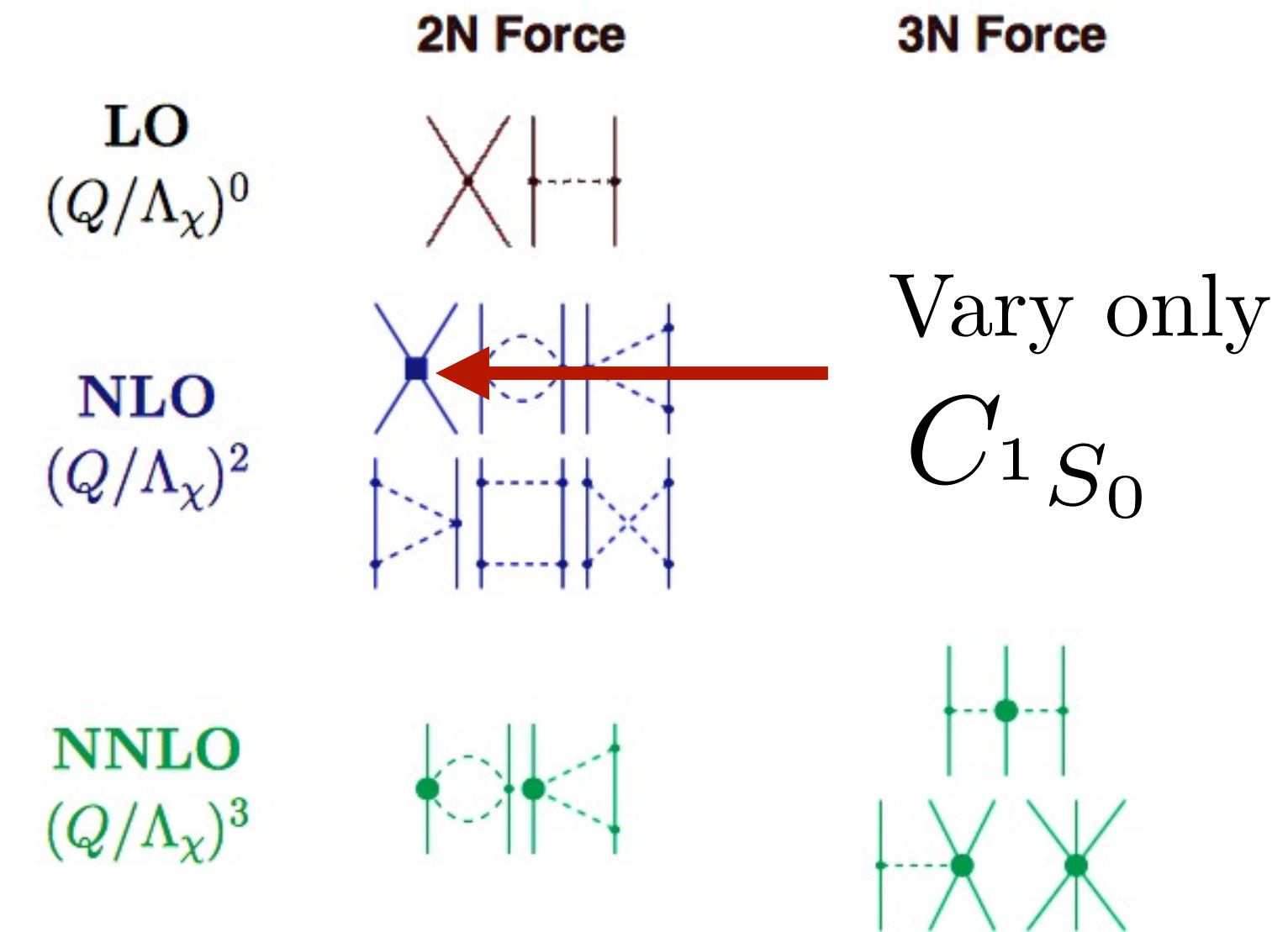


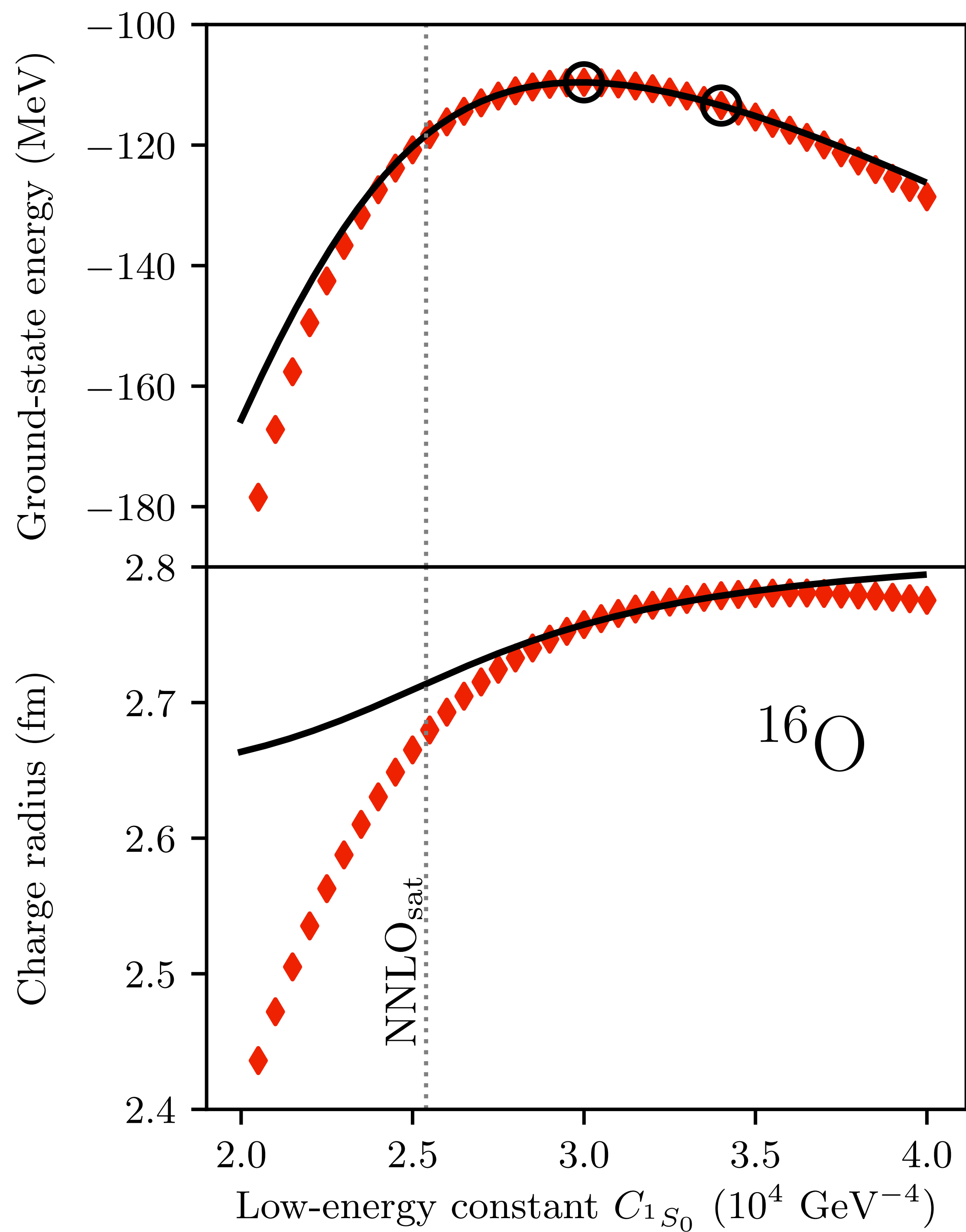
Exact coupled cluster calculations at the singles and doubles level



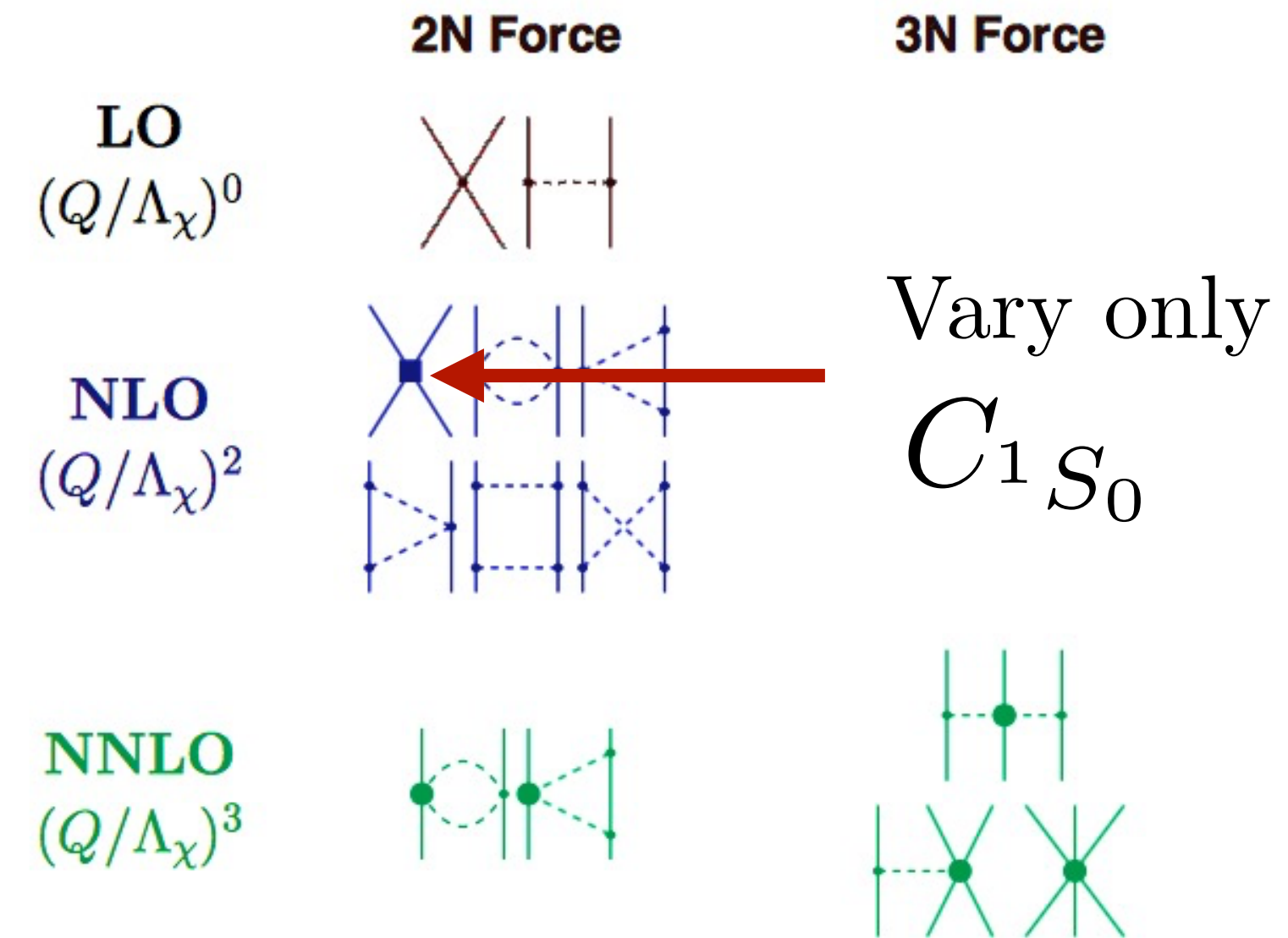


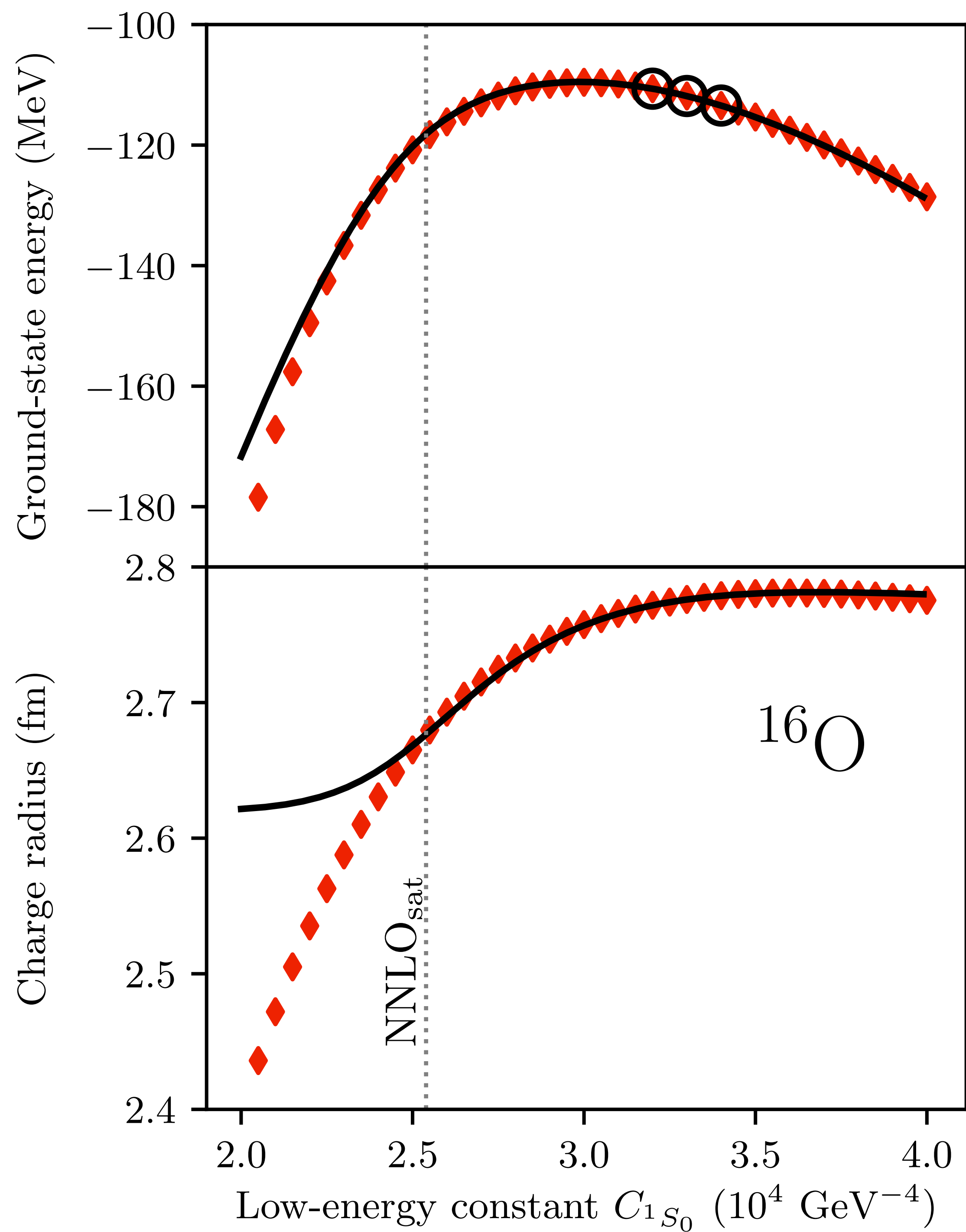
Exact coupled cluster calculations at the singles and doubles level



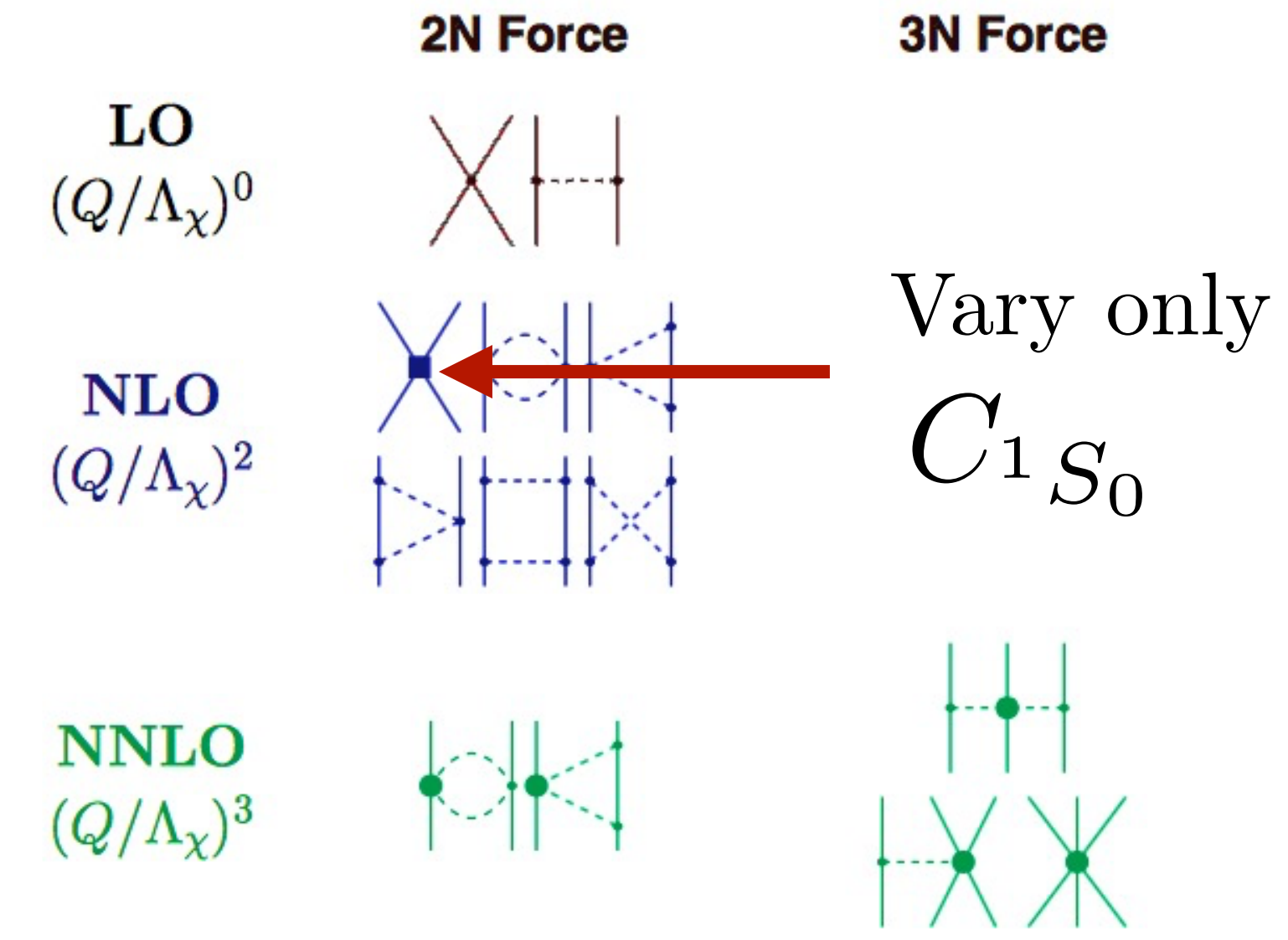


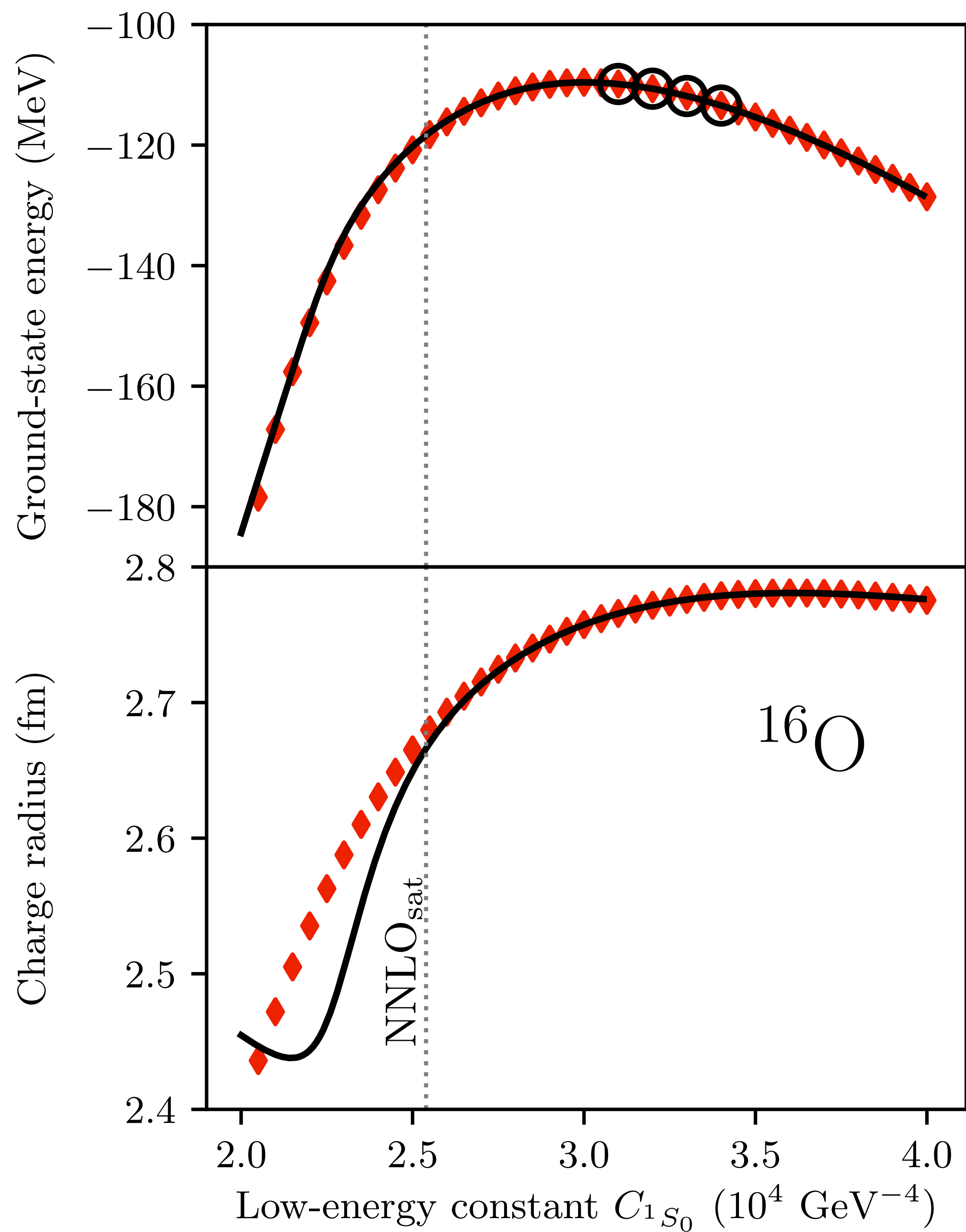
Exact coupled cluster calculations at the singles and doubles level



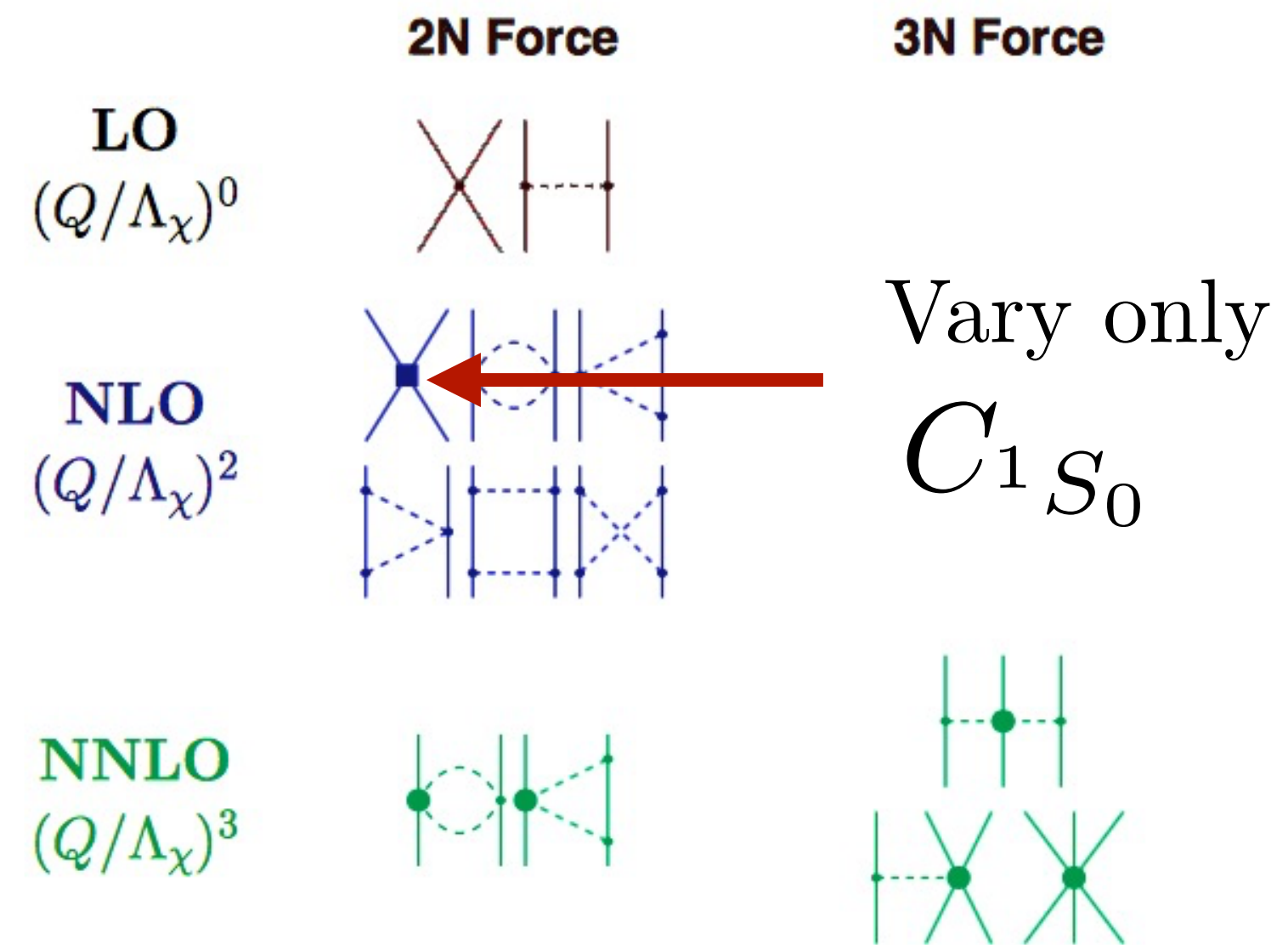


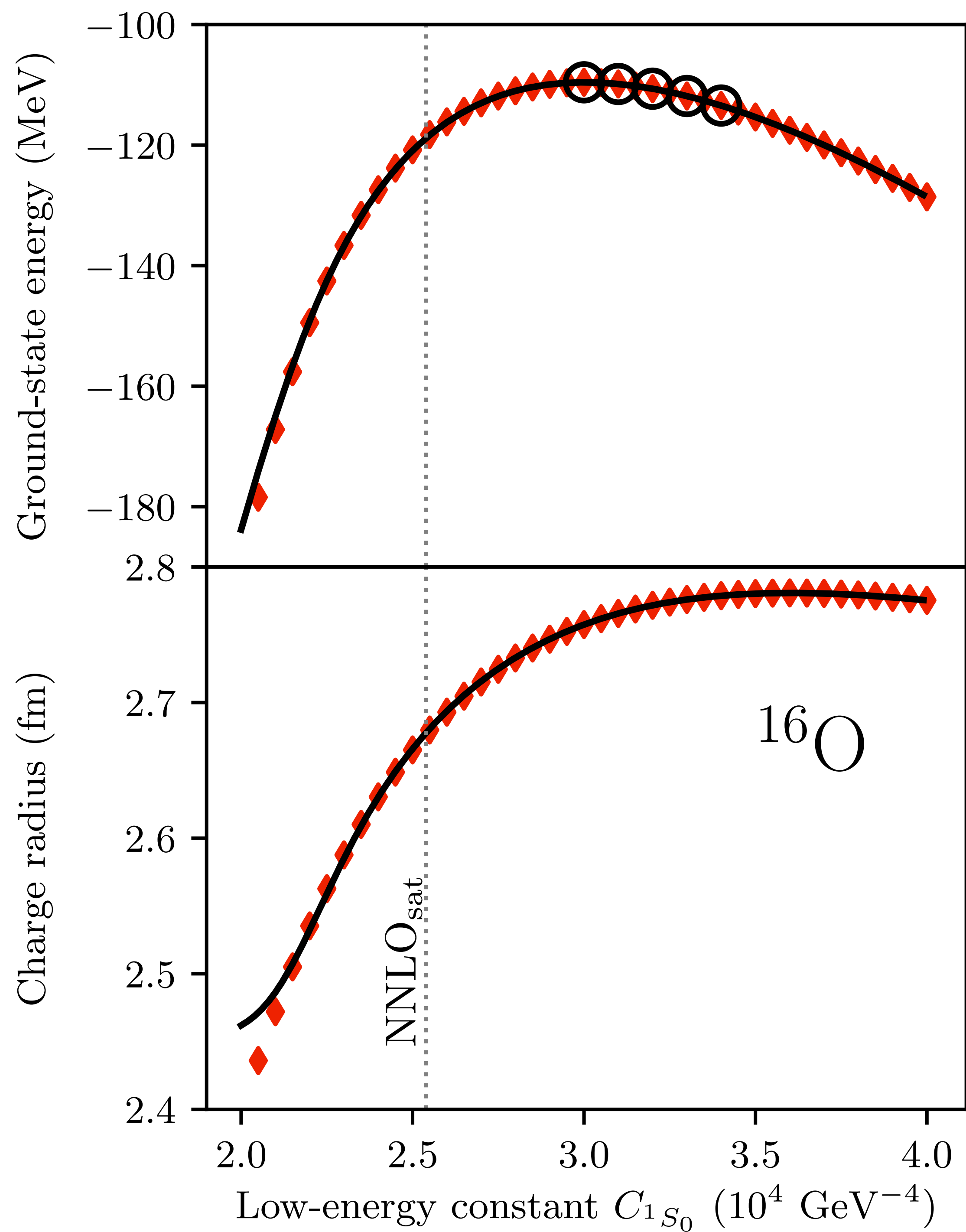
Exact coupled cluster calculations
at the singles and doubles level



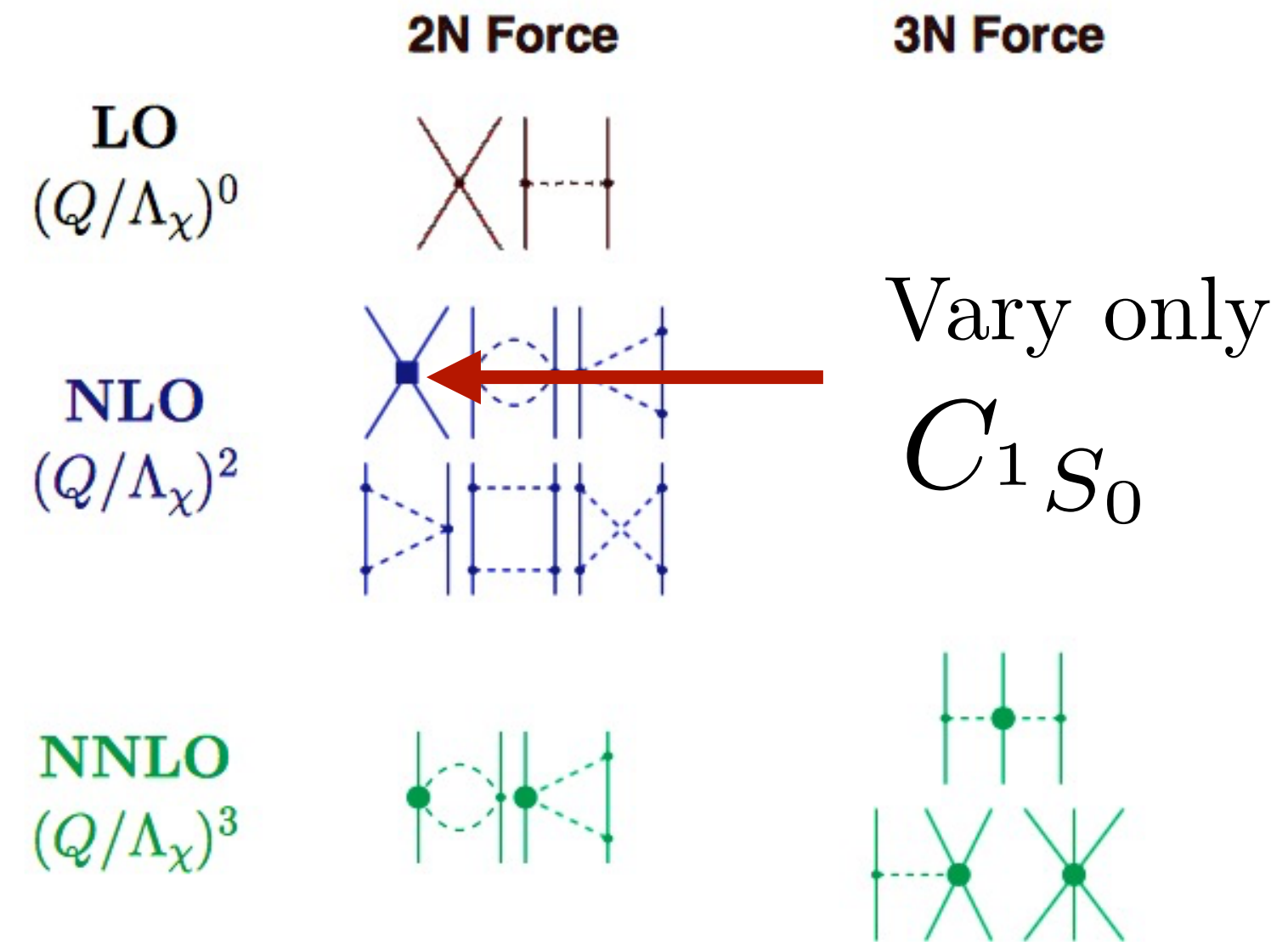


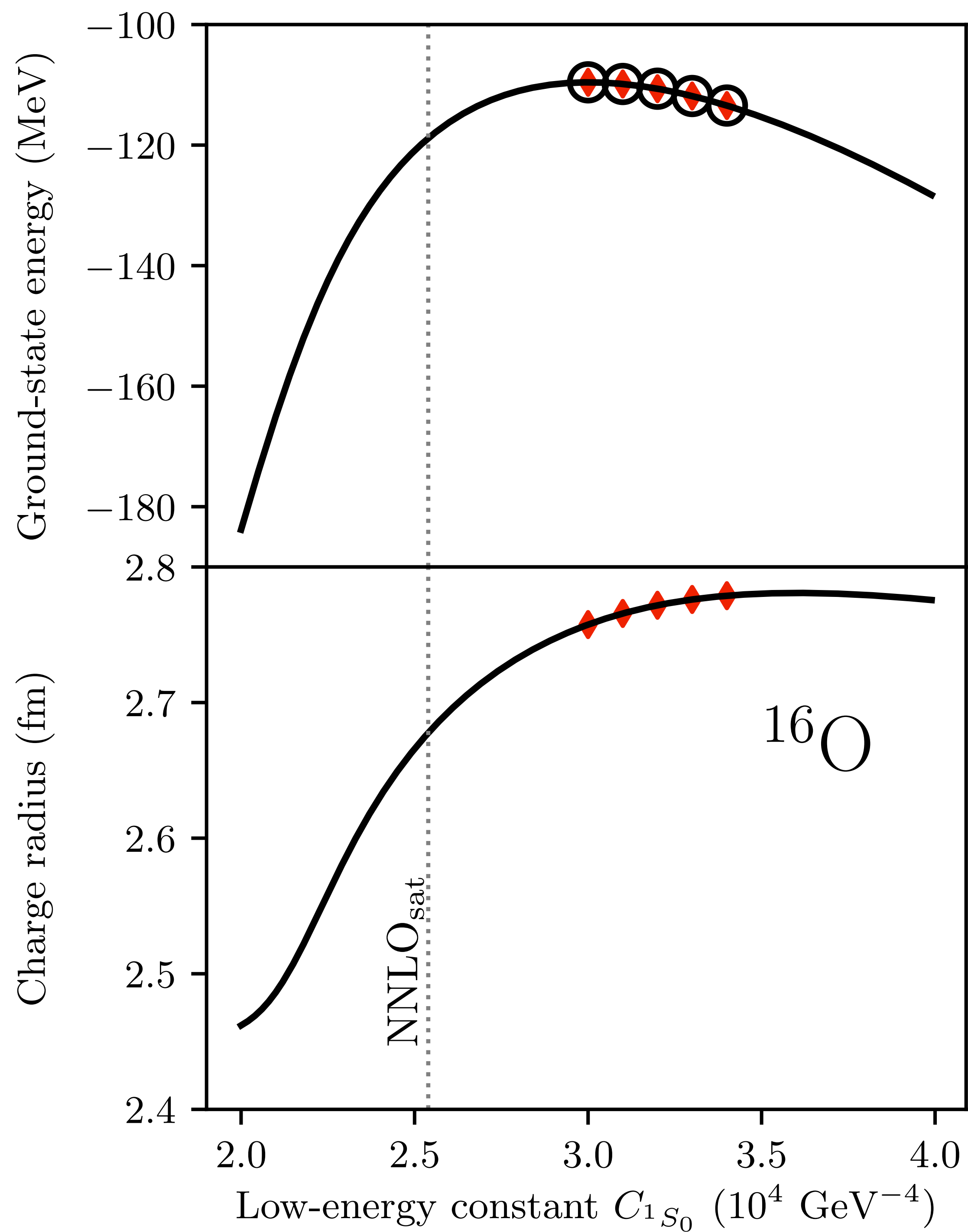
Exact coupled cluster calculations at the singles and doubles level





Exact coupled cluster calculations at the singles and doubles level





Exact coupled cluster calculations at the singles and doubles level

